

Modelling the role of HIV and its treatment in non-Hodgkin lymphoma growth dynamics

by

Rosemary Akinyi Aogo

*Thesis presented in partial fulfilment of the requirements
for the degree of Master of Science in Mathematics in the
Faculty of Science at Stellenbosch University*



Department of Mathematical Sciences,
Mathematics Division,
University of Stellenbosch,
Private Bag X1, Matieland 7602, South Africa.

Supervisor: Prof. Farai Nyabadza

December 2015

Declaration

By submitting this thesis electronically, I declare that the entirety of the work contained therein is my own, original work, that I am the sole author thereof (save to the extent explicitly otherwise stated), that reproduction and publication thereof by Stellenbosch University will not infringe any third party rights and that I have not previously in its entirety or in part submitted it for obtaining any qualification.

Signature:

Rosemary Akinyi Aogo

October 20, 2015

Date:

Copyright © 2015 Stellenbosch University
All rights reserved.

Abstract

Modelling the role of HIV and its treatment in non-Hodgkin lymphoma growth dynamics

Rosemary Akinyi Aogo

*Department of Mathematical Sciences,
Mathematics Division,
University of Stellenbosch,
Private Bag X1, Matieland 7602, South Africa.*

Thesis: MSc. (Mathematical Biology)

December 2015

HIV/AIDS associated cancers are cancers whose incidences are much higher in HIV/AIDS patients than in the general population. HIV as one of the chronic infections involves chronic antigenic stimulation by persistent self-antigens or foreign antigens and the stimulation activates B cells and induces their uncontrollable growth. Cancer and HIV co-existence both *in vivo* and *in vitro* in a cancer immune environment leads to specific cytokines being produced by various immune cells and the cancer cells. In this thesis, we develop a mathematical model describing the cancer-immune system interaction in the presence of HIV and HIV treatment. In particular, we focus on the most common cancer in AIDS patients; the non-Hodgkin's lymphoma (NHL). The formulated model, described by non-linear ordinary differential equations, shows existence of multiple equilibria whose stability and bifurcation analysis are presented. Our results suggest existence of a low endemic state (non-aggressive) and a higher endemic (aggressive state). At a low

cancer state, patients can live for a longer period of time with the cancer. However, initiation of HIV treatment in patients with NHL is observed to reduce the cancer cell density to lower endemic states and this might explain why some of the HIV-infected patients can live with cancer for many years. Highly active antiretroviral therapy (HAART) used for HIV treatment is a combination therapy ("cocktail" of drugs), that includes reverse transcriptase inhibitor (RTI) and protease inhibitor (PI) in different proportions; it is more effective in treating HIV than a single drug therapy. In many communities in sub-Saharan Africa, HAART is available but not anti cancer drugs. We explore how effective the combination therapy in HIV associated cancer is in reducing cancer growth. Our model simulations show how to best choose the proportions of RTI and PI in order to maintain an acceptable level of CD⁺4 T cells and, at the same time, reduce the growth of cancer cells as much as possible. The results obtained also give an estimate of the efficacies of the drugs in the HAART regimen given to people living with HIV. In addition, the results also explain why late initiation of HIV treatment might not be helpful to cancer patients. Furthermore, in case of chemotherapeutic intervention, our results might explain why a few of these chemotherapeutic drugs are more effective when given at a slow continuous rate. The models present some interesting research outcomes on treatment of HIV related cancers that can influence their treatment and management.

Opsomming

Modellering van die rol van MIV in die behandeling van Hodgkin limfoom groei dinamika

(“*Modelling the role of HIV and its treatment in non-Hodgkin lymphoma growth dynamics* ”)

Rosemary Akinyi Aogo

*Departement Wiskundige Wetenskappe,
Universiteit van Stellenbosch,
Privaatsak X1, Matieland 7602, Suid Afrika.*

Tesis: MSc. (Wiskunde)

Desember 2015

MIV/VIGS-verwante kankers is kankers wie se voorkoms in MIV/VIGS pasiënte baie groter is as in die algemene bevolking. MIV, as een van die kroniese infeksies, vereis kroniese antigeniese stimulus deur aanhoudende self- of vreemde antigene. Hierdie stimulus aktiveer B-selle en gee aanleiding tot hul onbeheerbare groei.

Die saambestaan van kanker en MIV, beide *in vivo* en *in vitro*, in ‘n kanker- immuunomgewing lei tot die produsering van spesifieke sitokiene deur verskeie immunselle en die kancerselle. In hierdie tesis ontwikkel ons ‘n wiskundige model wat die kanker-immuunstelsel se interaksie in die teenwoordigheid van MIV en MIV behandelings toon. Ons fokus, in die besonder, op die mees algemene kanker in MIV pasiënte: nie-Hodgkin se limfoom (NHL). Die geformuleerde model, wat nie-lineere gewone differensiaalvergelykings beskryf, toon die bestaan van verskeie ewewigte wie se stabiliteit en bifurkasie analise verskaf word. Ons resultate dui daarop bestaan te āNâNvan ‘n lae endemiese staat (nie- aggressiewe) en ‘n

hoër endemies (aggressiewe staat) . Op 'n lae kanker toestand is, kan pasiënte leef vir 'n langer tydperk van die tyd met die kanker. Dit word egter waargeneem in pasiënte met NHL dat die begin van MIV- behandeling hierdie lae epidemiese state van die kancerselle verminder.

Hoogs aktiewe antiretrovirale terapie (HAART) wat gebruik word vir MIV behandeling is 'n kombinasie terapie ("cocktail" van geneesmiddels) wat omgekeerde transkriptase inhibeerder (RTI) en protease-inhibeerder (PI) in verskeie proporsies insluit; dit is meer effektief in die behandeling van MIV as 'n enkele geneesmiddelterapie. In baie van die gemeenskappe in sub-Saharan Afrika is HAART, eerder as antie-kanker geneesmiddels, beskikbaar.

Ons ondersoek hoe effektief die kombinasie terapie in HIV-verwante kankers is om kankergroei te verminder. Ons modelsimulasies toon hoe om die beste proporsie van RTI en PI te kies om 'n aanvaarbare vlak van CD⁺4 selle te handhaaf, en ter selfde tyd, die groei van kancerselle soveel as moontlik te verminder. Die resultate toon ook 'n beraming van die effektiwiteit van die geneesmiddels in die HAART prosedure wat gegee word aan die wat MIV het. Ook verduidelik die resultate hoe kom die MIV behandeling nie so nuttig onder kankerpasiënte, wat die behandeling laat begin, is nie. Bykomend, in die geval van chemoterapeutiese intervensie, mag ons resultate verduidelik hoekom sommige van die chemoterapeutiese geneesmiddelle meer effektief is wanneer dit teen 'n stadige deurlopende tempo verskaf word. Die model toon interessante uitkomste van die navorsing oor die behandeling van MIV-verwante kankers wat hul behandeling en bestuur kan beïnvloed.

Acknowledgements

First and foremost I would like to thank the Almighty God for His infinite mercy upon me. His abundant blessings upon me has made me stronger each and every day throughout this entire research period. I owe it all to the Almighty; my stronghold.

Secondly, I would like to express my deep and profound gratitude to my academic supervisor, Prof. Farai Nyabadza for his patient guidance, effort, enthusiastic encouragement and useful critiques throughout the course of this research work. He has not only instilled in me more self-independence but also critical thinking amongst others. Prof. Nyabadza would encourage and make me laugh when I needed it the most. This kept me moving even at the verge of giving up. A big thank you Prof. I would also like to acknowledge with much appreciation the crucial role played by Prof. Avner Friedman of Mathematical Biology Institute at the Ohio State University. Your tireless support and the great zeal in helping me prepare a manuscript out of my thesis has not only improved my understanding of the research area but to a great extent my manuscript preparation skills.

My great appreciation to the Department of Mathematical Sciences, University of Stellenbosch and African Institute for Mathematical Science (AIMS) for their financial support during the study period.

Lastly, to my dad and siblings, their warm love and encouragement gave me strength to work harder and never give up at any moment. Thank you for believing in me. My friends and student colleagues, thank you so much for the encouragement and the fruitful discussions we had the entire time. I did learn quite a lot from you guys. Thank you.

God bless you all.

Dedications

This thesis is dedicated to my dad, Mr. Paul Aogo and my siblings for their unwavering love. To my late beloved mum, Jane Odhiambo Aogo and brother Erick Aogo for believing in me. You constantly reminded me that I was destined for greater things.

Publications

The publications presented below are extracts from my thesis. Both submitted to the Bulletin of Mathematical Biology. The manuscripts are appended at the end of the thesis.

- 1). Modelling the dynamics of HIV-related non-Hodgkin lymphomas in the presence of HIV treatment and chemotherapy (Manuscript under Review).
- 2). The effect of anti HIV drugs on HIV associated cancer (Manuscript under Review).

Contents

Declaration	i
Abstract	ii
Opsomming	iv
List of Figures	xii
List of Tables	xiv
1 Introduction	1
1.1 Cancers and HIV	1
1.2 Motivation	2
1.3 Objectives of the study	5
1.4 Project outline	5
2 Literature review	7
2.1 Cancer models	7
2.2 HIV-related non-Hodgkin's lymphoma epidemiology	11
2.3 Summary	15
3 HIV-related non-Hodgkin model with HIV treatment	16
3.1 Introduction	16
3.2 Mathematical model formulation	17
3.2.1 Model equations	20
3.3 Model analysis	23
3.3.1 The simplified model	23
3.3.2 Model properties	24

Contents

x

3.3.3 Steady states	30
3.4 Numerical simulations	34
3.4.1 Parameter estimation.	34
3.4.2 Sensitivity analysis	36
3.4.3 Numerical results	39
3.4.4 Bifurcation analysis	40
3.5 Conclusion	44
4 NHL model with HIV treatment and chemotherapy	46
4.1 Introduction	46
4.2 Model equations	47
4.3 Parameter estimation	48
4.4 Simulation results	50
4.4.1 Results with no chemotherapeutic drug	50
4.4.2 Results with chemotherapeutic drug	59
4.5 Conclusion	61
5 Discussions	63

List of references**i**

List of Figures

2.1	Source: Hashmi et al.[24]. Schematic diagram showing the interaction between the cellular populations of the cancer cells,Natural Killer cells and Effector cells cultured with chemo-immunotherapy and Interleukin IL-2 under the impact of Immunodeficiency Viruses. We have used the bold lines with square head arrows to represent inhibition or killing of the cells by either the chemotherapy or the effector cells incase of the tumor. The arrow heads have been used to represent cell activation.	9
2.2	Transmission dynamics of HIV-related NH Lymphoma.	13
3.1	Schematic representation of interactions of cells and cytokines in HIV-NH Lymphoma. We have macrophages M_1, M_2 , T-cells (immune cells) T_4, T_4^i, T_8 , cytokines ($T_\beta, I_6, I_{10}, I_{12}, I_2$), the cancer cells, C and HIV, V . The pool of viruses V , through infection, affects the movement of the healthy CD4 $^+$ T cells, T_4 into the infected CD4 $^+$ T cells, T_4^i compartment. We have used the dotted lines with arrow heads to represent cytokine production, and cell activation and with square head to represent inhibition. The bold lines with arrow head represent induction, transition or activation, and with square head represents killing.	17
3.2	Partial Rank scatter plots of the ranks for the cancer cell count, C and each of the sampled input parameters with significant PRCCs using the values in Table 3.3 and 1000 simulations per run.	37
3.3	Partial Rank scatter plots of the ranks for the cancer cell count, C and each of the sampled input parameters with significant PRCCs using the values in Table 3.3 and 1000 simulations per run.	38

3.4	The $g(C)$ as a function of C with different values of β_3 (rate of cancer loss in the population) with other parameters as in Table 3.3 and the other variables at their steady states. No chemotherapy treatment initiated.	39
3.5	Bifurcation diagram: Non-trivial solutions of $g(C^*) = 0$ as a function of β_3 with the rest of parameters as in Table 3.3 with the other variables at their steady states.	41
3.6	Population dynamics of the cancer cells in model system (4.2.1) with the parameters as in Table 3.3. Initial conditions: $M_1(0) = 40000$ cells/ml, $M_2(0) = 10000$ cells/ml, $T_4(0) = 5 \times 10^5$ cells/ml, $T_4^i(0) = 0$ cells/ml, $V(0) = 1000$ copies/mL, $T_8(0) = 100$ cells/ml and $C(0) = 100$ cells/ml.	42
3.7	Population dynamics of the cancer cells in model system (4.2.1) with only HAART therapy, with $\zeta_r = \zeta_p = 0.5$ and the rest of the parameters as in Table 3.3. Initial conditions: $M_1(0) = 400000$ cells/ml, $M_2(0) = 100000$ cells/ml, $T_4(0) = 5 \times 10^5$ cells/ml, $T_4^i(0) = 0$ cells/ml, $V(0) = 1000$ copies/mL, $T_8(0) = 100$ cells/ml and $C(0) = 100$ cells/ml.	43
3.8	Numerical simulation of model system (4.2.1) for the evolution of the CD8 ⁺ T cells (effector cells) with RTIs and PIs treatment of efficacies, $\zeta_r = \zeta_p = 0.5$ and the rest of the parameters as in Table 3.3. Initial conditions: $M_1(0) = 400000$ cells/ml, $M_2(0) = 100000$ cells/ml, $T_4(0) = 5 \times 10^5$ cells/ml, $T_4^i(0) = 0$ cells/ml, $V(0) = 1000$ copies/mL, $T_8(0) = 100$ cells/ml and $C(0) = 100$ cells/ml.	43
4.1	Combination therapy Map: $C(t)$ as a function of RTIs (ζ_r) and PIs (ζ_p) combination with the rest of parameters as defined in Table 3.3. The color bar shows the $C(t)$ values for various drug combination.	51
4.2	Cancer reduction curves after various time, t with the rest of the parameters as in Table 3.3. The dots correspond to the cancer load at each anti-virus drug combination, with $\zeta_r = \zeta_p$	52
4.3	Evolution of cancer cells in system (3.3.1) over 2000 days with the rest of the parameters as defined in Table 3.3.	52
4.4	Combination therapy map: $T_4(t)$, for $t=350, 1000$ and 2000 days as a function of RTI (ζ_r) and PI (ζ_p) combination, the parameters are as in Table 3.3. The color bar shows the $T_4(t)$ values for various drug combination.	54

4.5 Combination therapy map: $T_4(t)$, for t=1000 days with no cancer in the host population as a function of RTI (ζ_r) and PI (ζ_p) combination, the parameters are as in Table 3.3. The color bar shows the $T_4(t)$ values for various drug combination.	54
4.6 Cancer cell density curve, $C(\zeta_r)$ at $t = 1000$ days, for each pair $(\zeta_r, h(\zeta_r))$, the parameters are as in Table 3.3.	55
4.7 Population dynamics of T helper cells (cells/ml) over a period of 2000 days for the case of no cancer in the host immune system, i.e $C = 0$. The rest of the parameters as defined in Table 3.3. The inset plots show the T helper cells dynamics over 20 days.	57
4.8 Population dynamics of T helper cells (cells/ml) with cancer in the host immune system over 2000 days with the rest of the parameters as defined in Table 3.3. The inset plots show the T helper cells dynamics over 20 days.	58
4.9 Chemotherapeutic drug dose concentration in the system administered 1 day every 21 days for 200 days i.e 9 doses every 21 days.	59
4.10 Population dynamics for a period of 200 days of the cancer cells in model system (4.2.1) with both therapies (HAART and chemotherapy) with parameters as in Table (3.3). Initial conditions: $M_1(0) = 2000$ cells/ml, $M_2(0) = 2500$ cells/ml, $T_4(0) = 3 \times 10^5$ cells/ml, $T_4^i(0) = 1 \times 10^3$ cells/ml, $V(0) = 4 \times 10^3$ copies/mL, $T_8(0) = 3000$ cells/ml.	60

List of Tables

1.1	Source:Moosa Patel.[42]. Patients with non-Hodgkin's Lymphoma at Chris Hani Baragwanath Academic Hospital, Johannesburg, South Africa from 1993-2008	2
1.2	Source: Mwamba et al. [43]. A summary of clinical data on the treatment of AIDS-related non-Hodgkins lymphoma (AR-NHL) in sub-Saharan Africa. The abbreviations used: CWRU: Case Western Reserve University, and ACTG: AIDS Clinical Trials Group; Nos. Pts.: number patients; ORR: objective response rate; (CR/PR): complete response/partial response; MST: median survival time, 1-yr : 1-year survival rate and OS: overall survival; and cART: combination antiretroviral therapy.	4
3.1	Variables and their units	18
3.2	Symbols, description and units of the parameters used in the model. . .	19
3.3	Parameter values used in the numerical simulations and sensitivity analysis.	35
4.1	Estimated Parameter values.	49

Chapter 1

Introduction

1.1 Cancers and HIV

AIDS was first described in 1981 and the first definitions included certain opportunistic infections, kaposi sarcoma and central nervous system (CNS) lymphoma. In 1984, a multicenter study described the clinical spectrum of non-Hodgkin's lymphomas in the populations at risk for AIDS [1]. Going forward, the Centers for Disease Control and Prevention (CDC) in 1985 and 1987 revised the AIDS definition to include the human immunodeficiency virus (HIV)-infected patients who had aggressive B-cell non-Hodgkin's lymphomas (NHL) [1]. While HIV infection leads to AIDS, complications of HIV for instance, opportunistic infections, cancers amongst others are being experienced by people living with HIV [24].

The majority of cancers affecting HIV-positive people are Kaposi sarcoma (KS), non-Hodgkin's lymphoma (NHL) and invasive cervical cancer [44]. Other types of cancer which occur somewhat more frequently in HIV/AIDS patients include anal cancer [44], lung cancer [41, 44], and colorectal cancer [15]. KS is an indolent cancer, involving multiple tumor of the lymph nodes or skin, and occurring mainly in people with depressed immune system. It occurs in less than 3 in 100,000 people in the USA. Cervical cancer is caused by several types of virus, the most common is human papillomavirus (HPV). Incidence of NHL has increased in an almost parallel course with the AIDS epidemic and accounts for 2% to 3% of the newly diagnosed AIDS cases [1]. Patients with HIV infection are noted to develop lymphomas about 100 times more often and Kaposi's sarcoma about 400 times more often than non-

infected individuals [49].

Lymphomas are cancers that begin in the immune cells and are divided into two main types: Hodgkins lymphomas (HLs) and non-Hodgkins lymphomas (NHLs). HLs are named after Dr.Thomas Hodgkins who first described them and are marked by Reed-Sternberg cells [3] whereas NHLs are the large and diverse group of cancers of the immune cells. NHLs start in the lymphocytes and are characterised as either slow-growing, that is the non-aggressive or fast-growing (aggressive) and are noted to be more common than the HLs.

1.2 Motivation

AIDS-related non-Hodgkin's lymphomas (AIDS-NHLs) are the cause of death in approximately 16% of HIV-infected individuals [16, 37, 52]. The non-Hodgkin's lymphoma (NHL) facts shows that about 71,000 patients will be diagnosed with NHL in 2015, and approximately 19,500 patients will die in the United States [3]. This implies that the disease continues to be a threat despite the advances in highly active antiretroviral therapy (HAART) [11, 17, 43, 48], since the most common type includes the diffuse large B-cell lymphoma which mostly occur due to HIV infection.

Year	Total No. of Patients	No. of HIV-seropositive Patients	No. of HIV-seronegative Patients	Percentage (%) of HIV Positive with NHL
1993	20	19	1	5
1994	20	18	2	10
1995	18	15	3	16.7
1996	28	25	3	10.7
1997	18	14	4	22.2
1998	34	18	16	47.1
1999	22	14	8	36.4
2000	30	16	14	46.7
2001	24	4	20	83.3
2002	40	15	25	62.5
2003	44	17	27	61.4
2004	58	23	351	60.3
2005	54	15	39	72.2
2006	72	17	55	76.4
2007	72	19	53	73.6
2008	76	10	66	86.8

Table 1.1: Source:Moosa Patel.[42]. Patients with non-Hodgkin's Lymphoma at Chris Hani Baragwanath Academic Hospital, Johannesburg, South Africa from 1993-2008

Clinical studies, that is, experimental and computational biological studies have documented a lot of findings in relation to these specific lymphomas as their eti-

ology and pathogenesis is well documented. On the other hand, mathematical models that provide an alternative way to study the growth of cancer both HIV-related and non-HIV related have been precisely developed and the findings have provided the oncologists with solutions to cancer problems. Despite these findings from the mathematical models linking experimental to computational biology, people living with HIV continue to be at a significantly increased risk for intermediate- and high-grade B-cell non-Hodgkin lymphoma. This still occurs in the era of advances in highly active antiretroviral therapy (HAART) [11].

More than a third of HIV-infected individuals residing in sub-Saharan Africa eligible for antiretroviral therapy (ART) receive combined ART [43]. Despite the increased roll-out of combined antiretroviral therapy, a meaningful decrease in the incidence of AIDS-associated malignancies is yet to be realised [43]. In many poor communities around the world where anti-HIV drugs are nevertheless available, anti-cancer treatment is almost non-existent. For example, the estimates regarding access to or coverage of the cytotoxic chemotherapy in sub-Saharan Africa are largely unknown and neither are they published [43]. The study by Gopal et al. also indicates that, treatment of haematologic malignancy for instance the HIV-related NHL in the developed countries is increasingly associated with unparalleled rates of long-term control and survival. Contrarily, in sub-Saharan Africa, the mechanisms for diagnosis, treatment and palliating of this disease are still inadequate [17]. Out of the 54 sub-Saharan Africa countries, only 21 have operational radiotherapy service units and map showing the distribution of these services is highlighted in [17]. Securing chemotherapies by the sub-Saharan African governments due to the limitation in their supply may be less practicable as they compete with developed countries. This may lead to drug shortages for lymphoma treatment in these regions [17].

The delay and misdiagnosis of lymphoma, more specifically the diffuse large B-cell NHL in HIV patients, remains a major problem in South Africa [48]. Cancer, is often misdiagnosed as tuberculosis and this implies that patients living with HIV and HIV-related NHL are only introduced to HAART, instead of receiving the anti-cancer drugs. A summary of data collected by Puvaneswara et al.[48] on some patients in the mentioned community is shown in Table 1.

Chapter 1. Introduction**4**

Regimen (Study/Year) Reference	Nos. Pts.	ORR(CR/PR)	Survival	Comments
Dose-modified oral chemo.(CWRU 2498/2009)[29]	49	78% (CR 58% PR 30%)	MST 12.3 months. (33% 1-yr)	Only published prospective treatment trial of AR-NHL in sub-Saharan Africa; conducted comparable HIV therapeutic era as ACTG 142 trial [45]; 6% treatment mortality rate
Uganda Cancer Institute (NHL study/2011)[35]	154 (32% HIV+)	No response data provided or types of chemotherapy	MST 61 days (13% 1-yr)	Largest retrospective study on NHL including HIV(-) and HIV(+) case ever reported with treatment and outcome data. Only 60% had acceptable clinical staging
Stellenbosch University[19]	512 (4 HIV+)	Overall CR range 46-75% for all sub-types; chemotherapy regimens not reported	MST 10 months (50% 1-yr)	Comprehensive retrospective study of spectrum lymphoproliferative disorders at a major private referral centre in Cape Town. Only 4 cases (<1% were HIV(+)) MST is for the 4 AR-NHL cases

Table 1.2: Source: Mwamba et al. [43]. A summary of clinical data on the treatment of AIDS-related non-Hodgkins lymphoma (AR-NHL) in sub-Saharan Africa. The abbreviations used: CWRU: Case Western Reserve University, and ACTG: AIDS Clinical Trials Group; Nos. Pts.: number patients; ORR: objective response rate; (CR/PR): complete response/partial response; MST: median survival time, 1-yr : 1-year survival rate and OS: overall survival; and cART: combination antiretroviral therapy.

In view of the inadequate supply of chemotherapeutic drugs and radiotherapy equipments as well as increased incidences of NHL misdiagnosis and lack of trained personnel in Sub-Saharan Africa [17, 43, 48], there is dire need to understand the role played by HIV and its treatment with the HAART in the dynamics of the AIDS-related NHLs due to the increased roll-out of the HAART in these regions. More precisely, we address the question that arises; Can RTIs and PIs be combined in a way that will reduce the cancer (NHL) load, while maintaining acceptable level of CD4⁺ T cells? We also seek to understand the role of T cells in killing the cancer cell, since in HIV infected individuals, the reduced number of T cells exacerbates cancer growth.

1.3 Objectives of the study

The main objective of this study is therefore, to use mathematical models to investigate the dynamics of HIV-related non-Hodgkin's lymphoma in the presence of HIV and HIV treatment. In order to achieve this, we develop a mathematical model that investigates the relationship between cancer growth, host tissues and the immune system components in the presence of HIV. More precisely, we aim;

- i. To describe the NHL-immune system interactions through a conglomerate of cytokines in the presence of HIV and its treatment.
- ii. To formulate a workable mathematical model for the process with the inclusion of anti-HIV drugs in the model.
- iii. To carry out a detailed mathematical analysis both analytically and numerically and establish the existence of cancer-free and cancer-persistence states.
- iv. To extend the model to include the anti-cancer drugs that is, chemotherapy.
- v. To investigate the effects of combined use of reverse transcriptase inhibitors (RTIs) and protease inhibitors (PIs) in the highly active antiretroviral therapy (HAART) regimen on cancer cell density through numerical analysis.
- vi. To investigate the effects of the chemotherapeutic treatment on the HIV-related NHL dynamics through numerical analysis.

The rest of the thesis is therefore organized as described in the following section.

1.4 Project outline

We explore the biology of HIV-related non-Hodgkin's lymphoma and review relevant mathematical models which include cancer-immune system interactions models and HIV-related cancer-immune system interactions models in Chapter 2. In Chapter 3 we present the main model for the role of HIV and its treatment on the dynamics of HIV-related non-Hodgkin's lymphoma. The model is formulated and analysed in this chapter where the numerical simulations and deductions from the

Chapter 1. Introduction

6

results obtained are also presented. We focus on the stability and bifurcation analysis to establish the existence of the equilibria and to understand the behaviour of the model formulated in the study. We extend the model to include chemotherapy as a cancer treatment in Chapter 4. Here, we explore the effect of the two types of drugs (RTIs and PIs) combination on the HIV-related NHL load and the effects of chemotherapeutic drugs as well. We present our numerical simulations and discussions of the results for the extended model in this chapter. In Chapter 5, we conclude the study with discussions and pertinent recommendations.

Chapter 2

Literature review

In order to develop a cancer mathematical model, knowledge in two different areas is ineluctable; understanding of the relevant biological phenomena and the response processes involved in the cancer growth and the appropriate mathematical tools employed in order to obtain logical qualitative and quantitative predictive results. We thus review some previously studied cancer mathematical models as a basis to our work and afterwards, explore the biology of the HIV-related non-Hodgkin lymphomas with the inclusion of HIV treatment with highly active antiretroviral therapy (HAART).

2.1 Cancer models

Various research in the field of mathematical biology have considered the dynamics of cancer-immune interactions in the presence of HIV for the HIV-related malignancies both at population level and cell level (inhost). Similar studies have been done for other types of malignancies (non-HIV related). We will therefore, consider a few of these studies so far done as a preliminary to our work.

The first mathematical model for cancer dynamics was studied by De Boer and his colleagues [9], where they modeled the anti-cancer immune response under the impact of external cytokine IL-2 that is, exogenous IL-2 in the form of ordinary differential equations. They deduced from their work that early T helper activity highly increases the magnitude of immune response and the cytotoxic effector cells responsible for tumor eradication is dependent on tumor-antigenicity. Kirsch et al. [33]

went ahead to model similar cellular interactions considering both the naturally produced (endogenous) and the exogenous IL-2. Following were L.G. de Pillis and his colleagues [38] who included the chemotherapeutic effect. They formulated a model cultured with chemo-immunotherapy under the influence of exogenous and endogenous IL-2. Their results showed that the more effectively CD8 T cells taken from peripheral blood kill tumour cells, the more useful immunotherapy may be in conjunction with chemotherapy [38].

Hashmi et al. [24], further developed a mathematical model for cancer regression by incorporating cancer cells, effector cells, natural cell populations cultured with chemotherapy and IL-2 under the influence of immunodeficiency virus. The model developed by Hashmi and his colleagues is represented in Figure 2.1 and system (2.1.1) represents the dynamical equations developed. Though, no numerical justification was given by the researchers, their theoretical interpretation showed that the analysis of their model with the inclusion of the treatment as explained may give better cancer regression efficiency that is, has potential to reduce cancer.

$$\left. \begin{array}{l} \frac{dT}{dt} = r_1 T(1 - bT) - \frac{aET}{g_2 + T} - K_T(1 - e^{-\xi M})T, \\ \frac{dN}{dt} = r_2 N(1 - eN) + kT \left(1 - \frac{T}{T^c}\right) - K_N(1 - e^{-\xi M})N, \\ \frac{dE}{dt} = cT - \mu_1 E + \frac{p_1 EI}{g_1 + I} - \alpha VE - K_E(1 - e^{-\xi M})E, \\ \frac{dI}{dt} = \frac{p_2 TE}{g_E + T} - \mu_2 I, \\ \frac{dV}{dt} = \frac{fV}{h + V} - \beta VE - \mu_3 V, \\ \frac{dM}{dt} = -\gamma M + V_M(t). \end{array} \right\} \quad (2.1.1)$$

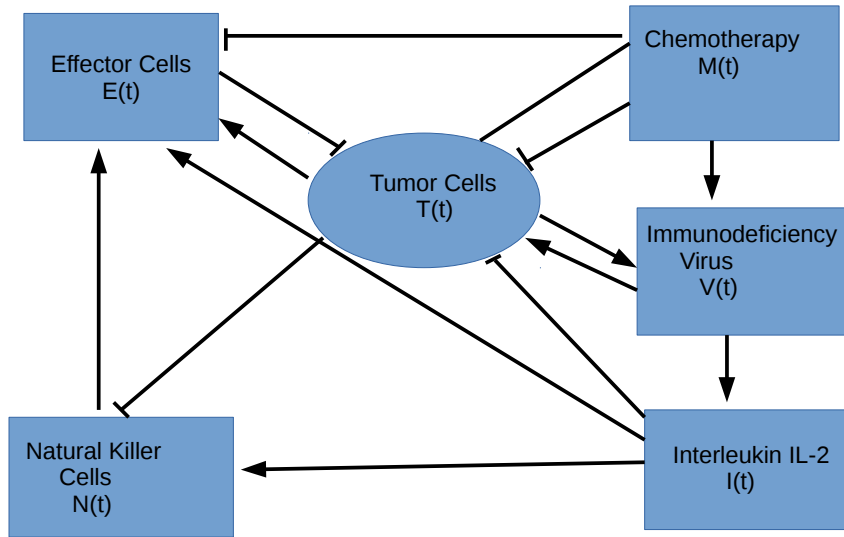


Figure 2.1: Source: Hashmi et al.[24]. Schematic diagram showing the interaction between the cellular populations of the cancer cells,Natural Killer cells and Effector cells cultured with chemo-immunotherapy and Interleukin IL-2 under the impact of Immunodeficiency Viruses. We have used the bold lines with square head arrows to represent inhibition or killing of the cells by either the chemotherapy or the effector cells incase of the tumor. The arrow heads have been used to represent cell activation.

Fathala et al. [49] on the other hand, introduced ODE and DDE models which described the tumor-immune system interactions *in vivo* in the presence of CD4⁺ T cells HIV infection. In their study, they considered the following populations; tumor cells, healthy CD4⁺ T cells, infected effector cells and the free viral particles.

Arciero et al. [5] later developed a model which consisted of a system of ODE's that describe the interactions between tumor cells, immune cells and the cytokines IL-2 and TGF- β . They described in their work, the essence of TGF- β in stimulation of

tumor growth and suppressing of immune system by inhibiting the activation of effector cells. Their results further showed how treatment with small interfering RNA (siRNA) is able to suppress the tumor by returning it to passive (non-aggressive state) that might not evade immune surveillance under some conditions.

Louzon et. al.[39] recently developed and discussed a model describing the pancreatic cancer-immune system interaction. They studied the profile of cancer growth and how different treatments considered in their work affect the cancer growth. Their study comprised of populations viz: cancer cells, immune system for instance, macrophages and the CTLs, and cytokines. Their results showed that the treatments aimed at suppressing cancer growth are only effective if the immune induced death lies within a specific range. This implies that, the parameter representing the immune response plays an important role in control of cancer growth. This analysis might be of great importance to the medical sector since it implies that bringing the parameter to some value may not be enough since we will still have the existence of both aggressive state and non-aggressive state. The parameter must thus be increased upto some value to ensure existence of non-aggressive cancer or no cancer cells in the system.

In this dissertation, we are motivated by the work in [39], in describing a model aimed at studying the role played by HIV and its treatment in the growth of NHLs.

Most of the research have always focused on modelling either cancer dynamics in a host immune system, HIV dynamics or the interaction of the cancer cells with the immune system in the presence of HIV *in vivo* [33, 49, 61] however, most importantly none of these studies to the best of our knowledge have incorporated all the cytokines present in the tumor microenvironment in an HIV-tumor coinfection scenario at individual level (*in vivo*). We will therefore, consider a combination of cytokines (which are other factors that might contribute to the occurrence of tumor) in modelling the role of HIV in the NHL growth. In our study, we consider the macrophages (pro-inflammatory, M_1 and anti-inflammatory, M_2), T cells (healthy $CD4^+$ T cells, HIV-infected $CD4^+$ T cells and $CD8^+$ T cells), the virus and cancer cells. The cells interact with each other through a conglomerate of cytokines.

We will investigate how these interactions (described in the following section) affect the growth of the cancer with and without the inclusion of anti-HIV and anti-cancer therapies most importantly the HAART and to some extent chemotherapy.

2.2 HIV-related non-Hodgkin's lymphoma epidemiology

The hallmark of Human immunodeficiency virus (HIV) is deficiency in CD4⁺ T cells, caused by the virus which infects them and causes their destruction. The disease is characterised as acquired immunodeficiency syndrome (AIDS) when the number of T cells falls from about 700000 in ml of blood to 200000. Since CD4⁺ T cells are an important component of the immune defense against diseases and in particular against cancer, people with advanced stage of HIV are at risk of developing cancer. This has been particularly observed in the case of non-Hodgkin Lymphoma (NHL) [26, 42, 56].

Lymphomas are generally white blood cells (T-cell or B-cell lymphocytes) that become abnormal i.e mutate and begin to divide uncontrollably, interfering with the body's production of healthy blood cells and ability to fight off infections and other diseases [28].

AIDS-related NHL, a blood disease which is characterised by abnormal growth of mutated lymphocytes are consistently derived from B-cells and are characterized by extreme aggressiveness. Gu Yian [21] noted that chronic infections for instance, HIV involve chronic antigenic stimulation by persistent self-antigens or foreign antigens; this stimulation activates B cells and induces their uncontrollable growth. Non-Hodgkin's lymphomas are classified as: AIDS-related Burkitt's lymphoma (AIDS-BL), AIDS-related diffuse large cell lymphoma (AIDS-DLCL) and AIDS-related primary effusion lymphoma (AIDS-PEL) [14].

The abnormal growth of these cells is a series of events that involves a heterogeneous assembly of cells and the immune response to the cancer growth exist in cancer-bearing hosts. Cancers often induce dysfunction in the response mechanisms by impairing the regulatory networks driven by cytokines. Cytokines are regulatory molecules that are secreted by various cell types for the regulation of immune response to infection. They are messenger molecules that cells use to communicate. The ones that play a crucial role in the pathological processes of cancers are classified as interleukins (ILs), tumor necrosis factors (TNFs), transforming growth factors (TGFs), interferons (IFNs) and colony-stimulating factors (CSFs) [27]. Cytokines influence the biology of cancers either by promoting cancer growth

or impairing anticancer responses [13]. There is a disruption of normal cytokine regulatory networks in the presence of immune suppression. This often leads to altered immune responses and can contribute to the development of malignant outgrowths [46].

Research into the cytokines expressed in AIDS- related lymphomas has shown elevated serum levels of IL-6 and IL-10 in HIV infected individuals [13, 14, 47]. Human tumor microenvironment includes macrophages and these tumor associated macrophages (TAMs) are phenotypically classified as M_1 and M_2 [18, 25]. M_1 macrophages are the macrophages that have undergone cell activation in response to interferon (IFN) while the M_2 are those that have undergone activation in response to IL-4. The M_1 macrophages are associated with acute inflammation and T-cell immunity and are characterized by the expression of high levels of pro- inflammatory cytokines. The M_2 macrophages are anti-inflammatory and are associated with the promotion of cancer growth [18, 25, 50]. TAMs can switch type between pro-inflammatory M_1 and anti-inflammatory M_2 in the tumor environment [25]. IL-6 has been identified as a key cytokine for the B-cell NHL's growth and survival [65]. As indicated in [32], TGF- β is likely to contribute to the deficit in T-cell surveillance. IL-6 and TGF- β induce polarization of M_2 into M_1 macrophages and promote an immunosuppressive environment [65]. One of the most important features of M_1 macrophages is the production of a T-cell stimulating cytokine IL-12 which enhances natural killer cell activities by activation of CD8 $^+$ effector T cells [62]. M_2 macrophages produce IL-10 cytokines which down regulates the activities of IL-12, and thus inhibits the activation of T cells by IL-12 [6, 19, 59]. It has also been shown that IL-12 induces IL-10 production as a negative feedback for IL-12-induced immune response [58, 59]. Interleukin 2 (IL-2) is a cytokine signaling molecule in the immune system naturally produced mainly by the CD4 T-cells. IL-2 may be administered from external sources that is, exogenous IL-2 while the naturally produced ones are the endogenous. Our study focusses on the endogenous IL-2. CD4 $^+$ T cells produce the cytokine IL-2 which induces growth, proliferation and activation of both CD4 $^+$ T cells and CD8 $^+$ T cells. CD8 $^+$ T cells are also called cytotoxic cells (CTL) and they are directly involved in killing cancer cells [36]. The CD8 effector cells are also responsible for the production of chemokines which inhibit the infection of the macrophages by the virus [4].

The greatest risk factor for the development of NHL is immune deficiency. Infec-

tion by HIV, is typified by a marked deficiency of $CD4^+$ T cells and a persistent stimulation of B cells [20], therefore NHL risk in people with HIV infection is high. More than 90% of HIV-associated NHLs are derived from B cells, and the majority are high-grade and extranodal [20]. We thus focus on the NHL derived from B cells. We schematically represent the process described above in Figure 2.2.

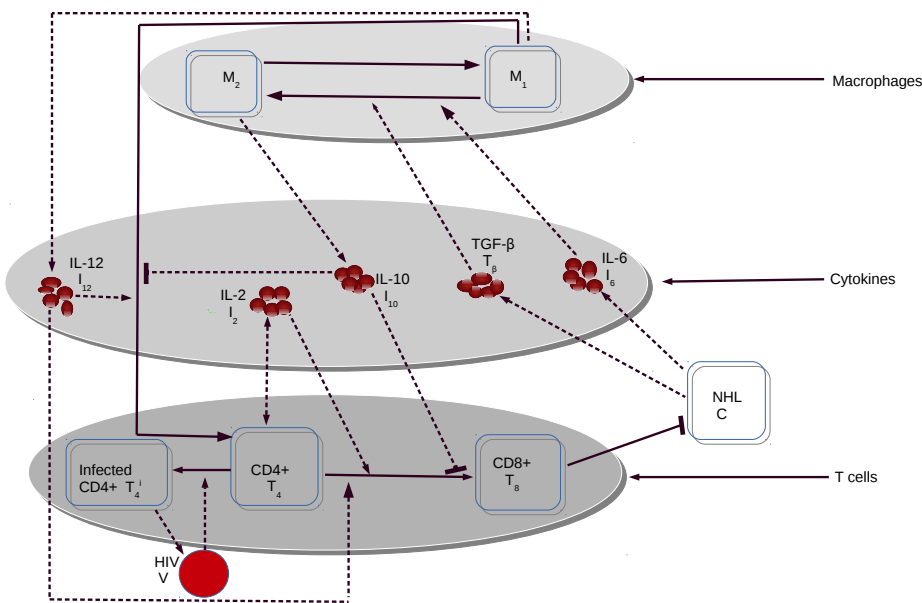


Figure 2.2: Transmission dynamics of HIV-related NH Lymphoma.

As HIV progresses to AIDS (latest stage of HIV), a major concern is the number of $CD4^+$ T cells due to the destructive effect of the HIV on these cells. They are the primary virus target and their depletion is of concern since immunodeficiency arises primarily as a result of the depletion. In HIV-infected patients, the extracellular virus infects the $CD4^+$ T cells and afterwards become productively infected and thus produce more virions whose presence in the host immune system has adverse effect on the elimination of the cancer since it is able to escape the immune 'surveillance'. The depletion of these cells is very vital in this study since it results in an immunosuppressive environment.

An individual with HIV who develops cancer, should be treated both for cancer and HIV. Highly active antiretroviral therapy (HAART) is the most effective anti HIV drug that have long been used to curb HIV infection (by reducing viral load and hence reduction in the depletion of CD4⁺ T cells). Since we are dealing with an HIV-related cancer, considering the HAART is important. We therefore consider in this study, the treatment of HIV with HAART which has at least two different antiretroviral drugs (ARVs) i.e. nucleotide reverse transcriptase inhibitors (NRTIs) and one non-nucleotide reverse transcriptase inhibitors (NNRTIs) or a protease inhibitor (PI). The reverse transcriptase inhibitor (RTI) and protease inhibitor (PI) drugs are therefore the important components of HAART for the treatment of AIDS. RTI works by blocking the reverse transcription of viral DNA and can therefore effectively prevent the target cell from becoming productively infected by the free virus. It is worth noting that the inhibition process by RTI occurs after the virus has been attached to the cell and therefore the drug does not directly affect the infection rate of the target cells. On the other hand, PI drug blocks the action of HIV protease by preventing it from cleaving the viral polyprotein into functional sub units which ultimately prevent the formation of new copies of functional virus. Cancer treatment is discussed later in Chapter 4 where we extended the model.

2.3 Summary

In this chapter we have reviewed some selected cancer models as a basis of our work and looked into the biology of cancer-immune system interactions of HIV-related NHL. To this point, we will therefore employ the biological phenomena and response processes involved in the non-Hodgkin's lymphoma growth and mathematical ideas discussed in this chapter to formulate our mathematical model in Chapter 3 that follows.

Chapter 3

HIV-related non-Hodgkin model with HIV treatment

3.1 Introduction

Considering the interactions of immune cells, cytokines, HIV and cancer cell (NHL) described in Chapter 2, we develop a mathematical model that describes the interaction incorporating treatment with the RTI and PI drugs; components of HAART. A mathematical model is a description of a system using mathematical language. Our model focuses on the role of T cells in killing the cancer cell, since in HIV infected individuals, the reduced number of T cells exacerbates cancer growth. We then show that the model is positively invariant, hence, both mathematically and biologically well posed and afterwards carry out mathematical analysis. We accomplish this by determining the steady states and numerically determine the stability of the steady states (both cancer-free and cancer-persistent). Recent studies for instance, the study by Louzon et al. [39] on pancreatic cancer show that the parameter representing immune-cancer cell induced death i.e responsible for the immune response play an important role in mathematical modelling of cancer since it influences the dynamics of the cancer states. We will therefore investigate the role played by this parameter in our model in the presence of HAART and without the HAART by numerically carrying out bifurcation analysis with this specific parameter as our bifurcation parameter. We will focus on the stability and bifurcation analysis to establish the existence of the equilibria and to understand the behaviour

of the model formulated in the study. We also carry out sensitivity analysis on our model parameters to find out the effects of these parameters on the cancer dynamics.

3.2 Mathematical model formulation

We first postulate a mathematical model driven by the following variables: tumor associated macrophages (pro-inflammatory M_1 and anti-inflammatory M_2), T cells (healthy $CD4^+$ T cells, infected $CD4^+$ T cells, and $CD8^+$ T cells), HIV virus, V and the cancer cells, C . The mathematical model is based on the network described in Figure 3.1.

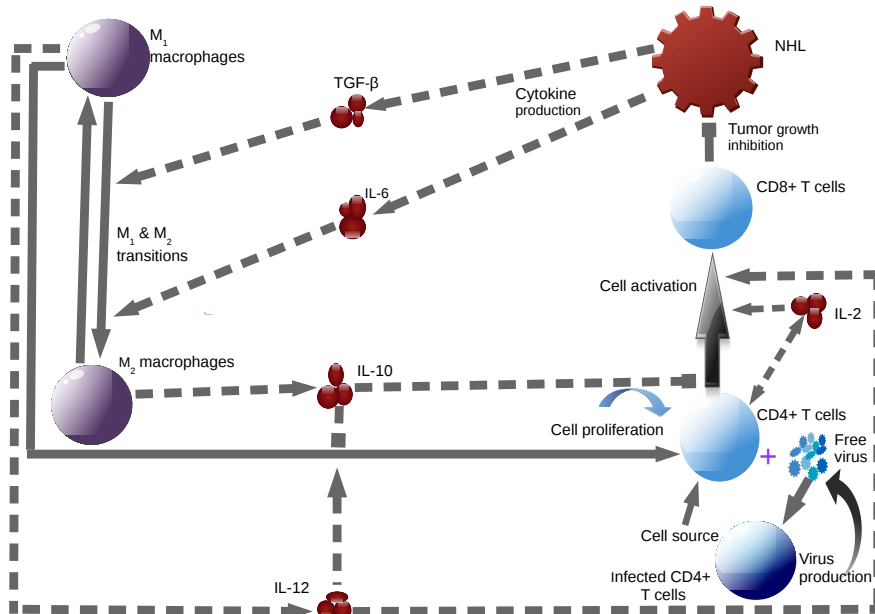


Figure 3.1: Schematic representation of interactions of cells and cytokines in HIV-NHL Lymphoma. We have macrophages M_1, M_2 , T-cells (immune cells) T_4, T_4^i, T_8 , cytokines ($T_\beta, I_6, I_{10}, I_{12}, I_2$), the cancer cells, C and HIV, V . The pool of viruses V , through infection, affects the movement of the healthy $CD4^+$ T cells, T_4 into the infected $CD4^+$ T cells, T_4^i compartment. We have used the dotted lines with arrow heads to represent cytokine production, and cell activation and with square head to represent inhibition. The bold lines with arrow head represent induction, transition or activation, and with square head represents killing.

Chapter 3. HIV-related non-Hodgkin model with HIV treatment**18**

Table 3.1 lists the variables used in the model and the parameters used in formulating our model equations are summarised in Table 3.2.

Table 3.1: Variables and their units

Variable	Description	Units
M_1	density of pro-inflammatory tumor associated macrophages	cells/ml
M_2	density of anti-inflammatory tumor associated macrophages	cells/ml
T_4	density of healthy CD4 ⁺ T cells	cells/ml
T_4^i	density of virus-infected CD4 ⁺ T cells	cells/ml
V	density of extracellular HIV	virus/ml
T_8	density of CD8 ⁺ T cells	cells/ml
C	density of cancer cells	cells/ml
T_β	concentration of transforming growth factor (TGF- β)	pg/ml
I_6	concentration of interleukin 6 (IL-6)	pg/ml
I_{10}	concentration of interleukin 10 (IL-10)	pg/ml
I_{12}	concentration of interleukin 12 (IL-12)	pg/ml
I_2	concentration of interleukin 2 (IL-2)	pg/ml

Table 3.2: Symbols, description and units of the parameters used in the model.

Parameter	Description	Units
α_1	production rate of TNF- α due to cancers cells	pg/cell day
α_2	production rate of IL-2 due to CD4 $^{+}$ T cells	pg/cell day
α_6	production rate of IL-6 due to cancers cells	pg/cell day
α_{10}	production rate of IL-10 due to M_2	pg/cell day
α_{12}	production rate of IL-12 due to M_1	pg/cell day
d_1	degradation rate of TNF- α	day $^{-1}$
d_2	degradation rate of IL-2	day $^{-1}$
d_6	degradation rate of IL-6	day $^{-1}$
d_{10}	degradation rate of IL-10	day $^{-1}$
d_{12}	degradation rate of IL-12	day $^{-1}$
s_1	influx rate of M_1	day $^{-1}$
s_2	influx rate of M_2	day $^{-1}$
s_3	production of CD4 $^{+}$ T cells by the sources	day $^{-1}$
k_1	per capita death rate of M_1	day $^{-1}$
k_2	per capita death rate of M_2	day $^{-1}$
λ_1	transformation rate of M_1 by TNF- α	ml/pg day
λ_2	transformation rate of M_2 by IL-6	ml/pg day
ν	transition rate from M_2 to M_1	ml/pg day
β_1	activation rate of T cells by IL-12	pg/cell day
β_2	proliferation rate of T cells by IL-2	pg/cell day
β_3	loss of cancer cells	day $^{-1}$
K_2	saturation constant of proliferation by IL-2	pg/ml
K_{10}	saturation constant for anti-proliferation by IL-10	pg/ml
ϵ	modification parameter	
μ_1	per capita death rate of uninfected CD4 $^{+}$ T cells	day $^{-1}$
μ_2	infection rate of CD4 $^{+}$ T cells due to infiltration by free viruses	day $^{-1}$
μ_4	per capita death rate of CD8 $^{+}$ T cells	day $^{-1}$
μ_v	clearance rate (loss) of free viruses	day $^{-1}$
μ_5	per capita death rate of infected CD4 $^{+}$ T cells	day $^{-1}$
δ_2	lytic death rate of infected CD4 $^{+}$ T cells	day $^{-1}$
N	Virions produced during a lifetime by an infected CD4 $^{+}$ T cells	
r	cancer growth rate	day $^{-1}$
C_0	maximum cancer density	
ζ_r	measure of efficacy of reverse transcriptase inhibitor (RTI)	
ζ_p	measure of efficacy of protease inhibitor (PI)	

3.2.1 Model equations

We now present the model equations by the following system of non-linear ordinary differential equations (ODEs). We consider cytokines dynamics and the cells dynamics.

3.2.1.1 Cytokine equations

In model system (3.2.1), the ordinary differential equations track the dynamics of the cytokines, where the positive terms show the secretion of the cytokines by respective cells into the cancer environment while the negative terms indicate the natural decay of the cytokines which occurs in a short time-scale as opposed to the dynamics of the cell population. The secretion and decay rates of the cytokines depend on the size of the cells causing the change. This assumption follows from the study by Louzoun et al. [39].

$$\left. \begin{array}{l} \frac{dT_\beta}{dt} = \alpha_1 C - d_1 T_\beta, \\ \frac{dI_6}{dt} = \alpha_6 C - d_6 I_6, \\ \frac{dI_{10}}{dt} = \alpha_{10} M_2 - d_{10} I_{10}, \\ \frac{dI_{12}}{dt} = \alpha_{12} M_1 - d_{12} I_{12}, \\ \frac{dI_2}{dt} = \alpha_2 T_4 - d_2 I_2, \end{array} \right\} \quad (3.2.1)$$

T_β and I_6 are produced by cancer cells [14, 39, 52], I_{12} and I_{10} are produced primarily by M_1 and M_2 macrophages [39, 58, 59] and I_2 is produced by T_4 cells [36]. Parameters, α_i represent the production rates by the respective cells, whereas d_i are the respective cytokine decay rates.

3.2.1.2 Immune cell equations

The dynamics of macrophages are given by the following equations

$$\frac{dM_1}{dt} = s_1 - k_1 M_1 + \nu M_2 - (\lambda_1 T_\beta + \lambda_2 I_6) M_1, \quad (3.2.2)$$

$$\frac{dM_2}{dt} = s_2 + (\lambda_1 T_\beta + \lambda_2 I_6) M_1 - k_2 M_2 - \nu M_2, \quad (3.2.3)$$

Here s_1 and s_2 are source terms for M_1 and M_2 macrophages, ν represents the unbiased interchange between these two macrophage phenotypes, and $(\lambda_1 T_\beta + \lambda_2 I_6)$ is the rate by which additional transformation occurs from M_1 to M_2 and it is activated by cytokines TGF- β and IL-6 [39]. The natural deaths of the macrophages M_1 and M_2 are assumed to be directly proportional to the concentration rate of the macrophages thus occur at the per capita rates k_1 and k_2 respectively.

The density of CD4⁺ T cells, T_4 satisfies the equation

$$\frac{dT_4}{dt} = s_3 + \beta_1 \frac{I_{12} M_1}{K_{10} + I_{10}} + \beta_2 \frac{I_2 T_4}{K_2 + I_2} - \mu_1 T_4 - (1 - \zeta_r) \mu_2 V T_4, \quad (3.2.4)$$

with a source term s_3 (from a source such as the thymus) and apoptosis rate μ_1 . T_4 is further activated (from naive T cells) by I_{12} while in contact with M_1 due to the molecule, major histocompatibility complex, class II (MHC-II) found on the surface of M_1 [23, 39] at a rate β_1 . The MHC-II molecule found on the surface of M_1 , an antigen presenting cell (APC) together with IL-12 activates the naive T helper cells, where the former also aid in the priming of the naive T helper cells into effector T cells and memory T cells. This process is resisted by IL-10. The third term on the right-hand side of equation (3.2.4) is the proliferation enhanced by I_2 [36], and the fourth term is the natural death of T_4 cells. We assume the proliferation is saturated thus we use the Michaelis-Menten kinetics in the proliferation term. The last term is the depletion of T_4 as a result of invasion by external virus, a process which is reduced by RTI drug as represented by the factor $1 - \zeta_r$, where $0 \leq \zeta_r \leq 1$. If $\zeta_r = 1$, then the RTIs offer 100% protection while if $\zeta_r = 0$, zero protection is offered. It is worth noting that the inhibition process by RTI occurs after the virus has been attached to the cell and therefore the drug does not directly affect the infection rate, μ_2 of the target cells.

The density of infected T_4 cells, T_4^i satisfies the equation

$$\frac{dT_4^i}{dt} = (1 - \zeta_r) \mu_2 V T_4 - \mu_5 T_4^i, \quad (3.2.5)$$

where in μ_5 we included both the natural death rate and the burst rate δ_2 of the infected T_4 cells, hence $\mu_5 > \delta_2$. We assume that without HIV drugs, upon burst of

one infected T_4 cell, N virions are released. However, this number will be decreased by a factor $1 - \zeta_p$, ($0 \leq \zeta_p \leq 1$) under treatment with PI drug. Hence

$$\frac{dV}{dt} = (1 - \zeta_p)N\delta_2 T_4^i - \mu_v V, \quad (3.2.6)$$

where μ_v is the death, or degradation rate of extracellular virus. Similar conclusions can be drawn for $\zeta_p = 0$ and $\zeta_p = 1$ as done for ζ_r .

T_8 cells are activated by I_{12} , a process inhibited by I_{10} [19, 58, 59] and I_2 [36]. ϵ included in the first term is a modification parameter which represents the proliferation potential of $CD8^+$ T cells when compared to that of $CD4^+$ T cells when influenced by I_{12} and I_{10} . Since HIV does not invade into T_8 cells, we have the following equation;

$$\frac{dT_8}{dt} = \epsilon\beta_1 \frac{I_{12}}{K_{10} + I_{10}} + \beta_2 \frac{I_2 T_8}{K_2 + I_2} - \mu_4 T_8, \quad (3.2.7)$$

where the loss of the cells is at a rate μ_4 given by the term $\mu_4 T_8$ assuming direct proportionality of the rate to the concentration of the $CD8^+$ T cells.

As in [39], we assume the dynamics of the cancer is governed by two processes: i.e. intrinsic growth of the cancer cells and the elimination due to the cytotoxic effector cells. Therefore, considering equation (3.2.8) describing the cancer dynamics, the first term models the growth of the cancer which we assume as most of the living organisms, follows universal law with r being the growth rate, C_0 , the maximum size of the cancer cells and the total body mass of the cancer cell is represented by C . For greater elucidation on the growth term, see [22, 39]. The killing rate of the cancer cells by T_8 cells occurs at a rate β_3 and follows the mass-action law.

$$\frac{dC}{dt} = rC^{\frac{3}{4}} \left(1 - \left(\frac{C}{C_0} \right)^{\frac{1}{4}} \right) - \beta_3 C T_8. \quad (3.2.8)$$

The parameters in the model system described in equations (3.2.1) - (3.2.8) are all assumed to be non-negative.

The model equations are thus given by

$$\left. \begin{aligned} \frac{dM_1}{dt} &= s_1 - k_1 M_1 + \nu M_2 - (\lambda_1 T_\beta + \lambda_2 I_6) M_1, \\ \frac{dM_2}{dt} &= s_2 + (\lambda_1 T_\beta + \lambda_2 I_6) M_1 - k_2 M_2 - \nu M_2, \\ \frac{dT_4}{dt} &= s_3 + \beta_1 \frac{I_{12} M_1}{K_{10} + I_{10}} + \beta_2 \frac{I_2 T_4}{K_2 + I_2} - \mu_1 T_4 - (1 - \zeta_r) \mu_2 V T_4, \\ \frac{dT_4^i}{dt} &= (1 - \zeta_r) \mu_2 V T_4 - \mu_5 T_4^i, \\ \frac{dV}{dt} &= (1 - \zeta_p) N \delta_2 T_4^i - \mu_v V, \\ \frac{dT_8}{dt} &= \epsilon \beta_1 \frac{I_{12}}{K_{10} + I_{10}} + \beta_2 \frac{I_2 T_8}{K_2 + I_2} - \mu_4 T_8, \\ \frac{dC}{dt} &= r C^{\frac{3}{4}} \left(1 - \left(\frac{C}{C_0} \right)^{\frac{1}{4}} \right) - \beta_3 C T_8, \end{aligned} \right\} \quad (3.2.9)$$

3.3 Model analysis

3.3.1 The simplified model

The first step is to reduce the model into a model that describes the interactions between cell populations i.e. CD4 cells, CD8 cells, macrophages and the cancer cells. We assume quasi-steady-state approximation for the cytokines concentration since in our model system the dynamics occur at different time scales. The dynamics of cytokines ,that is, their secretion and decay is on a much faster scale than the dynamics of cells and thus we assume they reach their equilibrium almost instantaneously [39]. Hence, we simplify the model (3.2.1) and (3.2.9) by taking the cytokines dynamics in system (3.2.1) to be at steady state, so that

$$T_\beta = \frac{\alpha_1}{d_1} C, \quad I_6 = \frac{\alpha_6}{d_6} C, \quad I_{10} = \frac{\alpha_{10}}{d_{10}} M_2, \quad I_{12} = \frac{\alpha_{12}}{d_{12}} M_1, \quad I_2 = \frac{\alpha_2}{d_2} T_4.$$

Substituting these cytokines into model system (3.2.9) we obtain

$$\left. \begin{array}{l} \frac{dM_1}{dt} = s_1 - k_1 M_1 + \nu M_2 - \gamma_c C M_1, \\ \frac{dM_2}{dt} = s_2 + \gamma_c C M_1 - k_2 M_2 - \nu M_2, \\ \frac{dT_4}{dt} = s_3 + \frac{\gamma_1 M_1 M_1}{K_{10} + \gamma_2 M_2} + \beta_2 \frac{\gamma_3 T_4 T_4}{K_2 + \gamma_3 T_4} - \mu_1 T_4 - (1 - \zeta_r) \mu_2 V T_4, \\ \frac{dT_4^i}{dt} = (1 - \zeta_r) \mu_2 V T_4 - \mu_5 T_4^i, \\ \frac{dV}{dt} = (1 - \zeta_p) N \delta_2 T_4^i - \mu_v V, \\ \frac{dT_8}{dt} = \epsilon \frac{\gamma_1 M_1}{K_{10} + \gamma_2 M_2} + \beta_2 \frac{\gamma_3 T_4 T_8}{K_2 + \gamma_3 T_4} - \mu_4 T_8, \\ \frac{dC}{dt} = r C^{\frac{3}{4}} \left(1 - \left(\frac{C}{C_0} \right)^{\frac{1}{4}} \right) - \beta_3 C T_8, \end{array} \right\} \quad (3.3.1)$$

where $\gamma_c = \lambda_1 \frac{\alpha_1}{d_1} + \lambda_2 \frac{\alpha_6}{d_6}$, $\gamma_1 = \beta_1 \frac{\alpha_{12}}{d_{12}}$, $\gamma_2 = \frac{\alpha_{10}}{d_{10}}$ and $\gamma_3 = \frac{\alpha_2}{d_2}$,

with the general initial conditions

$$M_1 \geq 0, M_2 \geq 0, T_4 \geq 0, T_4^i \geq 0, V \geq 0, T_8 \geq 0 \quad \text{and} \quad C \geq 0.$$

The model system (3.3.1) represents the dynamics of the cell population and the HIV virus in the presence of cytokines in a cancer environment and HIV treatment. The analysis of system (3.3.1) is therefore central in this study. We state two important model properties of model system (3.3.1) before embarking on steady-state analysis.

3.3.2 Model properties

Before commencing the steady-states analysis of the model system (3.3.1), we look at some properties to ensure existence of biologically meaningful solutions.

3.3.2.1 Positivity of the solutions

We need to ensure that the state variables remain non-negative and solutions of the system remain positive for all $t \geq 0$ given positive initial conditions i.e. to establish the long term behaviour of the solutions. We thus have the following lemma.

Lemma 3.3.1. *Given the initial conditions $M_1 \geq 0, M_2 \geq 0, T_4 \geq 0, T_4^i \geq 0, V \geq 0, T_8 \geq 0$ and $C \geq 0$, then the solutions of $M_1(t), M_2(t), T_4(t), T_4^i(t), V(t), T_8(t)$ and $C(t)$ remain positive for all $t \geq 0$*

Proof. Suppose $\tilde{t} = \sup \{t > 0 : M_1 \geq 0, M_2 \geq 0, T_4 \geq 0, T_4^i \geq 0, V \geq 0, T_8 \geq 0, C \geq 0\} \in [0, t]$, implying $\tilde{t} \geq 0$. The first equation of system (3.3.1) gives

$$\frac{dM_1}{dt} \geq s_1 - k_1 M_1 - \gamma(t) M_1, \quad \text{where } \gamma_c C = \gamma(t).$$

Integration, yields

$$M_1(\tilde{t}) \geq M_1(0) e^{-[k_1 t + \int_0^t \gamma(s) ds]} + e^{-[k_1 t + \int_0^t \gamma(s) ds]} \int_0^{\tilde{t}} s_1 e^{[k_1 t + \int_0^t \gamma(s) ds]} \geq 0.$$

Hence M_1 is always positive for all $\tilde{t} > 0$. Similarly

$$M_2(\tilde{t}) \geq M_2(0) e^{(-(k_2 + \nu)t)} + e^{(-(k_2 + \nu)t)} \int_0^{\tilde{t}} s_2 e^{(k_2 + \nu)t} \geq 0.$$

Considering the CD4 T cells we have

$$\frac{dT_4}{dt} \geq s_3 - \Theta(t) T_4, \quad \text{where } \Theta(t) = \mu_1 + (1 - \zeta_r) \mu_2 V.$$

The solution of the differential equation is

$$T_4(\tilde{t}) \geq T_4(0) \exp \left[- \int_0^t \Theta(s) ds \right] + \exp \left[- \int_0^t \Theta(s) ds \right] \left(\int_0^{\tilde{t}} s_3 \exp \left[\int_0^t \Theta(s) ds \right] \right) \geq 0.$$

Similarly we have

$$T_4^i(\tilde{t}) \geq T_4^i(0) \exp(-\mu_5 t) \geq 0.$$

Also

$$T_8(\tilde{t}) \geq T_8(0) \exp \left[- \left(\mu_4 t - \int_0^t \Phi(s) ds \right) \right] \geq 0, \quad \text{where } \Phi(t) = \beta_2 \frac{\gamma_3 T_4}{K_2 + \gamma_3 T_4}.$$

Hence $T_4(\tilde{t}), T_4^i(\tilde{t})$ and $T_8(\tilde{t})$ are positive for all $\tilde{t} > 0$.

For the virus population we have

$$\frac{dV}{dt} \geq -\mu_v V, \quad \Rightarrow V(t) \geq V(0) \exp(-\mu_v t) \geq 0.$$

Lastly, for the cancer cell population, we have

$$\Rightarrow C(\tilde{t}) \geq C(0) \exp \left[-\beta_3 \int T_8(s) ds \right] \geq 0.$$

Hence $V(\tilde{t})$ and $C(\tilde{t})$ are positive for all $\tilde{t} > 0$. This implies that all the state variables are non-negative and the solutions of our system remain positive for all $\tilde{t} \geq 0$. \square

3.3.2.2 Feasible region

Since the model examines the dynamics of the cell populations, it then follows that all the parameters and state variables should be non-negative for a biologically feasible model. We will therefore analyse model system (3.3.1) in the feasible region Ω . We thus have the following lemma on the region where the system exist.

Lemma 3.3.2. *The solution of our system with initial conditions $M_1 \geq 0, M_2 \geq 0, T_4 \geq 0, T_4^i \geq 0, V \geq 0, T_8 \geq 0$ and $C \geq 0$ are contained (bounded) for all $t \geq 0$ in the biologically feasible region defined by the set*

$$\Omega = \left\{ (M_1, M_2, T_4, T_4^i, V, T_8, C) \in \mathbb{R}_+^7 : M \leq \frac{(s_1 + s_2)}{k}, T \leq \frac{s_3 + K}{\mu}, V \leq \frac{N\delta_2 W}{\mu_v}, C \leq \left(\frac{rC_0^{\frac{1}{4}}}{r - \beta_3 W C_0^{\frac{1}{4}}} \right)^4 \right\}, \quad (3.3.2)$$

with $M = M_1 + M_2$ and $T = T_4 + T_4^i + T_8$.

Proof. Summing the two macrophage populations from the first two equations of system (3.3.1) we obtain

$$\frac{d}{dt}(M_1 + M_2) = \frac{dM}{dt} \leq s_1 + s_2 - kM, \quad \text{for } k = \min \{k_1, k_2\}, \quad (3.3.3)$$

Integration of (3.3.3) yields

$$M(t) \leq \frac{(s_1 + s_2)}{k} + \left(M(0) - \frac{(s_1 + s_2)}{k} \right) e^{-kt}.$$

When we take the limit supremum of M as $t \rightarrow \infty$, we have

$$\limsup_{t \rightarrow \infty} M(t) \leq \frac{(s_1 + s_2)}{k} = S.$$

This implies that

$$M_1 \leq S \quad \text{and} \quad M_2 \leq S.$$

Hence the macrophage population is bounded.

Again considering the sum of the T cell populations we have

$$\begin{aligned} \frac{dT}{dt} &\leq s_3 + \frac{\gamma_1 S^2}{K_{10} + \gamma_2 S} + \epsilon \frac{\gamma_1 S}{K_{10} + \gamma_2 S} - \mu_1 T_4 - \mu_5 T_4^i - \mu_4 T_8, \\ &\leq s_3 + \frac{\gamma_1 S}{K_{10} + \gamma_2 S} (S + \epsilon) - \mu T, \\ \text{where } \mu &= \min \{\mu_1, \mu_5, \mu_4\} \text{ and } M_1, M_2 \leq \frac{(s_1 + s_2)}{k} = S. \end{aligned}$$

Through integration, we obtain

$$T(t) \leq \frac{s_3 + K}{\mu} + \left(T(0) - \frac{s_3 + K}{\mu} \right) e^{-\mu t}, \text{ where } K = \frac{\gamma_1 S}{K_{10} + \gamma_2 S} (S + \epsilon).$$

Therefore

$$\limsup_{t \rightarrow \infty} T(t) \leq \frac{s_3 + K}{\mu} = W.$$

This implies that $T_4 \leq W$, $T_4^i \leq W$ and $T_8 \leq W$, hence each of the T-cell population is bounded.

Considering the virus population we have

$$\frac{dV}{dt} \leq (1 - \zeta_p) N \delta_2 W - \mu_v V, \quad \text{since} \quad T_4^i \leq W.$$

Integration gives

$$V(t) \leq \frac{(1 - \zeta_p) N \delta_2 W}{\mu_v} + \left(V(0) - \frac{(1 - \zeta_p) N \delta_2 W}{\mu_v} \right) e^{-\mu_v t}.$$

We also have

$$\limsup_{t \rightarrow \infty} V(t) \leq \frac{(1 - \zeta_p) N \delta_2 W}{\mu_v} = Q.$$

Hence $V(t)$ is thus bounded.

Lastly, we consider the cancer cell population. From the last equation in system (3.3.1), we have

$$\begin{aligned} \frac{dC}{dt} &= C \left[rC^{-\frac{1}{4}} \left(1 - \left(\frac{C}{C_0} \right)^{\frac{1}{4}} \right) - \beta_3 T_8 \right], \\ \Rightarrow \frac{dC}{dt} &\leq C \left[\frac{r}{C^{\frac{1}{4}}} - \frac{r}{C_0^{\frac{1}{4}}} - \beta_3 W \right], \quad \text{since } T_8 \leq \frac{s_3 + K}{\mu} = W. \\ &= \frac{C \left[rC_0^{\frac{1}{4}} - rC^{\frac{1}{4}} - \beta_3 W(C_0^{\frac{1}{4}} C^{\frac{1}{4}}) \right]}{C_0^{\frac{1}{4}} C^{\frac{1}{4}}}. \end{aligned}$$

Through integration , we obtain

$$\begin{aligned} \int \frac{C_0^{\frac{1}{4}} C^{\frac{1}{4}} dC}{C \left[rC_0^{\frac{1}{4}} - rC^{\frac{1}{4}} - \beta_3 W(C_0^{\frac{1}{4}} C^{\frac{1}{4}}) \right]} &\leq \int dt, \\ \left(-\frac{4C_0^{\frac{1}{4}}}{(r - \beta_3 WC_0^{\frac{1}{4}})} \right) \int \frac{-\frac{1}{4}(r - \beta_3 WC_0^{\frac{1}{4}}) C^{-\frac{3}{4}} dC}{\left[rC_0^{\frac{1}{4}} - C^{\frac{1}{4}}(r - \beta_3 WC_0^{\frac{1}{4}}) \right]} &\leq \int dt, \\ \left(-\frac{4C_0^{\frac{1}{4}}}{(r - \beta_3 WC_0^{\frac{1}{4}})} \right) \ln \left(rC_0^{\frac{1}{4}} - C^{\frac{1}{4}}(r - \beta_3 WC_0^{\frac{1}{4}}) \right) &\leq t, \end{aligned}$$

we thus have

$$\begin{aligned} \ln \left(rC_0^{\frac{1}{4}} - C^{\frac{1}{4}}(t)(r - \beta_3 WC_0^{\frac{1}{4}}) \right) &\leq \left(-\frac{(r - \beta_3 WC_0^{\frac{1}{4}})}{4C_0^{\frac{1}{4}}} \right) t, \\ -C^{\frac{1}{4}}(t)(r - \beta_3 WC_0^{\frac{1}{4}}) &\leq \exp \left(\left(-\frac{(r - \beta_3 WC_0^{\frac{1}{4}})}{4C_0^{\frac{1}{4}}} \right) t \right) - rC_0^{\frac{1}{4}}, \end{aligned}$$

$$C^{\frac{1}{4}}(t) \leq \frac{\exp\left(\left(-\frac{(r-\beta_3WC_0^{\frac{1}{4}})}{4C_0^{\frac{1}{4}}}\right)t\right) - rC_0^{\frac{1}{4}}}{-(r-\beta_3WC_0^{\frac{1}{4}})},$$

$$C(t) \leq \left(\frac{rC_0^{\frac{1}{4}} - \exp\left(\left(-\frac{(r-\beta_3WC_0^{\frac{1}{4}})}{4C_0^{\frac{1}{4}}}\right)t\right)}{r-\beta_3WC_0^{\frac{1}{4}}} \right)^4.$$

So

$$\limsup_{t \rightarrow \infty} C(t) \leq \left(\frac{rC_0^{\frac{1}{4}}}{r-\beta_3WC_0^{\frac{1}{4}}} \right)^4 = P.$$

Therefore $C(t)$ is also bounded.

From the above we observe that as $t \rightarrow \infty$, $M(t) \rightarrow \frac{(s_1+s_2)}{k}$, $T \rightarrow \frac{s_3+K}{\mu}$, $V \rightarrow \frac{N\delta_2W}{\mu_v}$ and $C \rightarrow \left(\frac{rC_0^{\frac{1}{4}}}{r-\beta_3WC_0^{\frac{1}{4}}} \right)^4$ where $M(t) = M_1(t) + M_2(t)$ and $T(t) = T_4(t) + T_4^i(t) + T_8(t)$.

So, for instance if $M_0 \leq \frac{(s_1+s_2)}{k}$ then $\lim_{t \rightarrow \infty} M(t) = \frac{(s_1+s_2)}{k}$. Clearly, $\frac{(s_1+s_2)}{k}$ is the upper bound of M , i.e. the non-negative solutions of the first two equations of system (3.3.1) are monotone increasing and are bounded above by $\frac{(s_1+s_2)}{k}$. On the other hand, if $M_0 > \frac{(s_1+s_2)}{k}$, then the solutions will decrease monotonically and are bounded below by $\frac{(s_1+s_2)}{k}$, i.e. they enter or approach the region asymptotically. Same applies to other state variables in system (3.3.1).

Our invariant region is therefore defined by Ω . Hence, any solution of our system that commences in the positive orthant \mathbb{R}_+^7 at $t \geq 0$ will either remain confined in the region, enters or approaches it asymptotically. We therefore deduce that the region Ω is positively invariant and attracting with respect to model system (3.3.1) for instance, the system is both mathematically and biologically well posed. That completes the proof. \square

3.3.3 Steady states

Definition 3.3.3. Given a system of differential equations $\mathbf{x}'(t)=\mathbf{f}(t)$, an equilibrium/steady state \mathbf{x}^* of this system is a point in the state space for which $\mathbf{x}(t)=\mathbf{x}^*$ is a solution for all time, t .

To obtain this, we set the right hand side of system (3.3.1) to zero, so that

$$s_1 - k_1 M_1^* + \nu M_2^* - \gamma_c C^* M_1^* = 0, \quad (3.3.4)$$

$$s_2 + \gamma_c C^* M_1^* - k_2 M_2^* - \nu M_2^* = 0, \quad (3.3.5)$$

$$s_3 + \frac{\gamma_1 M_1^* M_1^*}{K_{10} + \gamma_2 M_2^*} + \beta_2 \frac{\gamma_3 T_4^* T_4^*}{K_2 + \gamma_3 T_4^*} - \mu_1 T_4^* - (1 - \zeta_r) \mu_2 V^* T_4^* = 0, \quad (3.3.6)$$

$$(1 - \zeta_r) \mu_2 V^* T_4^* - \mu_5 T_4^{i*} = 0, \quad (3.3.7)$$

$$(1 - \zeta_p) N \delta_2 T_4^{i*} - \mu_v V^* = 0, \quad (3.3.8)$$

$$\epsilon \frac{\gamma_1 M_1^*}{K_{10} + \gamma_2 M_2^*} + \beta_2 \frac{\gamma_3 T_4^* T_8^*}{K_2 + \gamma_3 T_4^*} - \mu_4 T_8^* = 0 \quad (3.3.9)$$

$$r C^{* \frac{3}{4}} \left(1 - \left(\frac{C^*}{C_0} \right)^{\frac{1}{4}} \right) - \beta_3 C^* T_8^* = 0. \quad (3.3.10)$$

We start by solving for the steady states M_1^* and M_2^* in equations (3.3.4) and (3.3.5) and we have respectively

$$M_1^* = \frac{\sigma_1}{\Lambda + \sigma_2 C^*} \quad \text{and} \quad M_2^* = \frac{\sigma_3 + \sigma_4 C^*}{\Lambda + \sigma_2 C^*},$$

$$\text{where } \sigma_1 = (\nu + k_2) s_1 + \nu s_2, \quad \Lambda = k_1 (\nu + k_2), \quad \sigma_2 = k_2 \gamma_c,$$

$$\sigma_3 = k_1 s_2, \quad \sigma_4 = (s_1 + s_2) \gamma_c.$$

We therefore assume a quasi steady-state for the viral population and thus from equation (3.3.8) we have

$$V^* = \frac{(1 - \zeta_p) N \delta_2 T_4^{i*}}{\mu_v}. \quad (3.3.11)$$

Substituting V^* in (3.3.11) into equation (3.3.7) we obtain

$$T_4^{i*} \left(\frac{(1 - \zeta_p)(1 - \zeta_r) \mu_2 N \delta_2 T_4^*}{\mu_v} - \mu_5 \right) = 0.$$

This gives

$$T_4^{i*} = 0 \quad \text{or} \quad T_4^* = \frac{\mu_v \mu_5}{(1 - \zeta_p)(1 - \zeta_r)\mu_2 N \delta_2}.$$

From the above, it implies that T_4 has one solution given by

$$T_4^* = \frac{\mu_v \mu_5}{(1 - \zeta_p)(1 - \zeta_r)\mu_2 N \delta_2}.$$

For $T_4^{i*} = 0$, our system at the steady state relates to HIV-free cancer equilibrium. Since our objective is to investigate the role of HIV in the NHLs, we therefore analyse hereinafter the steady state in which there is HIV in the system, that is, co-infection of HIV and the cancer in the presence of HIV treatment.

We now solve for the steady states, $E = (M_1^*, M_2^*, T_4^*, T_4^{i*}, V^*, T_8^*, C^*)$ where the state of the cancer is also influenced by the presence of the HIV in the cancer environment. Firstly, we substitute the solution T_4^* into equations (3.3.6) and (3.3.9). We notice that in the solution T_4^* , the number of virions, N , has an effect on the concentration of the CD4⁺ T cells in the cancer environment, therefore the virus and the infected T cells play a crucial role in our model.

From (3.3.6) we solve for the solution of V at HIV-related NHL steady state denoted by V^* so that

$$V^* = \frac{\left(\left(s_3 + \frac{T_4^{*2} \beta_2 \gamma_3}{K_2 + T_4^* \gamma_3} + \frac{\gamma_1 \sigma_1^2}{K_{10}(\Lambda + C^* \sigma_2)^2 + (\sigma_3 + C^* \sigma_4)(\Lambda + C^* \sigma_2)} \right) - \mu_1 T_4^* \right)}{(1 - \zeta_r) \mu_2 T_4^*}.$$

From equation (3.3.11), we have

$$T_4^{i*} = \mu_v \left(\frac{\left(\left(s_3 + \frac{T_4^{*2} \beta_2 \gamma_3}{K_2 + T_4^* \gamma_3} + \frac{\gamma_1 \sigma_1^2}{K_{10}(\Lambda + C^* \sigma_2)^2 + (\sigma_3 + C^* \sigma_4)(\Lambda + C^* \sigma_2)} \right) - \mu_1 T_4^* \right)}{(1 - \zeta_p)(1 - \zeta_r)\mu_2 N \delta_2 T_4^*} \right).$$

We then obtain the steady state T_8^* as a function of C from equation (3.3.9). We have

$$T_8^* = \frac{\epsilon \gamma_1 \sigma_1 [(1 - \zeta_p)(1 - \zeta_r)\mu_2 \delta_2 N K_2 + \gamma_3 \mu_5 \mu_v]}{[(1 - \zeta_p)(1 - \zeta_r)\mu_2 \mu_4 \delta_2 N K_2 - \gamma_3 \mu_5 (\beta_2 - \mu_4) \mu_v] [K_{10}(\Lambda + C^* \sigma_2) + \gamma_2 (\sigma_3 + C^* \sigma_4)]}.$$

Since β_2 is the proliferation/activation rate of T_8 due to IL-2 and μ_4 , the decay rate of T_8 , it therefore suffice to assume that, for the existence of CD8⁺ T- cells, the

proliferation rate must always be greater than the death rate, that is $\beta_2 > \mu_4$. This implies that, the solution T_8^* is positive if and only if

$$N > \frac{\gamma_3 \mu_5 \mu_v (\beta_2 - \mu_4)}{(1 - \zeta_p)(1 - \zeta_r) \mu_2 \mu_4 \delta_2 K_2} = N_{\text{crit}}^*.$$

The existence of T_8^* at endemic steady state is subject to $N > N_{\text{crit}}^*$. Therefore, the virions released per bursting of infected T cell must exceed a certain threshold, N_{crit}^* .

From equation (3.3.10) we have

$$g(C) = C \left[rC^{-1/4} \left(1 - (C/C_0)^{1/4} \right) - \beta_3 T_8^* \right] = 0. \quad (3.3.12)$$

The solutions of (3.3.12) are

$$C^* = 0 \quad \text{or} \quad rC^{-1/4} \left(1 - (C/C_0)^{1/4} \right) - \beta_3 T_8^* = 0.$$

$C^* = 0$ corresponds to a cancer free environment.

We define

$$g(C^*) = rC^{-1/4} \left(1 - (C/C_0)^{1/4} \right) - \beta_3 T_8^* = 0,$$

for the non-zero steady states.

Once the solutions of T_8 are in terms of C , their substitution into the non-zero equilibria i.e endemic equilibria result in an implicit function whose solutions can only be established numerically.

We begin by considering the cancer free steady state. The non-zero solutions of C are subject to $N > N_{\text{crit}}^*$.

3.3.3.1 Cancer-free steady state, E_0

The model given by the system (3.3.1) has a unique feasible cancer-free steady state, E_0 and it represents the state of HIV infection in the presence of HIV treatment with no cancer cells in the host immune system. It reflects the possibility of cancer development prevention by the immune system (i.e the cancers are not able to evade

the immune system). The state, E_0 is therefore given by

$$\begin{aligned} \text{Cancer-free equilibrium, } E_0 &= (M_1^*, M_2^*, T_4^*, T_4^{0*}, V^*, T_8^*, C^*), \quad \text{where} \\ M_1^* &= \frac{\sigma_1}{\Lambda}, \quad M_2^* = \frac{\sigma_3}{\Lambda}, \quad T_4^* = \frac{\mu_v \mu_5}{(1 - \zeta_p)(1 - \zeta_r)\mu_2 N \delta_2}, \quad C^* = 0, \\ T_4^{i*} &= \frac{s_3}{\mu_5} + \frac{\beta_2 \gamma_3 \mu_v^2 \mu_5}{((1 - \zeta_r)(1 - \zeta_p)N K_2 \mu_2^2 \delta_2 + \gamma_3 \mu_5 \mu_v \mu_2)((1 - \zeta_r)(1 - \zeta_p)N \delta_2)} \\ &\quad + \frac{\gamma_1 \sigma_1^2}{\Lambda^2 K_{10} \mu_5 + \Lambda \gamma_2 \mu_5 \sigma_3} - \frac{\mu_1 \mu_v}{(1 - \zeta_r)(1 - \zeta_p)N \delta_2 \mu_2}, \\ T_8^* &= \frac{(\epsilon \gamma_1 ((1 - \zeta_p)(1 - \zeta_r)\mu_2 \delta_2 N K_2 + \gamma_3 \mu_5 \mu_v) \sigma_1)}{((1 - \zeta_p)(1 - \zeta_r)\mu_2 \mu_4 \delta_2 N K_2 + \gamma_3 \mu_5 (\mu_4 - \beta_2) \mu_v)(K_{10} \Lambda + \gamma_2 \sigma_3)}, \\ V^* &= \frac{(1 - \zeta_r)N \delta_2 s_3}{\mu_v \mu_5} + \frac{\beta_2 \gamma_3 \mu_v \mu_5}{(1 - \zeta_r)(1 - \zeta_p)^2 N K_2 \mu_2^2 \delta_2 + \gamma_3 \mu_5 \mu_v \mu_2} \\ &\quad + \frac{N \delta_2 \gamma_1 \sigma_1^2}{\Lambda^2 K_{10} \mu_v \mu_5 + \Lambda \gamma_2 \mu_v \mu_5 \sigma_3} - \frac{\mu_1}{(1 - \zeta_p)\mu_2}. \end{aligned}$$

The existence of cancer-free equilibrium, E_0 is subject to $\bar{N}_{\text{crit}} < N$, where $\bar{N}_{\text{crit}} = \max \{N_{\text{crit}}, N_{\text{crit}}^*\}$, and

$$\begin{aligned} N_{\text{crit}} &= \frac{\mu_5 \mu_v \mu_1}{(1 - \zeta_p)(1 - \zeta_r)\mu_2 \delta_2 s_3} \\ N_{\text{crit}}^* &= \frac{\gamma_3 \mu_5 \mu_v (\beta_2 - \mu_4)}{(1 - \zeta_p)(1 - \zeta_r)\mu_2 \mu_4 \delta_2 K_2} = N_{\text{crit}} \frac{\gamma_3 s_3 (\beta_2 - \mu_4)}{\mu_1 \mu_4 K_2}. \end{aligned}$$

The stability of this state is not easy to show analytically, we therefore use numerical simulations in Section 3.4 to help us assess the local stability of the cancer-free steady state.

3.3.3.2 Cancer-persistence steady states

The steady-state analysis for the model discussed in this section clearly shows the existence of some feasible (non-negative) and non-zero cancer equilibria (cancer-persistence steady states). However, due to mathematical intractability we are unable to explicitly express the endemic states in terms of the model parameters. We resort to numerical simulations.

3.4 Numerical simulations

3.4.1 Parameter estimation.

Table 3.3 provides the description and values of all the parameters that appear in model system (3.3.1). Due to lack of data, the parameter values used in the numerical simulation were taken from the literature, although not always from cancer experimental data. Some of the parameters were estimated as follows;

We assume that at steady state of HIV infected person, when he/she still appears to be normal, $T_4 = 500000$ cells/ml. Since $\mu_1 = 0.02/\text{day}$ [61], from the cancer-free steady state equation $s_3 - \mu_1 T_4 = 0$ we then get $s_3 = 10000$ cells/ml day. In normal healthy individual at steady state, the average monocyte content is 400000cells/ml [2]. We assume that monocytes differentiate mostly into M_1 macrophages as they move from the blood into the tissue, thus take $M_1 = 400000$ cells/ml. From the cancer-free steady state equation $s_1 - k_1 M_1 = 0$ and $k_1 = 0.02/\text{day}$, we get $s_1 = 8000$ cells/ml/day. It is known that tumor attracts myeloid derived suppressor cells (MDSC), cells that have similar behaviour to M_2 cells [54]. We identify MDSC with M_2 , and for simplicity consider this source of macrophages as a source term s_2 . We assume that this source is small in comparison to the source of M_1 macrophages, and take $s_2 = s_1/10 = 800$ cells/ml/day. Since $k_2 = 0.008/\text{day}$, the steady state equation $s_2 - k_2 M_2 = 0$ yields the steady state density $M_2 = 100000$ cells/ml. We take the values of parameters λ_1 and λ_2 to be 0.075 day^{-1} as in [64]. We finally take $N = 1000$, although this number varies in different studies [61].

Parameter	Description	Baseline Values	Min Values	Max Values	Units	Baseline Source
α_1	production rate of TGF- β due to cancers cells	7×10^{-4}	6.8×10^{-4}	7.5×10^{-4}	pg/cell day	[5, 60]
α_2	production rate of IL-2 due to CD4 $^{+}$ T cells	5	4	6	pg/cell day	[5, 33]
α_6	production rate of IL-6 due to cancers cells	7×10^{-5}	5×10^{-5}	8×10^{-5}	pg/cell day	Estimated
α_{10}	production rate of IL-10 due to M_2	5×10^{-4}	4.9×10^{-4}	5.3×10^{-4}	pg/cell day	[29, 30, 64]
α_{12}	production rate of IL-12 due to M_1	3×10^{-2}	2.9×10^{-2}	3.1×10^{-2}	pg/cell day	Estimated in [29]
d_1	degradation rate of TGF- β	10	9	11	day $^{-1}$	Estimated in [5]
d_2	degradation rate of IL-2	10	9	11	day $^{-1}$	[33, 51]
d_6	degradation rate of IL-6	0.173	0.1	0.2	day $^{-1}$	[40]
d_{10}	degradation rate of IL-10	5	3	6	day $^{-1}$	[29]
d_{12}	degradation rate of IL-12	1.188	1	2	day $^{-1}$	[29, 45]
s_1	influx rate of M_1	8000	7500	8500	day $^{-1}$	Estimated
s_2	influx rate of M_2	800	750	850	day $^{-1}$	Estimated
s_3	production of CD4 $^{+}$ T cells by the sources	1.0×10^4	9.9×10^3	1.10×10^4	cells/ml day	Estiamted
k_1	per capita death rate of M_1	0.02	0.01	0.04	day $^{-1}$	[29]
k_2	per capita death rate of M_2	8×10^{-3}	7×10^{-3}	9×10^{-3}	day $^{-1}$	[29, 31]
λ_1	transformation rate of M_1 by TGF- β	0.075	0.07	0.08	day $^{-1}$	Estimated in [64]
λ_2	transformation rate of M_2 by IL-6	0.075	0.07	0.08	day $^{-1}$	Estimated in [64]
ν	transition rate from M_2 to M_1	5×10^{-2}	4×10^{-2}	6×10^{-2}	day $^{-1}$	[57, 64]
β_1	activation rate of T cells by IL-12	1×10^6	9×10^5	1.1×10^6	cells/ ml day	[23]
β_2	proliferation rate of T cells by IL-2	0.1245	0.1	0.2	pg/cell day	[5, 33, 34]
β_3	loss of cancer cells	$10^{-5} \sim 10^{-9}$	10^{-5}	10^{-9}	day $^{-1}$	[39, 53, 63] and estimated (10^{-7})*
K_2	saturation constant of proliferation by IL-2	2×10^7	1.9×10^7	2.1×10^7	pg/ml	[33, 34]
K_{10}	saturation constant for anti-proliferation by IL-10	2.5×10^7	2.4×10^7	2.6×10^7	pg/ml	[23]
ϵ	modification parameter	0.5	0.4	0.6		Estimated
μ_1	per capita death rate of uninfected CD4 $^{+}$ T cells	0.02	0.01	0.03	day $^{-1}$	Estimated in [61]
μ_2	infection rate of CD4 $^{+}$ T cells due to infiltration by free viruses	2.4×10^{-8}	2×10^{-8}	3×10^{-8}	ml/ day	Estimated in [61]
μ_4	per capita death rate of CD8 $^{+}$ T cells	0.03 ~ 0.0412	0.02	0.05	day $^{-1}$	[33, 34] 0.03*
μ_v	clearance rate (loss) of free viruses	2.4	2.	3	day $^{-1}$	Estimated in [61]
μ_5	per capita death rate of infected CD4 $^{+}$ T cells	0.26	0.2	0.5	day $^{-1}$	Estimated in [61]
δ_2	lytic death rate of infected CD4 $^{+}$ T cells	0.24	0.2	0.3	day $^{-1}$	Estimated in [61]
r	cancer growth rate	$0.18 \sim 0.19$	0.15	0.2	day $^{-1}$	[5, 33, 34, 63] 0.19*
C_0	maximum cancer density	10^6			cells/ml	[39]
N	number of virions released upon burst by an infected CD4 $^{+}$ T cell	1000	500	1500	cells/ml	[61] and assumed
ζ_r	the measure of efficacy of reverse transcriptase inhibitors(RTI)	[0, 1]				
ζ_p	the measure of efficacy of protease inhibitors(PI)	[0, 1]				

Table 3.3: Parameter values used in the numerical simulations and sensitivity analysis.

3.4.2 Sensitivity analysis

We carry out sensitivity analysis in order to find out the contribution of vital parameters on the model dynamics, most specifically to establish the parameters that have significant influence on the HIV-related NHL dynamics. We employ, among the numerous sensitivity methodologies, the Latin Hypercube Sampling (LHS) scheme which is a form of Monte Carlo stratified sampling technique that can be applied to multiple variables. The technique used during LHS is sampling without replacement. It is designed to accurately recreate the input distribution through sampling in fewer iterations when compared to the Monte Carlo Method. LHS allows us to simultaneously obtain an unbiased estimate of the model output for a given set of input parameter values. We use the LHS by computation of Partial Rank Correlation Coefficients (PRCC) of each parameter value sampled by LHS scheme, and the outcome values derived from uncertainty analysis [8].

3.4.2.1 Results

We use the model parameter values defined in Table 3.3 to simulate the full range of parameters. To achieve this, we employ the LHS technique with 1000 simulations per run to analyse the sensitivity of the parameters to the dynamics of the cancer cells. We observe from Figures 3.2 and 3.3, that parameters $\beta_1, \alpha_{12}, s_1, s_2, d_{12}, d_1, d_{10}, k_1$ and K_{10} , mostly associated with the cytokines present in the cancer-immune environment have significant influences on the number of cancer cell count, i.e significant PRCC. As observed in Figure 3.2, the parameters $\beta_1, \alpha_{12}, s_1, d_1, s_2$ and d_{10} have positive correlation, implying that an increase in the magnitude of these parameters will result in an increase in the number of cancer cell count, for instance, they have the potential to aggravate the cancer growth. On the other hand, as observed in Figure 3.3 parameters d_{12}, k_1 and K_{10} have great potential to considerably minimize the aggressive growth of the cancer cells when increased (negative correlation). Intervention measures in terms of immunotherapy should therefore aim at controlling the mentioned parameters in order to curb the cancer growth since the system is truly sensitive to the change in these parameters.

3.4. Numerical simulations

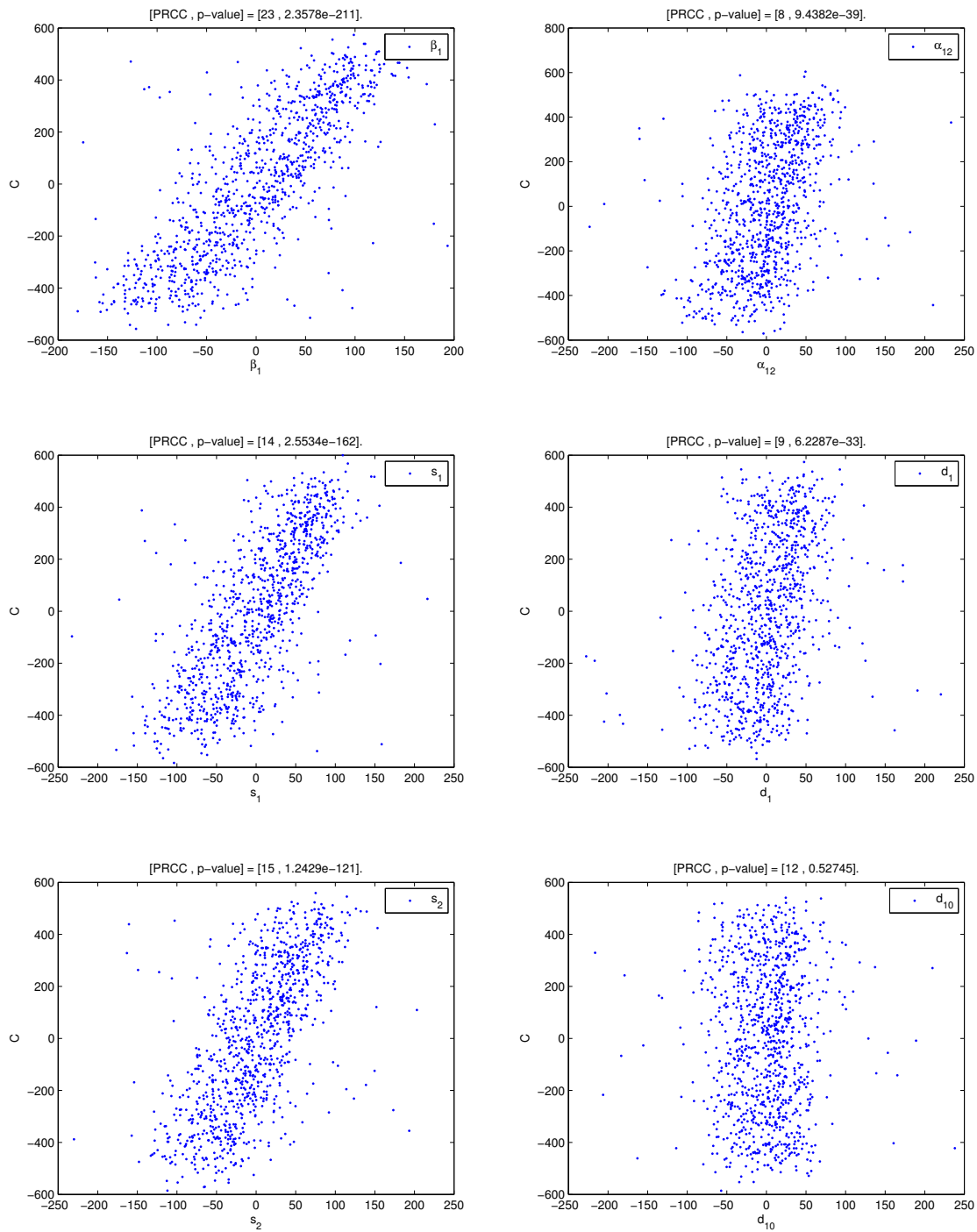


Figure 3.2: Partial Rank scatter plots of the ranks for the cancer cell count, C and each of the sampled input parameters with significant PRCCs using the values in Table 3.3 and 1000 simulations per run.

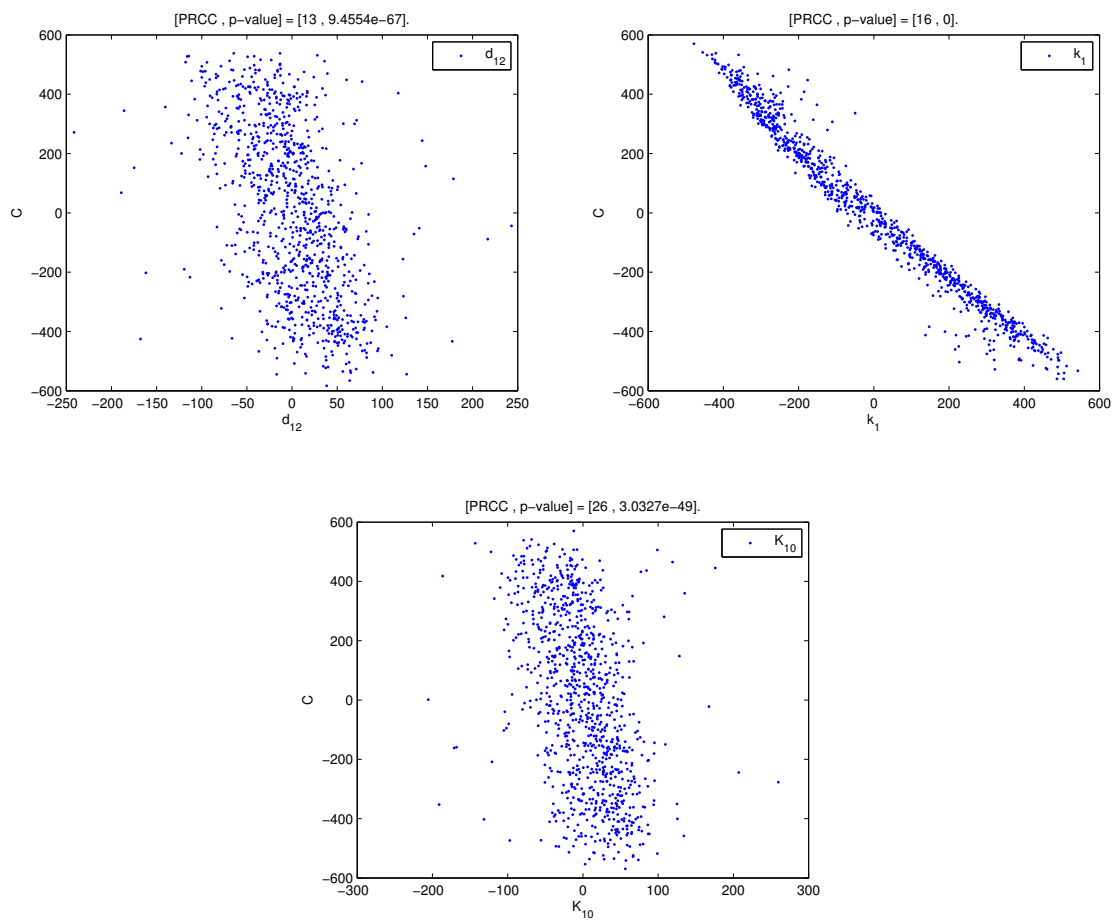
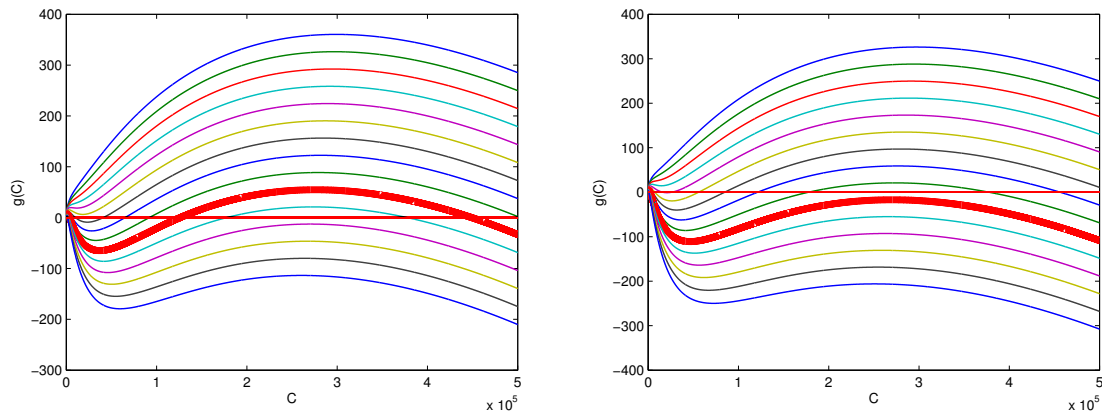


Figure 3.3: Partial Rank scatter plots of the ranks for the cancer cell count, C and each of the sampled input parameters with significant PRCCs using the values in Table 3.3 and 1000 simulations per run.

3.4.3 Numerical results

The results presented below of the numerical simulations for system (3.3.1) were obtained using Matlab ODE45 Solver which employ simultaneously the fourth and fifth order Runge Kutta schemes. Unless otherwise stated, parameters are as stated in Table 3.3. The initial conditions used in the numerical simulations unless stated otherwise, were set as follows; the initial value for the cancer density was set at; $C(0) = 100$ cells/ml while the rest of the state variables used in our model the initial values were set at their quasi steady-states. For instance, the patients are assumed to be in homeostasis, constant cell population/concentration.



(a) With no HIV treatment; $\zeta_p = \zeta_r = 0$ and (b) With HIV treatment; $\zeta_p = \zeta_r = 0.8$ and $\beta_3 = 2.0 \times 10^{-5} - 5.5 \times 10^{-5}$ steps of $2.5 \times \beta_3 = 2.0 \times 10^{-5} - 5.5 \times 10^{-5}$ steps of 2.5×10^{-6}

Figure 3.4: The $g(C)$ as a function of C with different values of β_3 (rate of cancer loss in the population) with other parameters as in Table 3.3 and the other variables at their steady states. No chemotherapy treatment initiated.

Figure 3.4 shows the results of our simulation for $g(C)$ as a function of C , with different values of cancer killing rate, β_3 . Every one of the trajectories represents different parameter value of β_3 and the values increase from top to the bottom trajectory/line. The values considered were in the range 2×10^{-5} to 5.5×10^{-5} for both cases; with and without HIV treatment with a step size of 2.5×10^{-6} (arithmetic distribution). A closer look at the trajectories, interestingly show that HIV treatment is important in cancer growth control. A typical example is to consider $\beta_3 = 4.25 \times 10^{-5}$ represented by the thicker trajectory. Without treatment we can

have three possible cancer steady states while one steady state is observed for the case with treatment.

3.4.4 Bifurcation analysis

This is a qualitative change in the behaviour/ dynamics of a dynamical system produced by varying a parameter in the equation. Bifurcation occurs when a fixed point of the system being considered changes its stability. According to [10] we have the following definition

Definition 3.4.1. Consider a class of ordinary differential equations (ODE's) that depend on one parameter δ ,

$$x' = f(x, \delta) \quad (3.4.1)$$

where $f : \mathbb{R}^{n+1} \rightarrow \mathbb{R}^n$ is analytic for $\delta \in \mathbb{R}$, $x \in \mathbb{R}^n$. Let $x = x_0(\delta)$ be a class of equilibrium points of equation (3.4.1), i.e $f(x_0(\delta), \delta) = 0$. We now set

$$y = x - x_0(\delta),$$

then

$$y' = A(\delta)y + \mathcal{O}(|y|^2),$$

where $A(\delta) = \frac{\partial f}{\partial x}(x_0(\delta), \delta)$.

Let $\delta_1, \delta_2, \dots, \delta_n(\delta)$ be the eigenvalues of $A(\delta)$. If for some i , $\text{Re}\delta_i(\delta)$ changes sign at $\delta = \delta_0$, we say that δ_0 is a bifurcation point of equation (3.4.1).

From the analysis in Figure 3.4, we observe that the parameter β_3 is important in our model since it plays an effective role in defining the cancer behaviour. We thus investigate numerically, the bifurcation of the model parameter β_3 , responsible for the immune response. The graphs in Figure 3.5, display the bifurcation diagrams for the treatment and no treatment cases. Figures 3.5(a) and 3.5(b) are plots of the non-zero steady state solutions of $g(C^*) = 0$ as a function of the parameter, β_3 . This analysis helps in understanding the behaviours of the model, i.e the critical values of the bifurcation parameter where the behaviour of the model system (4.2.1) changes. Figure 3.5 shows two saddle node bifurcation points. We observe the existence of

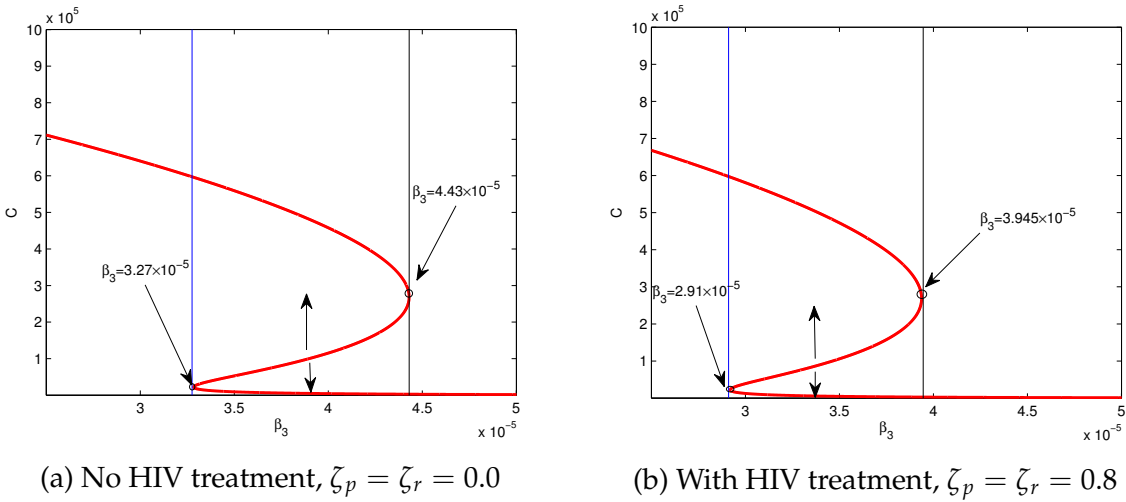


Figure 3.5: Bifurcation diagram: Non-trivial solutions of $g(C^*) = 0$ as a function of β_3 with the rest of parameters as in Table 3.3 with the other variables at their steady states.

multiple equilibria with respect to the different range of values for β_3 . Considering Figure 3.5(a), one steady state exists for both $\beta_3 < 3.27 \times 10^{-5}$ and $\beta_3 > 4.43 \times 10^{-5}$. These exact values where the bifurcation occurs are obtained from the plots in Figure 3.4(a). However, for $3.27 \times 10^{-5} < \beta_3 < 4.43 \times 10^{-5}$ we have three equilibria. It is also clear from the figure that the upper branch where $\beta_3 < 4.43 \times 10^{-5}$ and the lower branch of the graph where $\beta_3 > 3.27 \times 10^{-5}$, we have stable equilibrium of the cancer whereas for the middle is unstable equilibrium. The same is evident for Figure 3.5(b) where one solution exists for both $\beta_3 < 2.91 \times 10^{-5}$ and $\beta_3 > 3.945 \times 10^{-5}$ and three for $2.91 \times 10^{-5} < \beta_3 < 3.945 \times 10^{-5}$. This implies that for the regions $\beta_3 > 4.43 \times 10^{-5}$ in Figure 3.5(a) and $\beta_3 > 3.945 \times 10^{-5}$ in Figure 3.5(b), all the trajectories are attracted to the trivial cancer solution or the non-aggressive steady state disregarding the initial conditions. For $\beta_3 < 3.27 \times 10^{-5}$ in Figure 3.5(a) and $\beta_3 < 2.91 \times 10^{-5}$ in Figure 3.5(b), the aggressive cancer equilibrium is an attractor for all the initial conditions.

A consideration of the same initial conditions, say $(C, \beta_3) = (1 \times 10^5, 3.5^{-5})$, in Figures 3.5(a) and 3.5(b) yields different long term dynamic results. In the absence of treatment, the system will eventually settle to the aggressive steady state. On the other hand, in the presence of treatment, the system settles to a non-aggressive steady state. This underscores the importance of HIV treatment and early identifi-

cation of the cancer.

The population dynamics of the cancer cell of our system is depicted in the time series plot, Figure 3.6, where the solution is observed to stabilize after around $5\frac{1}{2}$ years for a value of $\beta_3 = 1 \times 10^{-7}$.

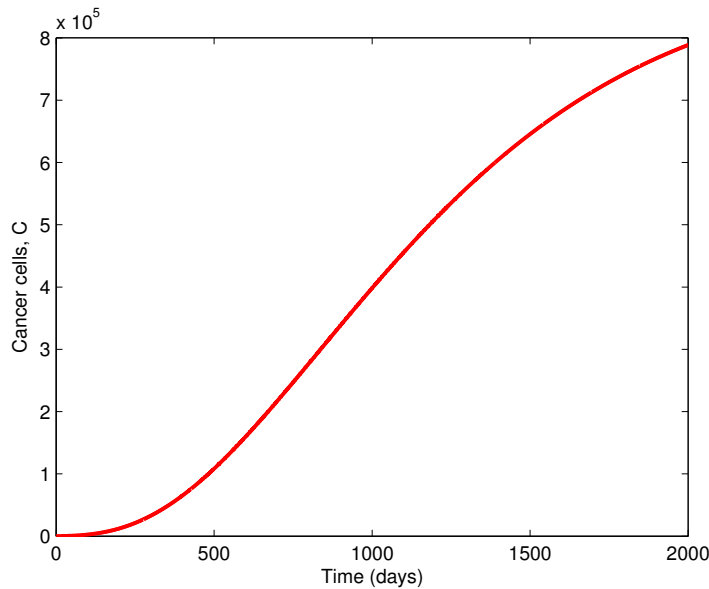


Figure 3.6: Population dynamics of the cancer cells in model system (4.2.1) with the parameters as in Table 3.3. Initial conditions: $M_1(0) = 40000$ cells/ml, $M_2(0) = 10000$ cells/ml, $T_4(0) = 5 \times 10^5$ cells/ml, $T_4^i(0) = 0$ cells/ml, $V(0) = 1000$ copies/mL, $T_8(0) = 100$ cells/ml and $C(0) = 100$ cells/ml.

The time series plot in Figure 3.6 is considered for different infection rates, $\mu_2 = 2.4 \times 10^{-8}$ and $\mu_2 = 2.4 \times 10^{-5}$ in the presence of HIV treatment. The results are presented in Figure 3.7. As seen in Figures 3.7(a) and 3.7(b), for a smaller infection rate, treatment reduces cancer growth while treatment has no effect on the cancer growth for high infection rate values. So, treatment alone in the absence of reduced infection rates does not have a significant impact on cancer growth dynamics.

Figure 3.8 shows the dynamics of the CD8 T cell population. For Figure 3.8(a), where the infection rate of the CD4⁺ T cells is low, we observe significant growth of the CD8 T cells in the presence of treatment. Similarly, as in Figure 3.7(b), no changes are obtained for higher infection rates.

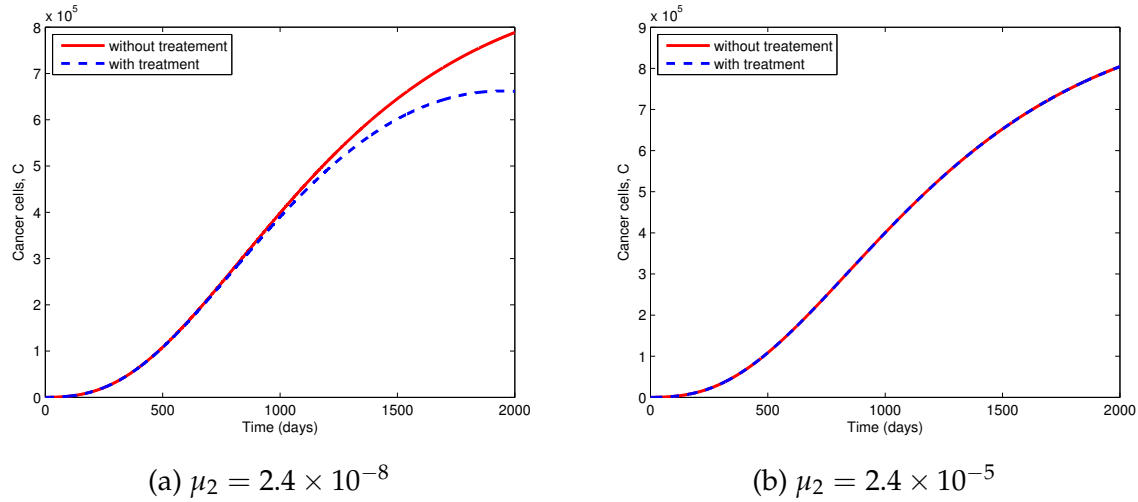


Figure 3.7: Population dynamics of the cancer cells in model system (4.2.1) with only HAART therapy, with $\zeta_r = \zeta_p = 0.5$ and the rest of the parameters as in Table 3.3. Initial conditions: $M_1(0) = 400000$ cells/ml, $M_2(0) = 100000$ cells/ml, $T_4(0) = 5 \times 10^5$ cells/ml, $T_4^i(0) = 0$ cells/ml, $V(0) = 1000$ copies/mL, $T_8(0) = 100$ cells/ml and $C(0) = 100$ cells/ml.

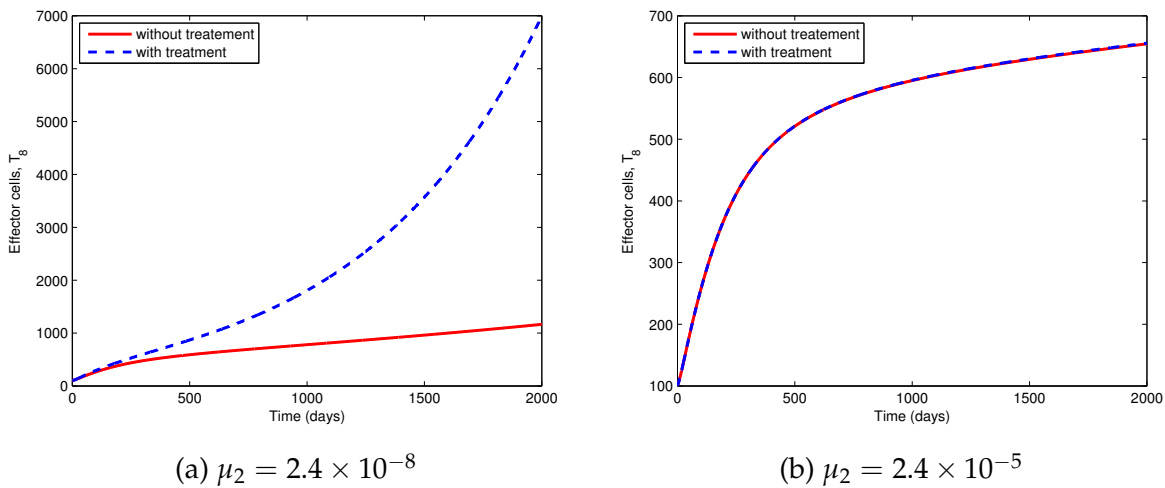


Figure 3.8: Numerical simulation of model system (4.2.1) for the evolution of the CD8⁺ T cells (effector cells) with RTIs and PIs treatment of efficacies, $\zeta_r = \zeta_p = 0.5$ and the rest of the parameters as in Table 3.3. Initial conditions: $M_1(0) = 400000$ cells/ml, $M_2(0) = 100000$ cells/ml, $T_4(0) = 5 \times 10^5$ cells/ml, $T_4^i(0) = 0$ cells/ml, $V(0) = 1000$ copies/mL, $T_8(0) = 100$ cells/ml and $C(0) = 100$ cells/ml.

3.5 Conclusion

In this chapter, we investigated the role of HIV in the model of AIDS-related non-Hodgkin Lymphoma by considering cytokines, macrophages, $CD4^+$ T helper cells, $CD8^+$ T effector cells and the virus in the cancer environment. The chapter has provided some interesting insights as discussed below.

From the numerical analysis, it suffices to deduce that when HIV is present in the cancer environment and no treatment of the HIV initiated in the patient, for a non-aggressive cancer state to be achieved the cancer killing rate has to be higher , i.e. higher immune response as compared to the case where treatment of HIV with HAART is initiated. This implies that the timing of initiating HIV treatment in patients with the cancer is an important factor since the cancer can remain in a non-aggressive state despite lower immune response (the comparison is done with respect to no treatment case).

The bifurcation analysis shows that treatment plays an important role in shifting the steady states. We notice that given the same value of parameter β_3 , the steady states values decrease when HIV treatment is included in the model system and for most of the parameter value β_3 , the existence of only low endemic cancer state is observed. This implies that, as opposed to the no HIV treatment scenario, the cancer can be controlled to a non-aggressive state despite low immune response. We also observe that when the HIV infection rate is low, initiating treatment in patients with HIV-related NHLs reduces cancer growth. Also, no effective control of the cancer will be observed despite HIV treatment as long as the cancer killing rate is small, i.e. weak immune response.

Our model represents a possible long-lasting coexistence of HIV-related NHLs and HIV, because of the existence of the non-zero equilibria. Despite a patient's strong immune response and treatment of the HIV with the reverse transcriptase inhibitors (RTIs) and protease inhibitors (PIs) drugs of efficacy for instance, 50% in our case, complete elimination of the cancer by the immune system is actually not possible. The cancer cell will still remain in the host system unless the cancer elimination rate is very high, though at a lower state that is not so destructive and thus the patient survives with the cancer for a longer period of time. This could also explain why some people live with cancer for many years. Moreover, it can also explain why late initiation of HIV treatment is not very helpful to NHL patients.

Having looked at the present model, and deduced that treatment with both PI and RTI drugs lower the steady state of the cancer, we now incorporate treatment of cancer with chemotherapy in the model as discussed in Chapter 4 that follows. This is with regard that an individual with HIV who develops cancer should be treated for both cancer and HIV. Firstly, we will focus on investigating how to best combine these two drugs i.e. PIs and RTIs in order to reduce cancer load as much as possible as well as maintaining the acceptable T-cell level. Later in the chapter, we will explore the effects of chemotherapeutic drugs on cancer cell dynamics.

Chapter 4

NHL model with HIV treatment and chemotherapy

4.1 Introduction

In this chapter, we relook at the model presented in Chapter 3, with the inclusion of chemotherapy. We first aim to establish the concept that drugs available only against HIV can also be judiciously adjusted to be useful against cancer. As discussed in Chapter 2, consideration of HIV treatment when dealing with the disease or diseases that arise due to HIV infection is very vital for any analysis involving the same. Likewise, individuals with HIV who develop cancer should also be treated for cancer. We therefore, consider cancer treatment administered to patients diagnosed with cancer, more precisely NHL which depends on the type, its stage and prognostic factors [55]. According to [55] the following are the main treatment types;

- i Radiotherapy: use of high energy radiation beams focused on cancerous sites in order to destroy the cancer cells.
- ii Biological therapy: also referred to as immunotherapy, is the administration of immune cells to the cancer site (referred to as local immunotherapy) or the whole body (systemic immunotherapy), in order to incite and strengthen the immune system.

iii Chemotherapy: a drug administered to kill the tumor cell due to their mode of action i.e killing cells that divide more rapidly, a feature associated with tumor cells. These drugs though targeted at the tumor cells, can also be destructive to other cells in the host immune system. The chemotherapy was discovered in chemical warfare during World War I and was actually first used in cancer treatment in the 1940s [7].

The above mentioned therapies are considered for the treatment of NHLs and HLs, but we will focus on chemotherapy as a means of treatment in this study. Our model formulation is as described in Chapter 3 except for the inclusion of the therapy parameters in the relevant model equations. We assume that the treatment will not affect the cytokine equations in our model, therefore for the equations that govern the model with the inclusion of HIV treatment and chemotherapy we will consider the final equations in system (4.2.1) where the state variables and the parameters are described as in Table 3.3.

4.2 Model equations

Following [12, 35], most of the chemotherapeutic drugs are only effective during certain phases of cell cycle (cell cycle specific) and pharmacokinetics indicate that the effectiveness of the chemotherapeutic drugs is bounded. We therefore have the term $(1 - e^{-D})$, a saturation term representing the fraction of the cell killed by a dose, D of chemotherapy. This prompts the inclusion of the cell dose-response term

$$Q_{D_i} = P_i(1 - e^{-D})i \quad \text{for } i = M_1, M_2, T_4, T_4^i, T_8, C.$$

Since the drug concentration in the bloodstream changes with time due to the processes involved, i.e absorption, distribution, metabolism and excretion, we include an equation that tracks that dynamics. Therefore, the terms in the non-homogeneous equation, dD/dt of system (4.2.1) reflects the rate of change in the dosage concentration over a given period of time. $u_{in}(t)$ is a function of time that describes the amount of drug influx into the system and the injection time assuming intravenous administration whereas d_D represents the drug elimination rate. The drug concentration equation assumes instantaneous distribution of the drug into all body parts.

Chapter 4. NHL model with HIV treatment and chemotherapy**48**

The model with the chemotherapy is thus as follows:

$$\left. \begin{array}{l} \frac{dM_1}{dt} = s_1 - k_1 M_1 + \nu M_2 - \gamma_c C M_1 - P_{M_1}(1 - e^{-D}) M_1, \\ \frac{dM_2}{dt} = s_2 + \gamma_c C M_1 - k_2 M_2 - \nu M_2 - P_{M_2}(1 - e^{-D}) M_2, \\ \frac{dT_4}{dt} = s_3 + \frac{\gamma_1 M_1 M_1}{K_{10} + \gamma_2 M_2} + \beta_2 \frac{\gamma_3 T_4 T_4}{K_2 + \gamma_3 T_4} - \mu_1 T_4 - (1 - \zeta_r) \mu_2 V T_4 \\ \quad - P_{T_4}(1 - e^{-D}) T_4, \\ \frac{dT_4^i}{dt} = (1 - \zeta_r) \mu_2 V T_4 - \mu_5 T_4^i - P_{T_4^i}(1 - e^{-D}) T_4^i, \\ \frac{dT_8}{dt} = \epsilon \frac{\gamma_1 M_1}{K_{10} + \gamma_2 M_2} + \beta_2 \frac{\gamma_3 T_4 T_8}{K_2 + \gamma_3 T_4} - \mu_4 T_8 - P_{T_8}(1 - e^{-D}) T_8, \\ \frac{dV}{dt} = (1 - \zeta_p) N \delta_2 T_4^i - \mu_v V, \\ \frac{dC}{dt} = r C^{\frac{3}{4}} \left(1 - \left(\frac{C}{C_0} \right)^{\frac{1}{4}} \right) - \beta_3 C T_8 - P_C(1 - e^{-D}) C, \\ \frac{dD}{dt} = u_{in}(t) - d_D D \end{array} \right\} \quad (4.2.1)$$

where $\gamma_c = \lambda_1 \frac{\alpha_1}{d_1} + \lambda_2 \frac{\alpha_6}{d_6}$, $\gamma_1 = \beta_1 \frac{\alpha_{12}}{d_{12}}$, $\gamma_2 = \frac{\alpha_{10}}{d_{10}}$ and $\gamma_3 = \frac{\alpha_2}{d_2}$.

4.3 Parameter estimation

Table 4.1 provides the description and values of all the parameters that appear in model system (4.2.1). As noted in Chapter 3, most of the parameters are taken from the literature, although not always from cancer experimental data.

Table 4.1: Estimated Parameter values.

Parameter	Description	Values	Units	Source
α_2	production rate of IL-2 due to CD4 ⁺ T cells	5	pg/cell day	[5, 33]
α_1	production rate of TGF- β due to cancers cells	7×10^{-4}	pg/cell day	[5, 60]
α_6	production rate of IL-6 due to cancers cells	7×10^{-5}	pg/cell day	Estimated
α_{10}	production rate of IL-10 due to M_2	5×10^{-4}	pg/cell day	[29, 30, 64]
α_{12}	production rate of IL-12 due to M_1	3×10^{12}	pg/cell day	Estimated in [29]
d_1	degradation rate of TGF- β	10	day ⁻¹	Estimated in [5]
d_2	degradation rate of IL-2	10	day ⁻¹	[33, 51]
d_6	degradation rate of IL-6	0.173	day ⁻¹	[40]
d_{10}	degradation rate of IL-10	5	day ⁻¹	[29]
d_{12}	degradation rate of IL-12	1.188	day ⁻¹	[29, 45]
s_1	influx rate of M_1	8000	cells/ml day	Estimated
s_2	influx rate of M_2	800	cells/ml day	Estimated
s_3	production of CD4 ⁺ T cells by the sources	10000	cells/ml day	Estimated
k_1	per capita death rate of M_1	0.02	day ⁻¹	[29]
k_2	per capita death rate of M_2	8×10^{-3}	day ⁻¹	[29, 31]
λ_1	transformation rate of M_1 by TGF- β	0.075	day ⁻¹	Estimated in [64]
λ_2	transformation rate of M_2 by IL-6	0.075	day ⁻¹	Estimated in [64]
v	transition rate from M_2 to M_1	5×10^{-2}	day ⁻¹	[57, 64]
β_1	proliferation rate of T cells due to IL-12	10^6	cells/ml day	[23]
β_2	proliferation rate of T cells by IL-2	0.1245	pg/cell day	[5, 33, 34]
β_3	loss of cancer cells	$10^{-5} \sim 10^{-9}$	day ⁻¹	[39, 53, 63] and estimated (10^{-9})*
K_2	saturation constant of proliferation by IL-2	2×10^7	pg/ml	[33, 34]
K_{10}	saturation constant for anti-proliferation by IL-10	2.5×10^7	pg/ml	[23]
μ_1	per capita death rate of uninfected CD4 ⁺ T cells	0.02	day ⁻¹	Estimated in [61]
μ_2	infection rate of CD4 ⁺ T cells due to infiltration by free viruses	2.4×10^{-8}	ml/day	Estimated in [61]
μ_4	per capita death rate of CD8 ⁺ T cells	$0.03 \sim 0.0412$	day ⁻¹	[33, 34] 0.03*
μ_v	clearance rate (loss) of free viruses	2.4	day ⁻¹	Estimated in [61]
μ_5	per capita death rate of infected CD4 ⁺ T cells	0.26	day ⁻¹	Estimated in [61]
δ_2	lytic death rate of infected CD4 ⁺ T cells	0.24	day ⁻¹	Estimated in [61]
r	cancer growth rate	$0.18 \sim 0.19$	day ⁻¹	[5, 33, 34, 63] 0.19*
C_0	maximum cancer density	10^6	cells/ml	Estimated in [39]
N	number of virions released upon burst by an infected T4 cell	1000	cells/ml	[61] and assumed
ζ_r	the measure of efficacy of reverse transcriptase inhibitors(RTIs)	[0, 1]		
ζ_p	the measure of efficacy of protease inhibitors(PIs)	[0, 1]		
$P_{M_1}, P_{M_2}, P_{T_4}, P_{T_4^i}, P_{T_8}$	chemo-induced immune cell death rates	0.6	day ⁻¹	[12, 35]
P_C	chemo-induced cancer cell death rate	0.9	day ⁻¹	[12, 35]
d_D	chemo drug elimination rate	0.9	day ⁻¹	[12, 35]

4.4 Simulation results

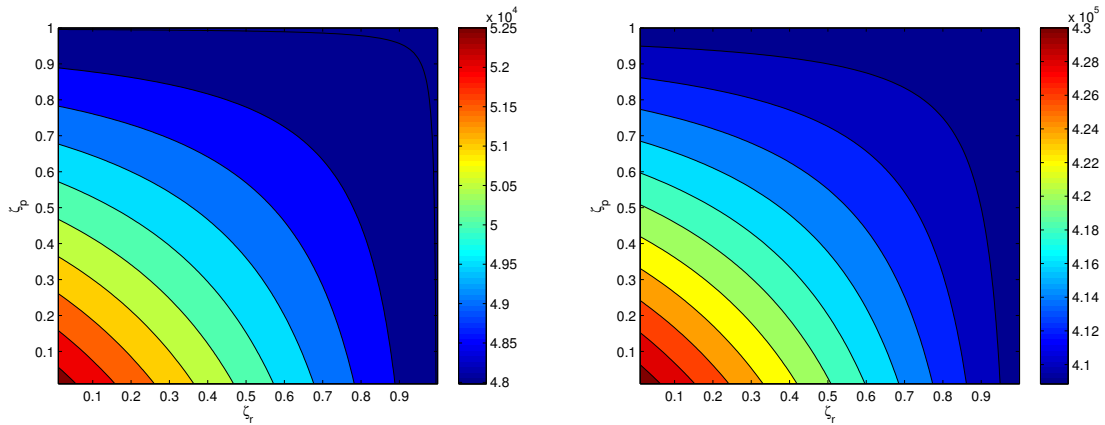
4.4.1 Results with no chemotherapeutic drug

As in Chapter 3, the results presented below of the numerical simulations for system (3.3.1) were obtained using Matlab ODE45 Solver which employs simultaneously the fourth and fifth order Runge Kutta schemes. Unless otherwise stated, parameters are as stated in Table 4.1.

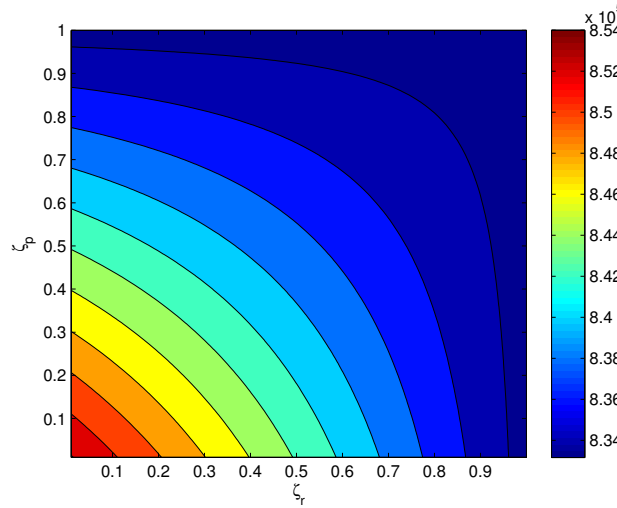
We take the following initial conditions: for instance, from steady state of equation (3.2.3), we get $s_2 = k_2 M_2$ and since $k_2 = 0.008/\text{day}$, implying that, $M_2 = 100000\text{cells/ml}$. Same applies for M_1 and T_4 . We have; $M_1(0) = 400000 \text{ cells/ml}$, $M_2(0) = 100000 \text{ cells/ml}$, $T_4(0) = 500000 \text{ cells/ml}$, $T_4^i(0) = 0 \text{ cells/ml}$, $V(0) = 1000 \text{ copies/ml}$, $T_8(0) = 100$ and $C(0) = 100 \text{ cells/ml}$. We explore the effect of combined HIV therapy on the cancer. Recall that one type of drugs (RTIs) reduces the infection of T_4 cells by virus by a factor $1 - \zeta_r$, while another type of drugs (PIs) reduces the proliferation rate of virus within infected T_4 cells by a factor $1 - \zeta_p$. We say that RTI has efficacy of $n\%$ if $\zeta_r = n/100$, and similarly PI has efficacy of $n\%$ if $\zeta_p = n/100$.

Figure 4.1 is a combination therapy map for cancer cells. Starting with $C(0) = 100 \text{ cells/ml}$, it shows the density of cancer cells at days 350, 1000 and 20000 for any combination of ζ_r and ζ_p . In particular, with no drugs, $C(350) = 5.25 \times 10^4 \text{ cells/ml}$, $C(1000) = 4.3 \times 10^5$ and $C(2000) = 8.54 \times 10^5$.

We observe from our analysis that a dose of 90% effective RTI drugs with as low as 10% effective PI drugs will reduce the state of the cancer and same applies for 90% effective PI drugs. Therefore, to achieve the best outcome, one of the drug efficacy should be approximately 90% and above or both drugs should be approximately 80% effective. From the convex shape of the equi-cancer-cell-number curves we see that if two drugs, ζ_r with efficacy $n\%$ and ζ_p with efficacy $m\%$, ($n + m < 100$) can be replaced by just one drug, say ζ_r , with efficacy $\zeta_r = (n + m)\%$ then the result will lead to a decrease in the growth of the cancer.



(a) Contour plot showing cancer cells density after 350 days
(b) Contour plot showing cancer cells density after 1000 days



(c) Contour plot showing cancer cells density after 2000 days

Figure 4.1: Combination therapy Map: $C(t)$ as a function of RTIs (ζ_r) and PIs (ζ_p) combination with the rest of parameters as defined in Table 3.3. The color bar shows the $C(t)$ values for various drug combination.

Figure 4.2 shows the reduction curves that represent the reduction of cancer load after time, $t = 350, 1000, 2000$ days for various $\zeta_r = \zeta_p$ anti-virus drugs combinations. The cancer load is observed to reduce though mildly as the efficacy, $\zeta_r = \zeta_p$ gets larger as observed in Figure 4.1 as well. This implies that best outcome, i.e. smaller cancer load will be achieved with the two drugs both of higher efficacies. After 350 days, initiating treatment with anti-virus drugs leads to a smaller cancer

Chapter 4. NHL model with HIV treatment and chemotherapy

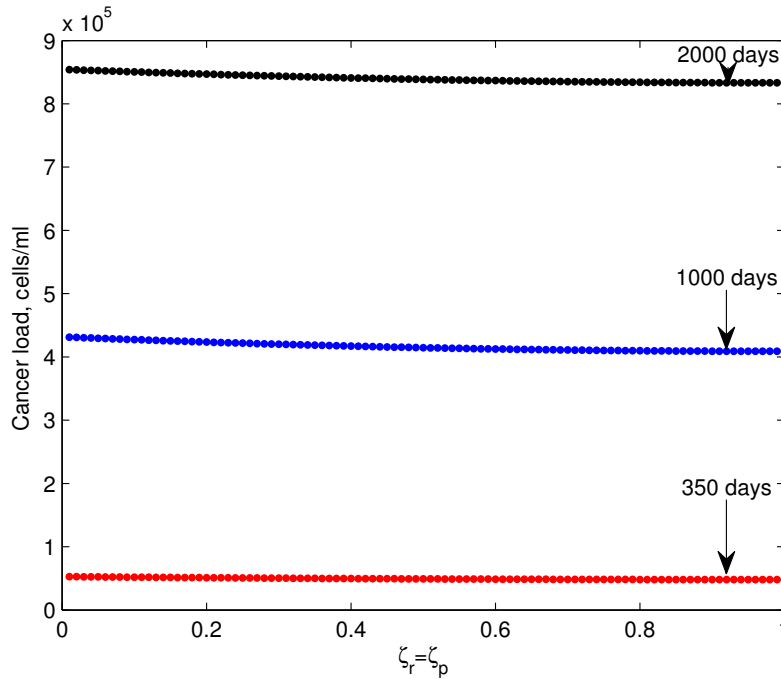
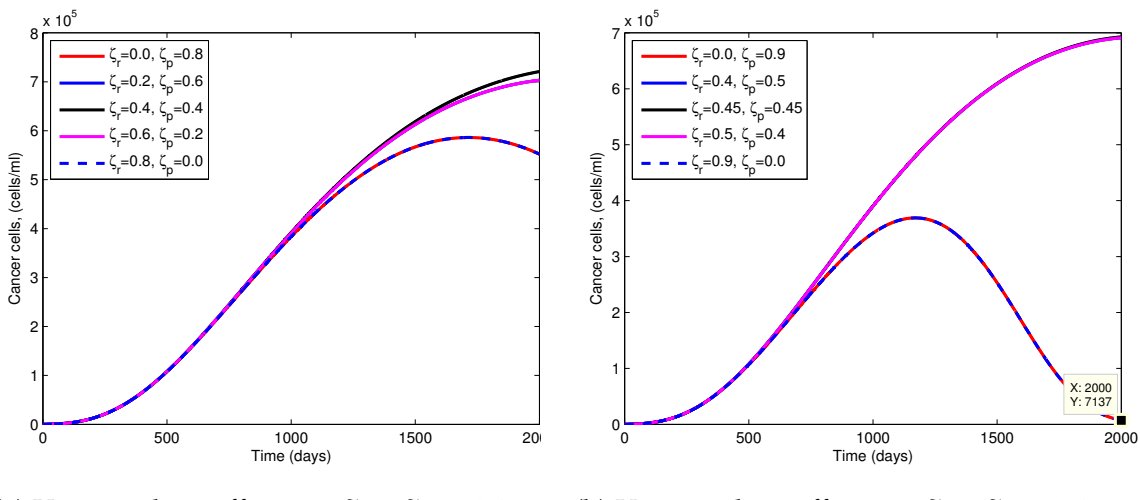


Figure 4.2: Cancer reduction curves after various time, t with the rest of the parameters as in Table 3.3. The dots correspond to the cancer load at each anti-virus drug combination, with $\zeta_r = \zeta_p$.



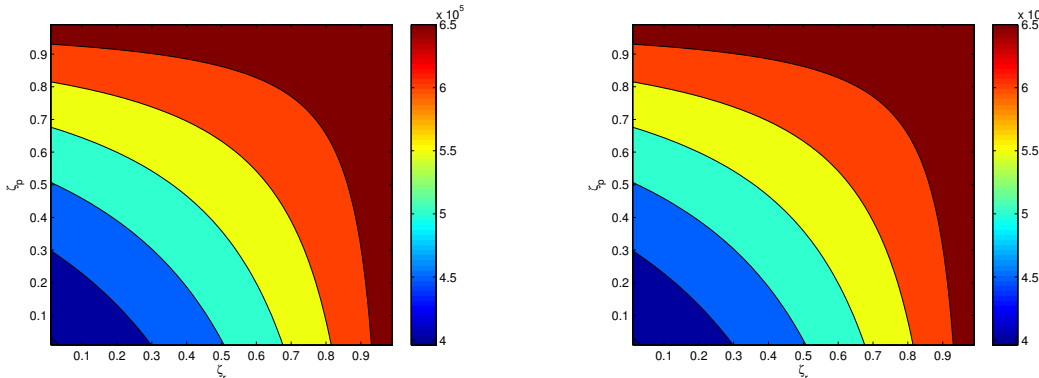
(a) Varying drug efficacies, $\zeta_r + \zeta_p = 0.8$ (b) Varying drug efficacies, $\zeta_r + \zeta_p = 0.9$

Figure 4.3: Evolution of cancer cells in system (3.3.1) over 2000 days with the rest of the parameters as defined in Table 3.3.

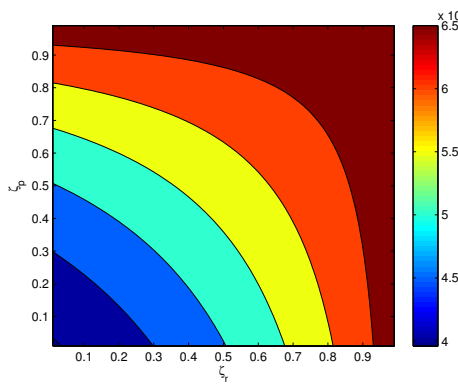
load as compared to $t = 1000$ or $t = 2000$ days. This might explain why early treatment of HIV would be preferred as it leads to reduction of the cancer density to a lower state.

Figure 4.3 shows the dynamics of cancer cells with inclusion of varying efficacies of the two drugs in the model. In Figure 4.3(a), we observe a slight decrease after the 2000 days in the growth of the cancer cells given either $\zeta_r = 0.0$ ($\zeta_p = 0.8$) and $\zeta_p = 0.8$ ($\zeta_r = 0.0$). However, given $\zeta_r = m, \zeta_p = n$, where $n, m < 0.8$, and $n + m = 0.8$, combining the drugs will not effectively reduce the cancer load and as discussed above from Figure 4.1 replacing the two drugs with one of higher efficacy would lead to a significant decrease in the cancer growth. Figure 4.3(b), shows varying the efficacies of the drugs such that we obtain 90% effective drug combination. Similarly, given $\zeta_r = 0.0$ ($\zeta_p = 0.9$) and $\zeta_p = 0.9$ ($\zeta_r = 0.0$), we observe the number density of cancer cells reducing to 7.137×10^3 as seen in Figure 4.3(b).

Figure 4.4 is a color map of T cells at $t=350, 100$ and 2000 days as a function of ζ_r and ζ_p . Similar to Figure 4.1, we see that if the two drugs with efficacies $m\%$ and $n\%$ can be replaced by one drug with efficacy $(n + m < 100)$ then the resulting number of CD4+ T cells will increase. However, Figure 4.5 shows the T cells color map without cancer in the host population. We observe an increase in number of T cells to a higher level after 1000 days as compared to Figure 4.4.

Chapter 4. NHL model with HIV treatment and chemotherapy

(a) Contour plot showing CD4 T cells density after 350 days
(b) Contour plot showing CD4 T cells density after 1000 days



(c) Contour plot showing CD4 T cells density after 2000 days

Figure 4.4: Combination therapy map: $T_4(t)$, for $t=350, 1000$ and 2000 days as a function of RTI (ζ_r) and PI (ζ_p) combination, the parameters are as in Table 3.3. The color bar shows the $T_4(t)$ values for various drug combination.

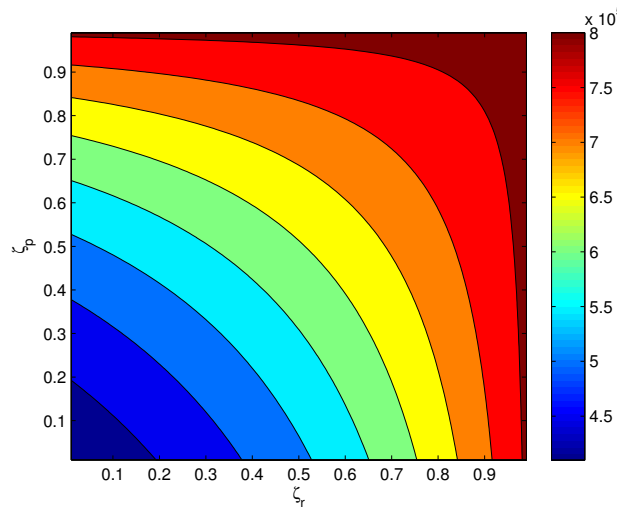


Figure 4.5: Combination therapy map: $T_4(t)$, for $t=1000$ days with no cancer in the host population as a function of RTI (ζ_r) and PI (ζ_p) combination, the parameters are as in Table 3.3. The color bar shows the $T_4(t)$ values for various drug combination.

Indeed, suppose we wish to maintain the CD4+ T cells population at level $\bar{T}_4 = 500000$ cells/ml after 1000 days. We use Figure 4.6 to determine the pairs ζ_r, ζ_p for which the corresponding equi-color curve indicates the level \bar{T}_4 ; we can write these pair of points as $\zeta_p = h(\zeta_r)$ where h is a monotone decreasing function. Next, for each pair $\zeta_r, h(\zeta_r)$ we depict from Figure 4.4 the corresponding value of $C(1000)$, and denote it by $C(\zeta_r)$. As we vary ζ_r over the range of all possible efficacy levels, say $a < \zeta_r < b$, for which $\zeta_r = h(\zeta_r)$ is also a realizable efficacy level, we obtain a range of values $C(\zeta_r)$. Figure 4.6 shows a typical curve $C = C(\zeta_r)$; we see that the smallest number of cancer cells occurs at one of the extreme points, i.e at $\zeta_r = a$ or $\zeta_r = b$. Thus, the best strategy is to choose the minimum or maximum level of efficacy for ζ_r and the corresponding ζ_p by $\zeta_p = h(\zeta_r)$.

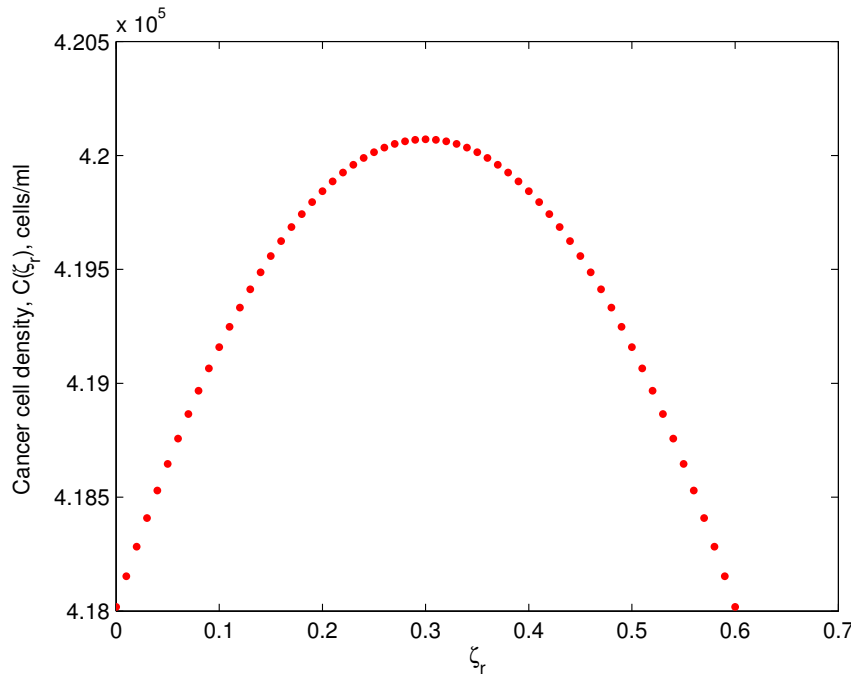


Figure 4.6: Cancer cell density curve, $C(\zeta_r)$ at $t = 1000$ days, for each pair $(\zeta_r, h(\zeta_r))$, the parameters are as in Table 3.3.

Considering Figure 4.7, we analyse the effect of inclusion and exclusion of HAART therapy on the dynamics of T_4 cells with no cancer in the host immune system. Note that the T_4 cell count in this case is cells per ml. Figure 4.7(a) shows the profile

of $CD4^+$ T cells over a period of 2000 days with no cancer in the host population, where we observe that the cells count increase then eventually decrease to a steady state of approximately 1.2×10^5 cells/ml (120 cells/ mm^3) and remain in that state for the rest of the time. We also observe from Figure 4.7(b), where treatment of HIV is initiated with the two drugs each of efficacy, 50% , i.e $\zeta_r + \zeta_p = 1$ an increase in the number of T_4 cells followed by a decrease that eventually stabilizes at approximately 5.0×10^5 cells/ml (500 cells/ mm^3). Similar results to Figure 4.7(b) hold when the efficacies of the drugs are not the same i.e $\zeta_r \neq \zeta_p$ (but $\zeta_r + \zeta_p = 1$) except for either $\zeta_r > 0.8$ or $\zeta_p > 0.8$, where we observe the steady state stabilizing at approximately 1.3×10^6 cells/ml (1300 cells/ mm^3) see Figure 4.8(b). This imply that for the T_4 cells count to stabilize at approximately 500 cells/ mm^3 , the efficacies of the drugs administered to the patients should be $m + n = 100\%$ with $m, n < 80\%$. Similar results are observed with cancer in the population.

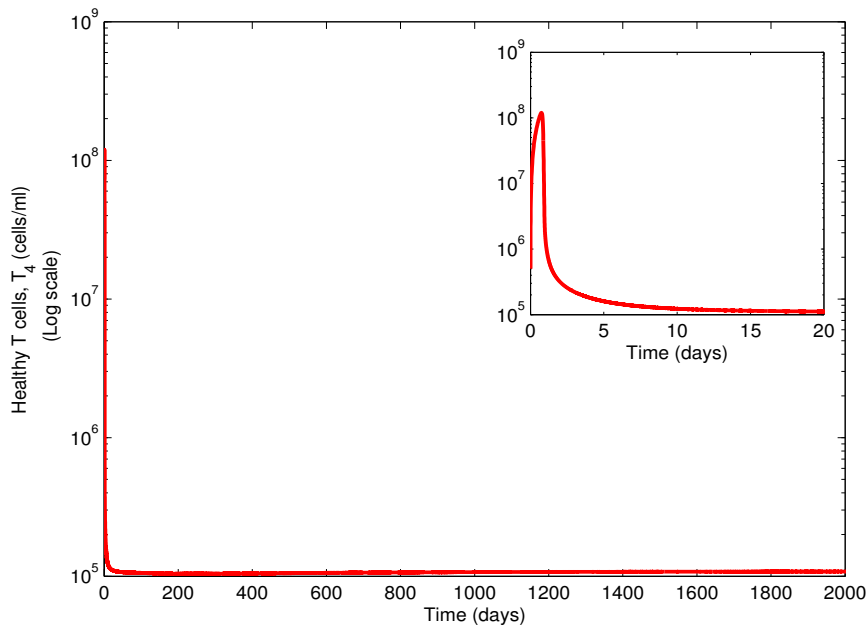
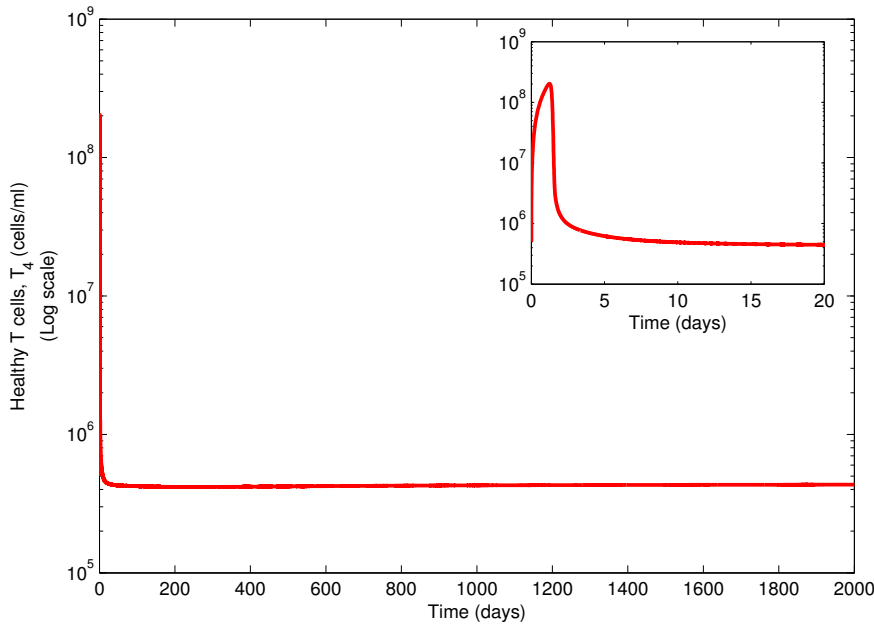
(a) No treatment, $\zeta_r = \zeta_p = 0.0$ (b) With treatment, $\zeta_r = 0.5, \zeta_p = 0.5$

Figure 4.7: Population dynamics of T helper cells (cells/ml) over a period of 2000 days for the case of no cancer in the host immune system, i.e $C = 0$. The rest of the parameters as defined in Table 3.3. The inset plots show the T helper cells dynamics over 20 days.

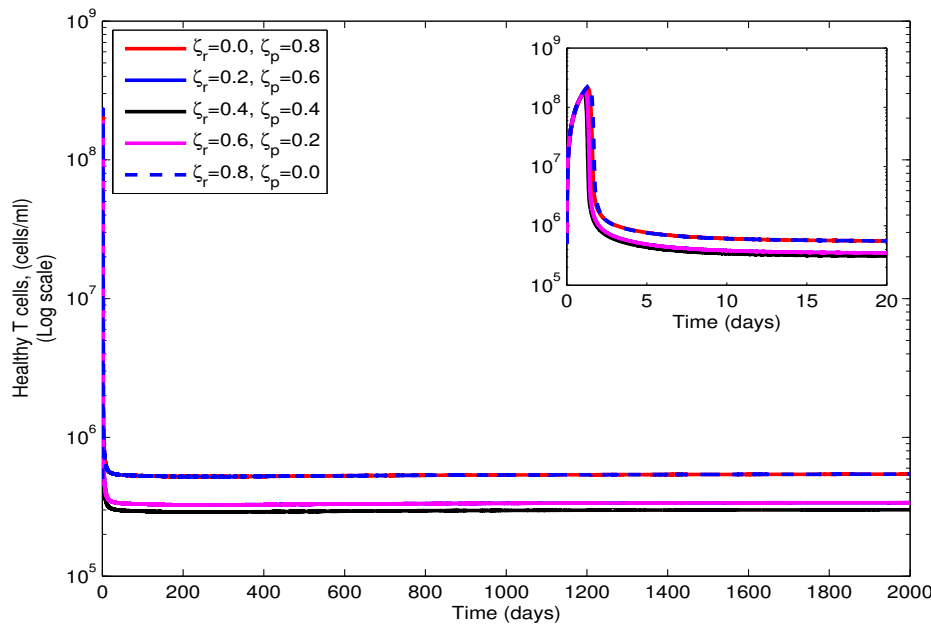
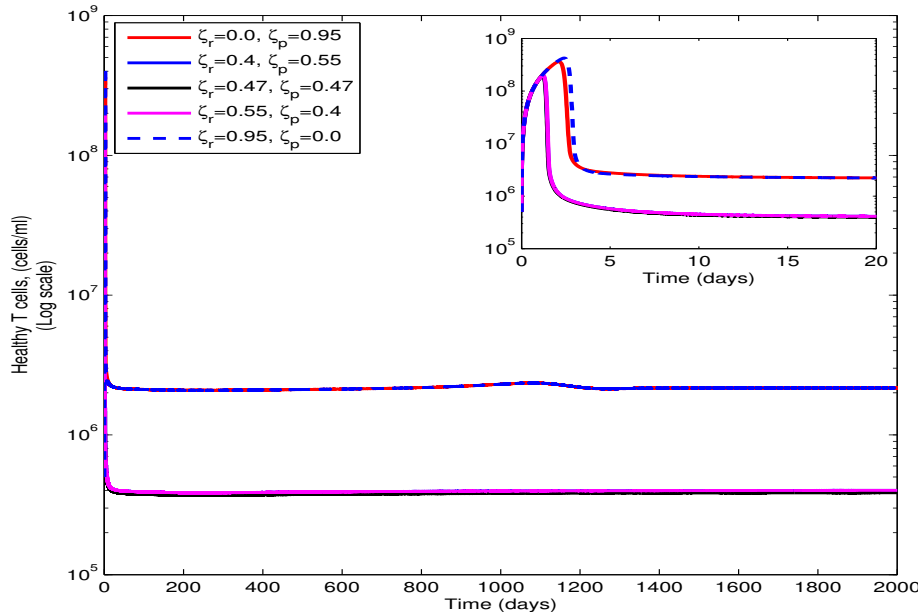
(a) Varying drug efficacies, $\zeta_r + \zeta_p = 0.8$ (b) Varying drug efficacies, $\zeta_r + \zeta_p = 0.95$

Figure 4.8: Population dynamics of T helper cells (cells/ml) with cancer in the host immune system over 2000 days with the rest of the parameters as defined in Table 3.3. The inset plots show the T helper cells dynamics over 20 days.

4.4.2 Results with chemotherapeutic drug

Considering the parameter associated with chemotherapy intervention, $u_{in}(t)$, we assume administration of $2.3869 \text{ mg/L} \simeq 2386900 \text{ pg/mL}$ per every 21 days for cancer cells, as suggested in [12]. Therefore, if T (every 21 days) is the drug infusion time, then the mass inflow is given by

$$u_{in} = \begin{cases} 2.3869, & t = T = 21n, \quad n = 1, 2, \dots \\ 0, & \text{otherwise} \end{cases}$$

The drug administration pattern is depicted in Figure 4.9.

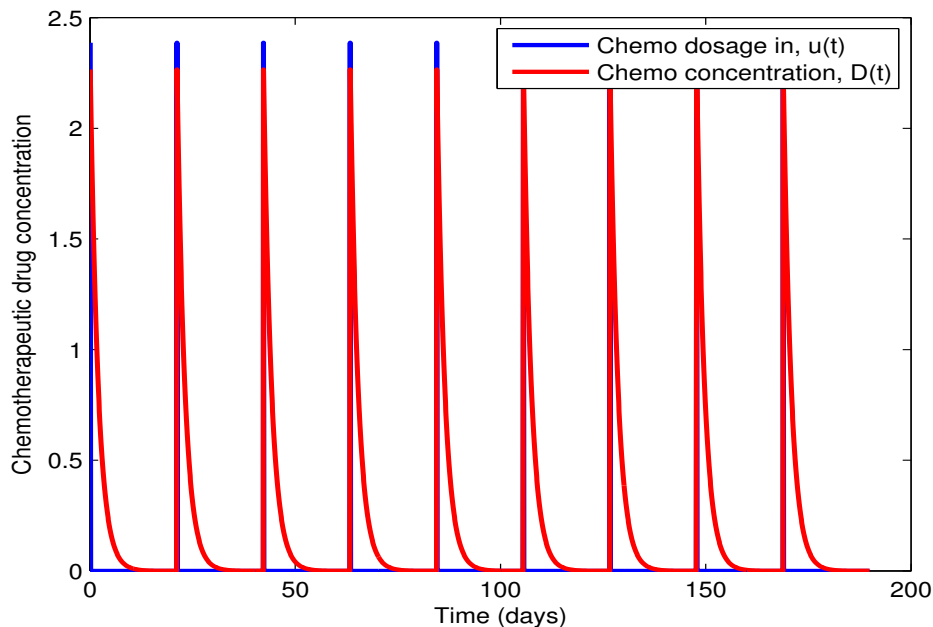
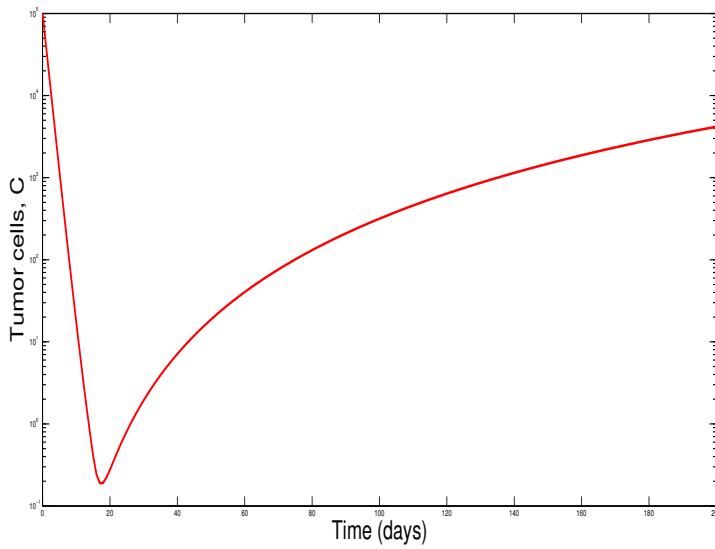
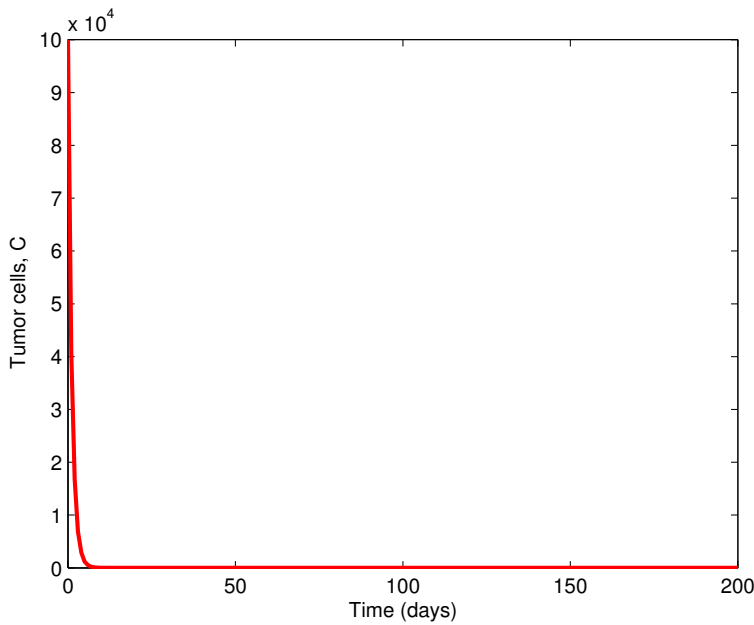


Figure 4.9: Chemotherapeutic drug dose concentration in the system administered 1 day every 21 days for 200 days i.e 9 doses every 21 days.



(a) Drug elimination rate, $d_D = 0.9$ with a log scale on the vertical axis.



(b) Drug elimination rate, $d_D = 0.1$

Figure 4.10: Population dynamics for a period of 200 days of the cancer cells in model system (4.2.1) with both therapies (HAART and chemotherapy) with parameters as in Table (3.3). Initial conditions: $M_1(0) = 2000$ cells/ml, $M_2(0) = 2500$ cells/ml, $T_4(0) = 3 \times 10^5$ cells/ml, $T_4^i(0) = 1 \times 10^3$ cells/ml, $V(0) = 4 \times 10^3$ copies/mL, $T_8(0) = 3000$ cells/ml .

With the inclusion of chemotherapy in the model, no difference is seen for the cases with and without HAART therapy. Chemotherapy administration occurs when the cancer cells are detectable, thus considering the initial state of the cancer as 1×10^5 cells/ml, we observe that the drug is very effective in eliminating the cancer cells when the decay rate in the system is smaller. Administering same therapy but with a higher decay rate in the system, the cancer will not be eliminated and instead the cancer will regrow as seen in Figure 4.10a. This implies that the length of time a chemotherapeutic drug has to act against the cancer is very critical since smaller decay/elimination rate implies a longer time required to act against the cancer. Figure 4.10b thus shows the effect of smaller decay rate on cancer elimination.

4.5 Conclusion

In this chapter we investigated the effect of HIV treatment and chemotherapy in the AIDS-related non-Hodgkin Lymphoma. We extended the model developed in Chapter 3 to include the chemotherapeutic intervention terms.

We investigated the effect of combined RTI and PI drugs on reduction of cancer load. We created a combination therapy map for cancer-cells number: $C(t)$ for $t=350, 1000$ and 2000 days as a function of ζ_r and ζ_p combination. The results clearly show the best combination of the two drugs that reduces the cancer load in the host environment while maintaining the CD4+ T cells at an 'acceptable' level.

The use of either of the drugs would be effective if the efficacy is approximately 90% and above which might not be plausible. For an effective suppression of the cancer cells growth, an optimal combination of PIs and RTIs presents the best treatment option, with the right efficacies as seen in our results. We can therefore, conclude from our model that using moderate efficacy from different classes of the HAART regimen can be as good as using a high efficacy therapy from a single drug.

However, despite patient's strong immune response and treatment of the HIV with the reverse transcriptase inhibitors (RTIs) and protease inhibitors (PIs) drugs of higher efficacy for instance, 80% efficacy, complete elimination of the cancer by the immune system is actually not possible unless the cancer elimination rate is very high i.e very strong immune response and thus early initiation of treatment might help reduce the cancer load in the system as in our results. It might also explain

Chapter 4. NHL model with HIV treatment and chemotherapy

62

why late initiation of treatment is not very helpful to NHL patients.

Our results might also give an insight on the approximate efficacies of the HAART regimen used in the treatment of HIV for instance, the PIs and RTIs. From the results we can deduce that the efficacies of each of the drug in HAART regimen given to HIV patients are approximately less than 80% since initiation of treatment with drugs of the said efficacies result in steady state of approximately $500 \text{ cells mm}^{-3}$ to $800 \text{ cells mm}^{-3}$ as the case mostly observed in HIV patients under highly active antiretroviral therapy.

In the case of chemotherapy intervention, the time taken by the drug to act on the cancer is an important factor and thus to reduce cancer related deaths, the chemotherapeutic drugs used should have low elimination rates. This implies that the absorption, distribution and clearance of the drugs take much longer time and this might explain why a few of these drugs are more effective when given at a slow continuous rate for a few days at a time.

Chapter 5

Discussions

In this dissertation, we have formulated a deterministic model showing the dynamics of HIV-related non-Hodgkin's lymphoma (NHL). Firstly, we analysed a HIV-related NHL with HIV treatment and later extended the model to include chemotherapeutic intervention.

The first model presented in Chapter 3, described the dynamics of HIV-related NHL with inclusion of HIV treatment. The model comprised immune cells population, cancer cells (NHL), cytokine population and lastly the free virus population. The proof that the state variables were positive and bounded was carried out to ensure that the region which the model is analysed is biologically feasible. The main aim here was to investigate the existence of steady states and analyse their stability by carrying out bifurcation analysis. Mathematical analysis in this chapter indicates existence of cancer-free steady states and existence of endemic (cancer-persistence) steady state. Sensitivity analysis on the parameters was carried out to establish the parameters that play a significant role in the dynamics of the cancer. Numerical simulations were then carried out to enhance the understanding of the theoretical results. Our numerical results indicate the existence of multiple equilibria with respect to different range of values for cancer elimination rate, the parameter responsible for immune response. This implies that the cancer elimination rate plays a crucial role in defining the cancer behaviour. Bifurcation analysis of this parameter, shows the immune response is crucial in suppressing the cancer growth and is only effective if it falls within a specific window of opportunity to effectively suppress the cancer growth. The results also indicate that despite initiation of HIV treat-

ment with the combined therapy, unless the HIV infection rate is low, no significant reduction in the cancer cell count would be realised.

In Chapter 4, we extended the model to incorporate chemotherapy treatment. Our main interest here was to explore the effect of combined HIV therapy on the cancer cell density and the effects of chemotherapy on the cancer growth. We determined how to optimally choose the proportions of RTI and PI in the anti HIV combination drug HAART in order to maintain an acceptable level of CD4+ T cells and, at the same time, to reduce cancer growth as much as possible. Our numerical results might give an insight on the approximate efficacies of the HAART regimen used in the treatment of HIV for instance, the PIs and RTIs. Our results also show that, for an effective suppression of the cancer cell growth, combination of PIs and RTIs is the best treatment to employ with the right efficacies as discussed in Chapter 4 in order to reduce the cancer growth as much as possible.

The study by Hoffman et al. [26], indicated that most of the NHL diagnosis occur when CD4 T cell count is less than 350 cells mm^{-3} and/or is less than 200 cells mm^{-3} . Our analysis was done with the T cells at steady states implying low CD4 T cell count and therefore, the predictions from our model results would be useful since most of the patients commence their HAART dosage when the count is less than 350 cells mm^{-3} and thus the appropriate combination would be better when initiated immediately after the diagnosis. Stebbing et al.[56] analysed the probability of developing NHL after initiation of HAART and deduced that combined antiretroviral regimen that is, PIs and RTIs when administered reduce the risk of developing NHL. In our study however, we have analysed and discussed the right combination of these two drugs that would reduce the cancer load to a manageable level when initiated at the right time in HIV-NHL patient.

We further investigated the effect of chemotherapy on the dynamics of the tumor and the numerical results pertaining to chemotherapeutic drugs might explain why a few of these drugs are more effective when given at a slow continuous rate. The results also explain why late initiation of HIV treatment might not be helpful to NHL patients.

The model presented in this thesis is a very simplified caricature of a complex biological interaction of immune cells, cytokines and HIV (with the inclusion of combination antiretroviral therapy treatment) in a cancer environment and therefore it

has some lucid limitations. The model does not take into account the spatial growth of the cancer and the associated metabolic elements and pathways. There is also paucity of experimental data for model verification. Despite these limitations, the model results have significant bearings on NHL dynamics and its coexistence with HIV. Our model provides a unique opportunity to influence policy on HIV related cancer treatment and management.

The model presented in this thesis is a very simplified description of a complex biological interaction of immune cells, cytokines and HIV (with the inclusion of combination antiretroviral therapy treatment) in a cancer microenvironment and therefore it has some lucid limitations. There is also paucity of experimental data for model verification. Despite these limitations, the model results have significant bearings on NHL dynamics with the inclusion of combined HIV treatment that might provide a unique opportunity to influence policy on NHL treatment and management.

List of references

- [1] *AIDS-Related Lymphoma Treatment-for health professionals.* Available at <http://www.cancer.gov/cancertopics/pdq/treatment/AIDS-related-lymphoma/HealthProfessional/page1>. Accessed 15 March, 2015.
- [2] Monocyte. Available at <http://en.wikipedia.org/wiki/Monocyte>. Accessed on 10 June, 2015.
- [3] NHL facts. Available at http://www.medicinenet.com/non-hodgkins_lymphomas/article.htm#non-hodgkins_lymphoma_facts. Accessed on May,14 2015.
- [4] B. J. Alimonti, T.B. Blake, and R.K. Fowke. Mechanisms of CD4⁺ T lymphocyte cell death in human immunodeficiency virus infection and AIDS. *Journal of General Virology*, 84(7):1649–1661, 2003.
- [5] J.C. Arciero, T.L. Jackson, and D.E. Kirschner. A mathematical model of tumor-immune evasion and siRNA treatment. *Discrete and Continuous Dynamical Systems - Series B*, 4(1):39–58, 2004. <http://AIMsciences.org>.
- [6] K. Asadullah, W. Sterry, and H.D. Volk. Interleukin-10 therapy-review of a new approach. *Pharmacological Reviews*, 55(2):241–269, 2003.
- [7] R.H. Blair, D.L. Trichler, and D.P. Gaille. Mathematical and statistical modeling in cancer systems biology. *Frontiers in Physiology*, 3(227), 2012. doi: 10.3389/fphys.2012.00227.
- [8] S. M. Blower and H. Dowlatabadi. Sensitivity and uncertainty analysis of complex models of disease transmission: an hiv model, as an example. *International Statistical Review*, pages 229–243, 1994.
- [9] R.J De Boer, P. Hogeweg, H.F. Dullens, R.A. De Weger, and W. Den Otter. Macrophage T lymphocyte interactions in the anti-tumor immune response: A mathematical model. *Journal of Immunology*, 134(4):2748–2758, 1985.

- [10] K. Canan Çelik. Bifurcation analysis and its applications. In Dr. Mykhaylo Andriychuk, editor, *Numerical simulation-from theory to industry*, 978-953-51-0749-1. InTech, 2012. Available from: <http://www.intechopen.com/books/numerical-simulation-from-theory-to-industry/bifurcation-analysis-and-its-applications>.
- [11] M. Aboulafia David, P. Liron, and J. Dezube Bruce. AIDS-related non-Hodgkin lymphoma: Still a problem in the era of HAART. *AIDS Reader*, 14(11):1–7, 2004.
- [12] L.G. de Pillis, W. Gu, and A.E.Radunskaya. Mixed immunotherapy and chemotherapy of tumors: modelling, applications and biological interpretations. *Journal of Theoretical Biology*, 238:841–862, 2006.
- [13] D.K. Duff, S. Thompson, S. Braye, D. Price, M. Loewenthal, and M.J. Boyle. The cytokine milieu of HIV-associated non-hodgkin's lymphoma favours aggressive tumors. *AIDS*, 14(1):92–94, 2000.
- [14] L. Fassone, G. Gaidano, C. Ariatti, D. Vivenza, D. Capello, A. Gloghini, A.M. Cilia, D. Buonaiuto, D. Rossi, C.Pastore, A. Carbone, and G. Saglio. The role of cytokines in the pathogenesis and management of AIDS-related lymphomas. *Leukemia & Lymphoma*, 38(5):81–488, 2000.
- [15] R.M. Ford, M.M. McMahon, and M.A. Wehbi. HIV / AIDS and colorectal cancer . *Gastroenterology and Hepatology*, 4(4):274–278, 2008.
- [16] J.J. Goedert. The epidemiology of acquired immunodeficiency syndrome malignancies. *Seminars in Oncology*, 27(4):390–401, 2000.
- [17] S. Gopal, W. A. Wood, S. J.Lee, T.C. Shea, K.N. Naresh, P.N. Kazembe, C. Casper, P.B. Hesseling, and R.T. Mitsuyasu. Meeting the challenge of hematologic malignancies in sub-Saharan Africa. *Blood*, 119(22):5078–87, 2012. doi: 10.1182/blood-2012-02-387092.
- [18] S. Gordon and F.O. Martinez. Alternative activation of macrophages: mechanism and functions. *Immunity*, 32(5):593–604, 2010.
- [19] H. Groux, M. Bigler, J..E de Vries, and M.G. Roncarolo. Inhibitory and stimulatory effects of il-10 on human cd8+ t cells. *Journal of Immunology*, 160(7):3188–3193, 1998.
- [20] A.E. Grulich and C.M. Vajdic. The epidemiology of non-hodgkin lymphoma. *Pathology*, 25:409–419, 2005.

- [21] Y. Gu. *Circulating cytokines and risk of B-cell non-Hodgkin lymphoma*. Number 3331864. UMI, 2008.
- [22] C. Guiota, P. P.Delsanto, A. Carpinteri, N. Pugno, Y. Mansurye, and T.S. Deisboeck. The dynamic evolution of the power exponent in a universal growth model of tumors. *Journal of Theoretical Biology*, 240(3):459–463, 2006. doi:10.1016/j.jtbi.2005.10.006.
- [23] W. Hao and A. Friedman. The LDL-HDL profile determines the risk of atherosclerosis: A mathematical model. *PLoS ONE*, 9(3), 2014. doi:10.1371/journal.pone.0090497.
- [24] M. U. Hashmi, M. Suleman, S. M. J. Zaidi, and M. Habib. Modeling the tumor-immune interaction cultured with chemotherapy and cytokine Interleukin IL-2 under the influence of Immunodeficiency Viruses. *American-Eurasian Journal of Toxicological Sciences*, 6(4):74–82, 2014. doi: 10.5829/idosi.aejts.2014.6.4.85241.
- [25] M. Heusinkveld and S.H. van der Burg. Identification and manipulation of tumor associated macrophages in human cancers. *Journal of Translational Medicine*, 9(216), 2011. doi:10.1186/1479-5876-9-216.
- [26] C. Hoffmann, M. Henrich, D. Gillor, G. Behrens, B. Jensen, A. Stoehr, S. Esser, J. van Lunzen, I. Krznaric, M. MÄijller, M. Oette, M. Hensel, J. Thoden, G. FÄd'tkenheuer, and C. Wyen. Hodgkin lymphoma is as common as non-Hodgkin lymphoma in HIV-positive patients with sustained viral suppression and limited immune deficiency: a prospective cohort study. *HIV Medicine*, 16(4):261–264, 2015. <http://dx.doi.org/10.1111/hiv.12200>.
- [27] S. Hsu, J.W. Waldron Jnr, P. Hsu, and A.J. Hough Jnr. Cytokines in malignant lymphomas. *Human Pathology*, 24:1040–1056, 1993.
- [28] National Cancer Institute. *What is Non-Hodgkin Lymphoma?* Available at <http://www.cancer.gov/cancertopics/wyntk/non-hodgkin-lymphoma/page2>. Accessed on October, 7 2014.
- [29] J.Day, A. Friedman, and L.S.Schlesinger. Modelling the immune rheostat of macrophages in the lung in response to infection. *Proceedings of the National Academy of Sciences U.S.A*, 106(27):11246–11251, 2009. doi: 10.1073/pnas.0904846106.
- [30] J.P.Edwards, X.Zhang, K.A. Frauwirth, and D.M. Mosser. Biochemical and functional characterization of three activated macrophage populations. *Journal of Leukocyte Biology*, 80(6):1298–1307, 2006.

- [31] J. Keane, M.K. Balcewicz-Sablinska, H.G. Remold, G.L. Chupp, B.B. Meek, M.J. Fenton, and H. Kornfeld. Infection by *Mycobacterium tuberculosis* promotes human alveolar macrophage apoptosis. *Infection and Immunity*, 65(1):298–304, 1997.
- [32] J. Kekow, W. Wachsman, J.A. McCutchan, W.L. Gross, M. Zachariah, Carson D.A, and M. Lotz. Transforming growth factor-beta and suppression of humoral immune responses in HIV infection. *Journal of Clinical Investigation*, 87(3):1010–6, 1991. doi:10.1172/JCI115059.
- [33] D. Kirschner and J.C. Panetta. Modeling immunotherapy of the tumor-immune interaction. *Journal of Mathematical Biology*, 37:235–252, 1998.
- [34] V.A. Kuznetsov, I.A. Makalkin, M. A. Taylor, and A. S. Perelson. Nonlinear dynamics of immunogenic tumors: Parameter estimation and global bifurcation analysis. *Bulletin of Mathematical Biology*, 56(2):295–321, 1994.
- [35] S.K. Kwang, C. Giphil, and H.J. Il. Optimal treatment strategy for a tumor model under immune suppression. *Computational and Mathematical Methods in Medicine*, 2014:13 pages, 2014. <http://dx.doi.org/10.1155/2014/206287>.
- [36] Y. Lai, C.J. Jeng, and S.C. Chen. The roles of CD4⁺ T cells in tumor immunity. *ISRN Immunology*, 2011:6 pages, 2011. doi:5402/2011/497397.
- [37] M. Alexandra Levine, L. Seneviratne, B.M. Espina, A.R. Wohl, A. Tulpule, B. N. Nathwani, and P.S. Gill. Evolving characteristics of AIDS-related lymphoma. *Blood*, 96(13):4084–4090, 2000.
- [38] G. Weiqing L.G de Pillis, F. K. Renee, C. Craig, M. Daub, D. Gross, J. Moore, and B. Preskill. Mathematical model creation for cancer chemo-immunotherapy. *Computational and Mathematical Methods in Medicine*, 10(3):165–184, 2009.
- [39] Y. Louzoun, C. Xue, G.B. Lesinski, and A. Friedman. A mathematical model for pancreatic cancer growth and treatment. *Journal of Theoretical Biology*, 351:74–82, 2014.
- [40] Z.Y Lu, H. Brailly, J. Wijdenes, R. Bataille, J.F. Rossi, and Klein B. Measurement of whole body interleukin-6 (il-6) production: prediction of the efficacy of anti-il-6 treatments. *Blood*, 86(8):3123–31, 1995.
- [41] D. Mani, M. Haigentz, and D.M. Aboulafia. Lung cancer in HIV infection. *Clinical Lung Cancer*, 13(1):5–13, 2012. doi:10.1016/j.clcc.2011.05.005.

- [42] P. Moosa. Hodgkin's lymphoma and human immunodeficiency virus infection. In Prof. Krassimir Metodiev, editor, *Immunodeficiency*, ISBN: 978-953-51-0791-0. In-Tech, 2012. Available from: <http://www.intechopen.com/books/immunodeficiency/hodgkin-s-lymphoma-and-human-immunodeficiency-virus-infection>.
- [43] P.M. Mwamba, W. O. Mwanda, N. W. Busakhala, R. M Strother, P. J. Loehrer, and S.C. Remick. AIDS-related non-Hodgkin's lymphoma in Sub-Saharan Africa: current status and realities of therapeutic approach. *Lymphoma*, page 9, 2012. <http://dx.doi.org/10.1155/2012/904367>.
- [44] J. Newcomb-Fernandez. Cancer in the HIV-infected population. *The Center for AIDS*, 2003.
- [45] R. Ohno, Y. Yamaguchi, T. Toge, T. Kinouchi, T. Kotake, M. Shibata, Y. Kiyohara, S. Ikeda, I. Fukui, A. Gohchi, Y. Sugiyama, S. Saji, S. Hazama, M. Oka, K. Ohnishi, Y. Ohhashi, S. Tsukagoshi, and T. Taguchi. A dose-escalation and pharmacokinetic study of subcutaneously administered recombinant human interleukin 12 and its biological effects in Japanese patients with advanced malignancies. *Clinical Cancer Research*, 6(7):2661–9, 2000.
- [46] C. Pastore, G. Gaidano, P. Ghia, L. Fassone, A.M. Cilia, A. Gloghini, D. Capello, D. Buonaiuto, S. Gonella, S. Roncella, A. Carbone, and G. Saglio. Patterns of cytokine expression in AIDS related non-hodgkin's lymphoma. *British Journal of Haematology*, 103:143–14, 1998.
- [47] J.M. Pluda, D.J. Venzon, G. Tosato, J. Lietzau, K. Wyvill, D.L. Nelson, E.S. Jaffe, J.E. Karp, S.Broder, and R.Yarchoan. Parameters affecting the development of non-Hodgkin's lymphoma in patients with severe human immunodeficiency virus infection receiving antiretroviral therapy. *Journal of Clinical Oncology*, 11:1099–1107, 1993.
- [48] B. Puvaneswaran and B. Shoba. Misdiagnosis of tuberculosis in patients with lymphoma. *South African Medical Journal*, 103(1), 2013.
- [49] F. A. Rihan, R. Abdel, and H. Duaa. Delay differential model for tumour-immune dynamics with HIV infection of CD4+ T-cells. *International Journal of Computer Mathematics*, 90(3):594–614, 2013. Available at <http://dx.doi.org/10.1080/00207160.2012.726354>.
- [50] J.M Roda, Y. Wang, L.A Sumner, G.S Phillips, C.B. Marsh, and T.D. Eubank. Stabilization of HIF-2 α induces sVEGFR-1 production from tumor-associated macrophages and

- decreases tumor growth in amurine melanoma model. *Journal of Immunology*, 189:3168–3177, 2012. <http://www.jimmunol.org/content/189/6/3168>.
- [51] S.A. Rosenberg and M.T. Lotze. Cancer immunotherapy using interleukin-2 and interleukin-2-activated lymphocytes. *Annual Review of Immunology*, 4:681–709, 1986.
- [52] K.R. Ruff, A. Puetter, and L.S. Levy. Growth regulation of simian and human AIDS-related non-hodgkin's lymphoma cell lines by TGF- β_1 and IL-6. *BMC Cancer*, 7(35), 2007.
- [53] N. Seki, A.D. Brooks, C.R. Carter, T.C. Back, E.M. Parsoneault, M.J. Smyth, R.H. Wiltzout, and T.J. Sayers. Tumor-specific CTL kill murine renal cancer cells using both perforin and Fas ligand-mediated lysis in vitro, but cause tumor regression in vivo in the absence of perforin. *Journal of Immunology*, 168(7):3484–3492, 2002.
- [54] A. Sevko and V. Umansky. Myeloid-derived suppressor cells interact with tumors in terms of myelopoiesis, tumorigenesis and immunosuppression; thick as thieves. *Journal of Cancer*, 4(1):3–11, 2013. doi:10.7150/jca.5047.
- [55] American Cancer Society. *Non-Hodgkin Lymphoma*. Available at <http://www.cancer.org/cancer/non-hodgkinlymphoma/detailedguide/non-hodgkin-lymphoma-what-is-non-hodgkin-lymphoma>. Accessed on 30 June, 2015.
- [56] J. Stebbing, B. Gazzard, S. Mandalia, A. Teague, A. Waterston, V. Marvin, M. Nelson, and M. Bower. Antiretroviral treatment regimens and immune parameters in the prevention of systemic AIDS-related non-Hodgkin's lymphoma. *Journal of Clinical Oncology*, 22(11):2177–2183, 2004.
- [57] C. SteinmÃijller, G. Franke-Ullmann, M.L. Lohmann-Matthes, and A. EmmendÃúrffer. Local activation of nonspecific defense against a respiratory model infection by application of interferon-gamma: comparison between rat alveolar and interstitial lung macrophages. *American Journal of Respiratory Cell and Molecular Biology*, 22(4):481–490, 2000.
- [58] E. Takeuchia, H. Yanagawaa, Y. Suzukia, K. Shinkawaa, Y. Ohmotoa, H. Bandob, and S. Sone. IL-12 induced production of IL-10 and interferon- γ by nonnuclear cells in lung cancer-associated malignant pleural effusions. *Lung Cancer*, 35(2):171–177, 2002.
- [59] G. Trinchieri. Cytokines acting on or secreted by macrophages during intracellular infection (IL-10, IL-12, IFN- γ). *Current Opinion in Immunology*, 9(1):17–23, 1997.

-
- [60] T.S. Tzai, A.L. Shiao, L.L. Liu, and C.L. Wu. Immunization with TGF-beta antisense oligonucleotide-modified autologous tumor vaccine enhances the antitumor immunity of MBT-2 tumor-bearing mice through upregulation of MHC class I and Fas expressions. *Anticancer Research*, 20(3A):1557–1562, 1999.
 - [61] V.C. Rebecca and R. Sigui. A delay-differential equation model of HIV infection of CD4⁺ T-cells. *Mathematical Biosciences*, 165:27–39., 2000.
 - [62] F. Villinger and A.A. Ansari. Role of IL-12 in HIV infection and vaccine. *European Cytokine Network*, 21(3):215–218, 2010.
 - [63] S. Wilson and D. Levy. A mathematical model of the enhancement of tumor vaccine efficacy by immunotherapy. *Bulletin of Mathematical Biology*, 74, 2012. doi: 10.1007/s11538-012-9722-4.
 - [64] W. Yunji, Y. Tianyi, M. Yonggang, V. H. Ganesh, Z. Jianqiu, L. L. Merry, and J. Yu-Fang. Mathematical modeling and stability analysis of macrophage activation in left ventricular remodeling post-myocardial infarction. *BMC Genomics*, 13(6), 2012. Available at <http://www.biomedcentral.com/1471-2164/13/S6/S21>.
 - [65] L. Zhang, J. Yang, J. Qian, H. Li, J.E. Romaguera, L.W. Kwak, M. Wang, and Q. Yi. Role of the microenvironment in mantle cell lymphoma: IL-6 is an important survival factor for the tumor cells. *Blood*, 120:3783–3792, 2012.

Modelling the dynamics of HIV-related non-Hodgkin lymphomas in the presence of HIV treatment and chemotherapy

Rosemary Aogo[†] and F. Nyabadza ^{†*}

[†]*Department of Mathematics, University of Stellenbosch, P. Bag X 1, Matieland, 7602, South Africa*

Abstract

Non-Hodgkin lymphomas (NHLs) and HIV co-existence both *in vivo* and *in vitro* in a tumor-immune environment has been studied to a large extent. Most of the studies have suggested that specific cytokines produced by the immune system cells and the tumor play an important role in the dynamics of NHLs. In this paper, a mathematical model describing the NHL-immune system interaction in the presence of the Human Immunodeficiency Virus (HIV), HIV treatment and chemotherapy is developed. The formulated model, described by non-linear ODEs shows existence of multiple equilibria whose stability and bifurcation analysis are presented. From the bifurcation analysis, bistability regions are evident. We observe that with and without HIV treatment, the system results in a non-aggressive tumor size or aggressive tumor (full-blown tumor) depending on the initial conditions. The results further suggest that at a low endemic state, patients can live for longer period of time with the tumor which might explain why some patients can live with cancer for many years. However, initiation of HIV treatment in patients with NHL is observed to lower these endemic states of the tumor. Our results explain why late initiation of HIV treatment might not be helpful to NHL patients. We further investigated the effect of chemotherapy on the dynamics of the tumor. Our simulation results might explain why a few of these chemotherapeutic drugs are more effective when given at a slow continuous rate. The model provides a unique opportunity to influence policy on HIV related cancer treatment and management.

Keywords: NHL; cytokines; modelling; simulation; bifurcation; HIV; chemotherapy.

1 Introduction

The greatest risk factor for the development of NHLs is immune deficiency often caused by the Human immunodeficiency virus (HIV) [38]. Patients with HIV infection develop lymphoma (cancers of the lymphocytes/immune system) about 100 times more often and Kaposi's sarcoma about 400 times more often than non-infected individuals [1, 38]. AIDS-related non-Hodgkin's lymphomas (AIDS-NHLs) are the second most frequent cancer in the wake of Kaposi's sarcoma associated with AIDS, and are the cause of death in approximately 16% of HIV-infected individuals [8, 14, 20]. NHLs are consistently derived from B-cells and are characterized by extreme aggressiveness. Non-Hodgkin's lymphoma, is a heterogeneous group of malignancies involving a controlled clonal expansion of transformed B cells [11, 17]. Untreated HIV infection as widely

*Corresponding author: Email: rosemary@aims.ac.za

discussed, causes reduction in the number of T cells and hence more B cells are made. When the latter occurs too fast, there are increased chances that they develop into NHL which are classified viz.: AIDS-related Burkitt's lymphoma (AIDS-BL), AIDS-related diffuse large cell lymphoma (AIDS-DLCL) and AIDS-related primary effusion lymphoma (AIDS-PEL) [7].

Immune response to tumor growth exist in tumor-bearing hosts. Tumors often induce dysfunction in the response mechanisms by impairing the regulatory networks driven by cytokines. The role of cytokines in the pathogenesis and management of AIDS-NHL has been studied extensively see for instance [5, 7, 11]. Cytokines are regulatory molecules that are secreted by various cell types for the regulation of immune response to infection. The ones that play a crucial role in the pathological processes of tumors are classified as interleukins (ILs), tumor necrosis factors (TNFs), transforming growth factors (TGFs), interferons (IFNs) and colony-stimulating factors (CSFs) [13]. Cytokines influence the biology of tumors either by promoting tumor growth or impairing antitumor responses [5]. There is a disruption of normal cytokine regulatory networks in the presence of immune suppression [18]. Research into the cytokines expressed in AIDS- related lymphomas has shown elevated serum levels of IL-6 and IL-10 in HIV infected individuals [5, 7, 19].

With regards to the functions of the cytokines expressed in patients with NHL, TGF- β acts as a negative growth regulator of the lymphoma-derived cell line and has been shown to be potentially, an inhibitory factor in the regulatory network of AIDS-related lymphomagenesis [3, 20]. It has an immunosuppressive role, mediated predominantly by its effects on T cells and antigen-presenting cells (APCs) [6], thus favouring the growth of malignancies. As indicated by [40], TGF- β is likely to contribute to the deficit in T-cell surveillance which is of paramount importance in suppressing tumor growth. Anti-tumor activities by the human body often involves the secretion of interleukin (IL)-12 which enhances natural killer cell activities [25] by activation of CD8 effector cells and the induction of interferon γ (IFN- γ) an essential cytokine in tumor regression [23]. It has also been shown that IL-12 induces IL-10 production as a negative feedback for IL-12-induced immune response [23, 24].

Interleukin 2 (IL-2) is a cytokine signaling molecule in the immune system produced mainly by the CD4 T-cells and is responsible for the growth, proliferation, and differentiation of CD4 $^{+}$ T cells, to become cytotoxic or CD8 $^{+}$ T cells (CTLs). The CD8 $^{+}$ T cells (adaptive immune system) are specialised for lytic function and therefore believed to be the main effector cells [39]. The CD8 effector cells are also responsible for lysis of the HIV infected CD4 T-cells [37, 43] and the production of chemokines which inhibit the infection of the macrophages by the virus [28]. The *in vivo* and *in vitro* experimental findings in [30] on the production of IL-10, IL-6, TNF- α and IL-2 cytokines in the tumor sites of NHL patients showed a correlation between the cytokines. IL-6 has been identified as a key cytokine for the B-cell NHLs' growth and survival [26].

Human tumors contain macrophages which are often phenotypically classified as M_1 and M_2 [9, 12]. M_1 are the macrophages that have undergone cell activation in response to interferon (IFN) while the M_2 are those that have undergone activation in response to IL-4. The activated macrophages (M_1) are associated with acute inflammation and T-cell immunity and the immune suppressive macrophages (M_2) are associated with active promotion of tumor growth and thus are mainly the tumor associated macrophages (TAMs) [9, 12]. The M_1 phenotype is characterized by the expression of high levels of pro-inflammatory cytokines, and M_2 macrophages are considered to be involved in tumor progression and to have immunoregulatory functions [2, 22]. TAMs can switch type between pro-inflammatory M_1 and anti-inflammatory M_2 in the tumor environment [12]. IL-6 and TGF- β induce M_2 polarization and promote an immunosuppressive environment [26]. One of the most important features of M_1 macrophages is the production of a

T-cell stimulating cytokine IL-12 while the M_2 macrophages are linked to the profuse production of IL-10, which down regulates the activities of IL-12 [24]. The IL-10 cytokines also have some direct inhibitory effects on the CD4 $^+$ T cells in that they inhibit proliferation and the cytokine synthesis, however, on CD8 $^+$ T cells research has shown indirect inhibitory effect by IL-10 [27].

Infection by the Human immunodeficiency virus (HIV), is typified by a marked deficiency of CD4 $^+$ T cells and a persistent stimulation of B cells [10], leading to increased NHL risk in people with HIV/AIDS. More than 90% of HIV-associated NHLs are derived from B cells, and the majority are high-grade and extranodal [10]. In this study, the depletion of these cells is very vital since it allows for an immunosuppressive environment that reduces the clearance rate of the tumor cells by the killer CD8 $^+$ T-cells of the host immune system. Highly active antiretroviral therapy (HAART) and chemotherapeutic drugs are two of the main therapeutic measures that have long been used to curb HIV infection and cancer growth respectively. We therefore consider the treatment of HIV with highly active retroviral therapy (HAART) by reverse transcriptase inhibitors (RTIs) and protease inhibitors (PIs). In addition, we also include chemotherapy which is a drug administered to kill the tumor cell due to their mode of action i.e killing cells that divide more rapidly, a feature associated with tumor cells. These drugs though targeted at the tumor cells, can also be destructive to other cells in the host immune system. Our study is motivated by the work in [16], where combination of cytokines were incorporated in modelling pancreatic cancer. We will therefore, consider a combination of cytokines in modelling the role of HIV in the NHL growth with and without the two drug interventions. In our study, we consider the macrophages (pro-inflammatory M_1 and anti-inflammatory M_2), T cells (healthy CD4 $^+$ T cells, HIV-infected CD4 $^+$ T cells and CD8 $^+$ T cells), the virus and cancer cells. The cells interact with each other through a conglomerate of cytokines. We will focus on the stability and bifurcation analysis to establish the existence of the equilibria and to understand the behaviour of the formulated model. Moreover, most of the research has always focused on modelling either tumor dynamics in a host immune system, HIV dynamics or the interaction of the tumor cells with the immune system in the presence of HIV *in vivo* [29, 32, 38]. However, most importantly, none of these studies to the best of our knowledge have incorporated all the cytokines present in the host immune system in an HIV and tumor co-infection scenario.

The paper is organized thereafter as follows : The formulation and analysis of the HIV-related non-Hodgkin lymphoma model with the inclusion of the two therapies i.e. chemotherapy and HAART are presented in Section 2. In Section 3, numerical simulations for the model and parameter estimation are carried out to illustrate the stability and bifurcation results as well as the effect of the two therapies on cancer evolution. We then discuss our conclusions in Section 4.

2 Methods

We postulate a mathematical model driven by the following variables: tumor associated macrophages (pro-inflammatory M_1 and anti-inflammatory M_2), T cells (healthy CD4 $^+$ T cells, infected CD4 $^+$ T cells, and CD8 $^+$ T cells), HIV virus, V and the cancer cells, C .

The postulated interactions described in Section 1 are depicted in Figure 1.

Table 1 shows the variables considered in our mathematical model and the parameters used in formulating our model equations are summarised in Table 2.

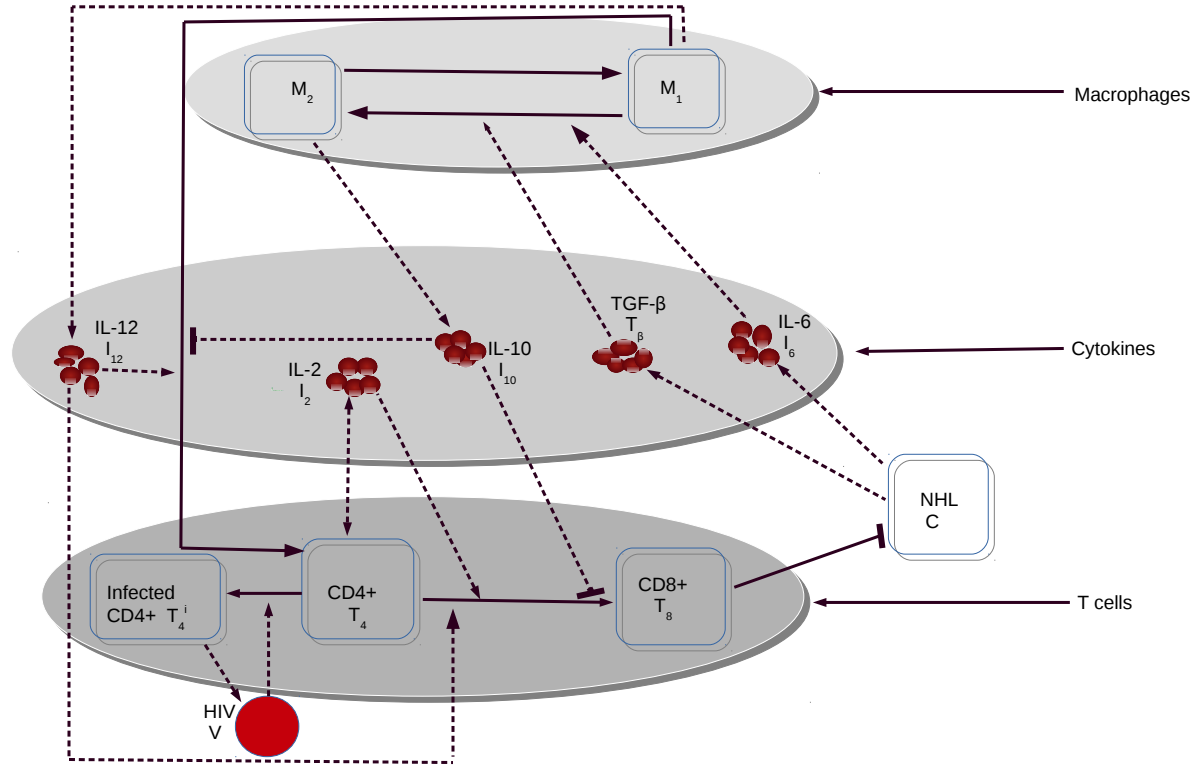


Figure 1: Transmission dynamics of HIV-related NH Lymphomas. We have macrophages M_1, M_2 , T-cells (immune cells) T_4, T_4^i, T_8 , cytokines ($T_\beta, I_6, I_{10}, I_{12}, I_2$), the tumor cell, C and HIV, V . The pool of viruses V , through infection, influence the movement of the $CD4^+$ T cells into the infected compartment T_4^i . We have used dotted lines with arrow heads to represent cytokine production, cell activation and viruses release. The bold lines represents induction of the $CD8^+$ memory by $CD4^+$ T-cells and activation of $CD4^+$ T-cells due to M_1 as well as the inflow of the infected T_4^i from T_4 compartment. Similarly, the bold lines represent transition of the macrophages. The inhibition are represented by the square heads lines where $IL-10$ hinders the proliferation and activation of both $CD4^+$ and $CD8^+$ T-cells and the killer cell ($CD8^+$) reduces the growth of the tumor by increasing its apoptosis.

2.1 Model Equations

We now present the model equations by considering cytokines dynamics and the cells dynamics. The parameters are assumed to be non-negative.

2.1.1 Cytokine dynamics

In model system (1), the ordinary differential equations track the dynamics of the cytokines, where the positive terms show the secretion of the cytokines by respective cells into the tumor environment while the negative terms indicate the natural decay of the cytokines which occurs in a short time-scale as opposed to the dynamics of the cell population. The secretion and

State Variable	Description	Units
M_1	density of pro-inflammatory tumor associated macrophages	cells/ml
M_2	density of anti-inflammatory tumor associated macrophages	cells/ml
T_4	density of healthy CD4 ⁺ T cells	cells/ml
T_4^i	density of virus-infected CD4 ⁺ T cells	cells/ml
V	density of HIV	virus/ml
T_8	density of CD8 ⁺ T cells	cells/ml
C	density of cancer cells	cells/ml
T_β	concentration of transforming growth factor (TGF- β)	pg/ml
I_6	concentration of interleukin 6 (IL-6)	pg/ml
I_{10}	concentration of interleukin 10 (IL-10)	pg/ml
I_{12}	concentration of interleukin 12 (IL-12)	pg/ml
I_2	concentration of interleukin 2 (IL-2)	pg/ml

Table 1: State variables and their units

decay of the cytokines are assumed to occur at constant rates. This assumption follows directly from [16].

$$\left. \begin{aligned} \frac{dT_\beta}{dt} &= \alpha_1 C - d_1 T_\beta & \frac{dI_6}{dt} &= \alpha_6 C - d_6 I_6, \\ \frac{dI_{10}}{dt} &= \alpha_{10} M_2 - d_{10} I_{10}, & \frac{dI_{12}}{dt} &= \alpha_{12} M_1 - d_{12} I_{12}, \\ \frac{dI_2}{dt} &= \alpha_2 T_4 - d_2 I_2, \end{aligned} \right\} \quad (1)$$

where parameters, α_1 and α_6 represent the production rates of T_β and I_6 by the cancer cell, d_1 and d_6 their respective decay rates. I_{12} and I_{10} are produced primarily by M_1 and M_2 respectively at the rates α_{12} and α_{10} . These two cytokines decay at the rates d_{12} and d_{10} respectively. Lastly, α_2 represents the production rate of I_2 by healthy T_4 cells and they decay at the rate d_2 .

2.1.2 State variables equations

$$\left. \begin{aligned}
 \frac{dM_1}{dt} &= s_1 - k_1 M_1 + \nu M_2 - (\lambda_1 T_\beta + \lambda_2 I_6) M_1 - P_{M_1}(1 - e^{-D}) M_1, \\
 \frac{dM_2}{dt} &= s_2 + (\lambda_1 T_\beta + \lambda_2 I_6) M_1 - k_2 M_2 - \nu M_2 - P_{M_2}(1 - e^{-D}) M_2, \\
 \frac{dT_4}{dt} &= s_3 + \beta_1 \frac{I_{12} M_1}{K_{10} + I_{10}} + \beta_2 \frac{I_2 T_4}{K_2 + I_2} - \mu_1 T_4 - (1 - \zeta_r) \mu_2 V T_4 - P_{T_4}(1 - e^{-D}) T_4, \\
 \frac{dT_4^i}{dt} &= (1 - \zeta_r) \mu_2 V T_4 - \mu_5 T_4^i - P_{T_4^i}(1 - e^{-D}) T_4^i, \\
 \frac{dT_8}{dt} &= \epsilon \beta_1 \frac{I_{12}}{K_{10} + I_{10}} + \beta_2 \frac{I_2 T_8}{K_2 + I_2} - \mu_4 T_8 - P_{T_8}(1 - e^{-D}) T_8, \\
 \frac{dV}{dt} &= (1 - \zeta_p) N \delta_2 T_4^i - \mu_v V, \\
 \frac{dC}{dt} &= r C^{\frac{3}{4}} \left(1 - \left(\frac{C}{C_0} \right)^{\frac{1}{4}} \right) - \beta_3 C T_8 - P_C(1 - e^{-D}) C, \\
 \frac{dD}{dt} &= u_{in}(t) - d_D D
 \end{aligned} \right\} \quad (2)$$

In system (2), the influx of the macrophages M_1 and M_2 due to the attraction to the tumor site are represented by s_1 and s_2 respectively. The switching of macrophages from M_1 to M_2 and vice versa is captured in the terms $(\lambda_1 T_\alpha + \lambda_2 I_6) M_1$ and νM_2 respectively, where the former is activated by cytokines TGF- β and IL-6. However, the transformation from M_2 to M_1 is assumed to be unbiased and occurs at a constant rate ν . The natural deaths of the macrophages M_1 and M_2 are assumed to be directly proportional to the concentration rate of the macrophages thus occurs at the rates k_1 and k_2 respectively.

The third equation of system (2) describes the dynamics of the healthy CD4 $^{+}$ T cells. The recruitment of the healthy CD4 $^{+}$ T cells is s_3 , from a source such as the thymus and their activation which is enhanced by IL-12 [16,44] occurs at a rate β_1 . The MHC-II molecule together with IL-12 activates the naive T helper cells, where the former also aid in the priming of the naive T helper cells into effector T cells and memory T cells. This process is hindered by IL-10. Proliferation due to IL-2 occurs at a rate β_2 . We thus have the terms $\beta_1 I_{12} M_1 / (K_{10} + I_{10})$ and $\beta_2 I_2 T_4 / (K_2 + I_2)$ since we assume saturation in proliferation of the CD4 $^{+}$ T cells. The natural decay rate of CD4 $^{+}$ T cells is μ_1 . Assuming that upon infection of the cells with the HIV viral particles at a rate μ_2 , all the healthy cells become productively infected and therefore, we ignore the latent stage of the infected cells which is captured in various models for instance the model discussed in [29]. Since RTI drugs affect the free virus-cell transmission, we thus have the term $(1 - \zeta_r) \mu_2 V T_4$, is the rate of reduction in the number of infected cells, with parameter $\zeta_r \in [0, 1]$ as a measure of efficacy of RTIs. If $\zeta_r = 1$, then the RTIs offer 100% protection while if $\zeta_r = 0$, zero protection is offered.

For the infected CD4 $^{+}$ T cells, the per capita death rate μ_5 , is assumed to include both natural death and the bursting. The rate at which the infected cells burst and produce viruses is δ_2 . We can safely assume that $\mu_5 > \delta_2$. Since the productively infected cells is assumed to produce N virions during its lifetime, the average virion production rate by infected cells is therefore given by $N \delta_2$. The role of PIs, is captured in the term, $(1 - \zeta_p) N \delta_2 T_4^i$, where $(1 - \zeta_p)$ measures the reduction in the number of mature viruses produced, with $\zeta_p \in [0, 1]$, the efficacy of PIs. The loss of virions due to clearance occurs at a constant rate μ_v . Similar conclusions can be drawn for $\zeta_p = 0$ and $\zeta_p = 1$ as done for ζ_r .

The dynamics of CD8⁺ T cells mirrors the dynamics of CD4⁺ T cells but with no source term. The proliferation of the effector T cells (CD8⁺ T cells) only occurs due to IL-12 produced by M_1 and the process is hindered by IL-10 and is modelled by the terms $\epsilon\beta_1 I_{12}/(K_{10} + I_{10})$ and $\beta_2 I_2 T_8/(K_2 + I_2)$. However, the ϵ included in the first term is a modification parameter which represents the proliferation potential of CD8⁺ T cells when compared to that of CD4⁺ T cells when influenced by IL-12 and IL-10. The loss of the cells is at a per capita rate μ_4 .

Following [16], we assume the dynamics of the tumor is governed by two processes: i.e. intrinsic growth of the tumor cells and the elimination due to the cytotoxic effector cells. Therefore, considering the equation describing the tumor dynamics, the first term $rC^{\frac{3}{4}}(1 - (C/C_0)^{\frac{1}{4}})$ models the growth of the tumor which we assume as most of the living organisms, follows universal law with r being the growth rate, C_0 , the maximum size of the tumor cell and the total body mass of the tumor cell is represented by C . For greater elucidation on the growth term, see [16, 45]. The clearance rate of the tumor cells occurs at a rate β_3 and follows the mass-action law.

Lastly, following [47, 48], most of the chemotherapeutic drugs are only effective during certain phases of cell cycle (cell cycle specific) and pharmacokinetics indicate that the effectiveness of the chemotherapeutic drugs is bounded. We therefore have the term $(1 - e^{-D})$, a saturation term representing the fraction of the cell killed by a dose, D of chemotherapy. This prompts the inclusion the cell dose-response term

$$Q_{D_i} = P_i(1 - e^{-D})i \quad \text{for } i = M_1, M_2, T_4, T_4^i, T_8, C.$$

Since the drug concentration in the bloodstream changes with time due to the processes involved, i.e absorption, distribution, metabolism and excretion, we include an equation that tracks that dynamics. Therefore, the terms in the non-homogeneous equation, dD/dt of system (3) reflects the rate of change in the dosage concentration over a given period of time. $u_{in}(t)$ is a function of time that describes the amount of drug influx into the system and the injection time assuming intravenous administration whereas d_D represents the drug elimination rate. The drug concentration equation assumes instantaneous distribution of the drug into all body parts.

2.2 Model Analysis

We assume quasi-steady-state approximation for the cytokines concentration since in our model system the dynamics occur at different time scales. The dynamics of the cytokines ,that is, their secretion and decay happen in a shorter time-scale when compared to that of the cells or virus and thus we assume they reach their equilibrium almost instantaneously, see also [16]. We therefore have, from model system (1) the following relations:

$$T_\beta = \frac{\alpha_1}{d_1}C, \quad I_6 = \frac{\alpha_6}{d_6}C, \quad I_{10} = \frac{\alpha_{10}}{d_{10}}M_2, \quad I_{12} = \frac{\alpha_{12}}{d_{12}}M_1, \quad I_2 = \frac{\alpha_2}{d_2}T_4.$$

Substituting the cytokine steady-states into equations in system (2), we obtain

$$\left. \begin{aligned} \frac{dM_1}{dt} &= s_1 - k_1 M_1 + \nu M_2 - \gamma_c C M_1 - P_{M_1}(1 - e^{-D}) M_1, \\ \frac{dM_2}{dt} &= s_2 + \gamma_c C M_1 - k_2 M_2 - \nu M_2 - P_{M_2}(1 - e^{-D}) M_2, \\ \frac{dT_4}{dt} &= s_3 + \frac{\gamma_1 M_1 M_1}{K_{10} + \gamma_2 M_2} + \beta_2 \frac{\gamma_3 T_4 T_4}{K_2 + \gamma_3 T_4} - \mu_1 T_4 - (1 - \zeta_r) \mu_2 V T_4 - P_{T_4}(1 - e^{-D}) T_4, \\ \frac{dT_4^i}{dt} &= (1 - \zeta_r) \mu_2 V T_4 - \mu_5 T_4^i - P_{T_4^i}(1 - e^{-D}) T_4^i, \\ \frac{dT_8}{dt} &= \epsilon \frac{\gamma_1 M_1}{K_{10} + \gamma_2 M_2} + \beta_2 \frac{\gamma_3 T_4 T_8}{K_2 + \gamma_3 T_4} - \mu_4 T_8 - P_{T_8}(1 - e^{-D}) T_8, \\ \frac{dV}{dt} &= (1 - \zeta_p) N \delta_2 T_4^i - \mu_v V, \\ \frac{dC}{dt} &= r C^{\frac{3}{4}} \left(1 - \left(\frac{C}{C_0} \right)^{\frac{1}{4}} \right) - \beta_3 C T_8 - P_C(1 - e^{-D}) C, \\ \frac{dD}{dt} &= u_{in}(t) - d_D D \end{aligned} \right\} \quad (3)$$

where $\gamma_c = \lambda_1 \frac{\alpha_1}{d_1} + \lambda_2 \frac{\alpha_6}{d_6}$, $\gamma_1 = \beta_1 \frac{\alpha_{12}}{d_{12}}$, $\gamma_2 = \frac{\alpha_{10}}{d_{10}}$ and $\gamma_3 = \frac{\alpha_2}{d_2}$, with the general initial conditions

$$M_1 \geq 0, M_2 \geq 0, T_4 \geq 0, T_4^i \geq 0, V \geq 0, T_8 \geq 0 \quad \text{and} \quad C \geq 0$$

The model system (3) above represents the dynamics of the cell population and the HIV virus in the presence of cytokines in a tumor environment, HIV treatment and chemotherapy. The analysis of system (3) is therefore central in this study. We state two important model properties of model system (3) before embarking on steady-state analysis. Our initial considerations focus only the model with HAART and with no chemotherapy treatment. Therefore, we exclude the equation tracking the concentration of the chemotherapy drug in the host system and the terms representing the effects of chemotherapy on the immune cells and cancer cells in the subsequent analysis.

2.2.1 Model Properties

Positivity of the solutions

Lemma 1. *Given the initial conditions $M_1 \geq 0, M_2 \geq 0, T_4 \geq 0, T_4^i \geq 0, V \geq 0, T_8 \geq 0$ and $C \geq 0$, then the solutions of $M_1(t), M_2(t), T_4(t), T_4^i(t), V(t), T_8(t)$ and $C(t)$ remain positive for all $t \geq 0$*

Proof. Suppose $\tilde{t} = \sup \{ t > 0 : M_1 \geq 0, M_2 \geq 0, T_4 \geq 0, T_4^i \geq 0, V \geq 0, T_8 \geq 0, C \geq 0 \} \in [0, t]$, implying $\tilde{t} \geq 0$. The first equation of system (3) gives

$$\frac{dM_1}{dt} \geq s_1 - k_1 M_1 - \gamma(t) M_1, \quad \text{where} \quad \gamma_c C = \gamma(t).$$

Integration, yields

$$M_1(\tilde{t}) \geq M_1(0)e^{-[k_1 t + \int_0^t \gamma(s)ds]} + e^{-[k_1 t + \int_0^t \gamma(s)ds]} \int_0^{\tilde{t}} s_1 e^{[k_1 t + \int_0^t \gamma(s)ds]} \geq 0.$$

Hence M_1 is always positive for all $\tilde{t} > 0$. Similarly

$$M_2(\tilde{t}) \geq M_2(0)e^{(-(k_2+\nu)t)} + e^{(-(k_2+\nu)t)} \int_0^{\tilde{t}} s_2 e^{(k_2+\nu)t} \geq 0.$$

Considering the CD4 T cells we have

$$\frac{dT_4}{dt} \geq s_3 - \Theta(t)T_4, \quad \text{where } \Theta(t) = \mu_1 + (1 - \zeta_r)\mu_2 V.$$

The solution of the differential equation is

$$T_4(\tilde{t}) \geq T_4(0) \exp \left[- \int_0^t \Theta(s)ds \right] + \exp \left[- \int_0^t \Theta(s)ds \right] \left(\int_0^{\tilde{t}} s_3 \exp \left[\int_0^t \Theta(s)ds \right] \right) \geq 0.$$

Similarly we have

$$T_4^i(\tilde{t}) \geq T_4^i(0) \exp(-\mu_5 t) \geq 0.$$

Also

$$T_8(\tilde{t}) \geq T_8(0) \exp \left[- \left(\mu_4 t - \int_0^t \Phi(s)ds \right) \right] \geq 0, \quad \text{where } \Phi(t) = \beta_2 \frac{\gamma_3 T_4}{K_2 + \gamma_3 T_4}.$$

Hence $T_4(\tilde{t})$, $T_4^i(\tilde{t})$ and $T_8(\tilde{t})$ are positive for all $\tilde{t} > 0$. For the virus population we have

$$\frac{dV}{dt} \geq -\mu_v V, \quad \Rightarrow V(t) \geq V(0) \exp(-\mu_v t) \geq 0.$$

Lastly, for the tumor cell population, we have

$$\Rightarrow C(\tilde{t}) \geq C(0) \exp \left[-\beta_3 \int T_8(s)ds \right] \geq 0.$$

Hence $V(\tilde{t})$ and $C(\tilde{t})$ are positive for all $\tilde{t} > 0$. This implies that all the state variables are non-negative and the solutions of our system remain positive for all $\tilde{t} \geq 0$. \square

Feasible Region

Lemma 2. *The solution of our system with initial conditions $M_1 \geq 0, M_2 \geq 0, T_4 \geq 0, T_4^i \geq 0, V \geq 0, T_8 \geq 0$ and $C \geq 0$ are contained (bounded) for all $t \geq 0$ in the biologically feasible*

region defined by the set

$$\Omega = \left\{ (M_1, M_2, T_4, T_4^i, V, T_8, C) \in \mathbb{R}_+^7 : M \leq \frac{(s_1 + s_2)}{k}, T \leq \frac{s_3 + K}{\mu}, V \leq \frac{N\delta_2 W}{\mu_v}, C \leq \left(\frac{rC_0^{\frac{1}{4}}}{r - \beta_3 W C_0^{\frac{1}{4}}} \right)^4 \right\}, \quad (4)$$

with $M = M_1 + M_2$ and $T = T_4 + T_4^i + T_8$.

Proof. Summing the two macrophage populations from the first two equations of system (3) we obtain

$$\frac{d}{dt}(M_1 + M_2) = \frac{dM}{dt} \leq s_1 + s_2 - kM, \quad \text{for } k = \min \{k_1, k_2\}, \quad (5)$$

The solution of (5) is

$$M(t) \leq \frac{(s_1 + s_2)}{k} + \left(M(0) - \frac{(s_1 + s_2)}{k} \right) e^{-kt}.$$

When we take the limit supremum of M as $t \rightarrow \infty$, we have

$$\lim_{t \rightarrow \infty} \sup M(t) \leq \frac{(s_1 + s_2)}{k} = S.$$

This implies that

$$M_1 \leq S \quad \text{and} \quad M_2 \leq S.$$

Hence the macrophage population is bounded.

Again considering the sum of the T cell populations we have

$$\begin{aligned} \frac{dT}{dt} &\leq s_3 + \frac{\gamma_1 S^2}{K_{10} + \gamma_2 S} + \epsilon \frac{\gamma_1 S}{K_{10} + \gamma_2 S} - \mu_1 T_4 - \mu_5 T_4^i - \mu_4 T_8, \\ &\leq s_3 + \frac{\gamma_1 S}{K_{10} + \gamma_2 S} (S + \epsilon) - \mu T, \quad \text{where } \mu = \min \{\mu_1, \mu_5, \mu_4\} \text{ and } M_1, M_2 \leq \frac{(s_1 + s_2)}{k} = S. \end{aligned}$$

Through integration, we obtain

$$T(t) \leq \frac{s_3 + K}{\mu} + \left(T(0) - \frac{s_3 + K}{\mu} \right) e^{-\mu t}, \quad \text{where } K = \frac{\gamma_1 S}{K_{10} + \gamma_2 S} (S + \epsilon).$$

Therefore

$$\lim_{t \rightarrow \infty} \sup T(t) \leq \frac{s_3 + K}{\mu} = W.$$

This implies that $T_4 \leq W$, $T_4^i \leq W$ and $T_8 \leq W$, hence each of the T-cell population is bounded.

Considering the virus population we have

$$\frac{dV}{dt} \leq (1 - \zeta_p)N\delta_2 W - \mu_v V, \quad \text{since } T_4^i \leq W.$$

Integration gives

$$V(t) \leq \frac{(1 - \zeta_p)N\delta_2 W}{\mu_v} + \left(V(0) - \frac{(1 - \zeta_p)N\delta_2 W}{\mu_v} \right) e^{-\mu_v t}.$$

We also have

$$\limsup_{t \rightarrow \infty} V(t) \leq \frac{(1 - \zeta_p)N\delta_2 W}{\mu_v} = Q.$$

Hence $V(t)$ is thus bounded.

Lastly, we consider the tumor cell population. From the last equation in system (3), integration of

$$\frac{dC}{dt} \leq C \left[\frac{r}{C^{\frac{1}{4}}} - \frac{r}{C_0^{\frac{1}{4}}} - \beta_3 W \right], \quad \text{since } T_8 \leq \frac{s_3 + K}{\mu} = W,$$

yields

$$C(t) \leq \left(\frac{rC_0^{\frac{1}{4}} - \exp \left(\left(-\frac{(r - \beta_3 W C_0^{\frac{1}{4}})}{4C_0^{\frac{1}{4}}} \right) t \right)}{r - \beta_3 W C_0^{\frac{1}{4}}} \right)^4.$$

So

$$\limsup_{t \rightarrow \infty} C(t) \leq \left(\frac{rC_0^{\frac{1}{4}}}{r - \beta_3 W C_0^{\frac{1}{4}}} \right)^4 = P.$$

Therefore $C(t)$ is also bounded.

Our invariant region is therefore defined by Ω . The population will approach the thresholds as $t \rightarrow \infty$. We therefore deduce that the region Ω is positively invariant and attracting with respect to model system (3). That completes the proof. \square

2.2.2 Steady states

Setting the right hand side of system (3) to zero (without the terms representing the effects of chemotherapeutic drug on the cells) we have

$$s_1 - k_1 M_1^* + \nu M_2^* - \gamma_c C^* M_1^* = 0, \quad (6)$$

$$s_2 + \gamma_c C^* M_1^* - k_2 M_2^* - \nu M_2^* = 0, \quad (7)$$

$$s_3 + \frac{\gamma_1 M_1^* M_1^*}{K_{10} + \gamma_2 M_2^*} + \beta_2 \frac{\gamma_3 T_4^* T_4^*}{K_2 + \gamma_3 T_4^*} - \mu_1 T_4^* - (1 - \zeta_r) \mu_2 V^* T_4^* = 0, \quad (8)$$

$$(1 - \zeta_r) \mu_2 V^* T_4^* - \mu_5 T_4^{i*} = 0, \quad (9)$$

$$(1 - \zeta_p) N \delta_2 T_4^{i*} - \mu_v V^* = 0, \quad (10)$$

$$\epsilon \frac{\gamma_1 M_1^*}{K_{10} + \gamma_2 M_2^*} + \beta_2 \frac{\gamma_3 T_4^* T_8^*}{K_2 + \gamma_3 T_4^*} - \mu_4 T_8^* = 0 \quad (11)$$

$$r C^{* \frac{3}{4}} \left(1 - \left(\frac{C^*}{C_0} \right)^{\frac{1}{4}} \right) - \beta_3 C^* T_8^* = 0. \quad (12)$$

We start by solving for the steady states of M_1^* and M_2^* in equations (6) and (7) and we have respectively

$$M_1^* = \frac{\sigma_1}{\Lambda + \sigma_2 C^*} \quad \text{and} \quad M_2^* = \frac{\sigma_3 + \sigma_4 C^*}{\Lambda + \sigma_2 C^*},$$

where $\sigma_1 = (\nu + k_2) s_1 + \nu s_2$, $\Lambda = k_1 (\nu + k_2)$, $\sigma_2 = k_2 \gamma_c$, $\sigma_3 = k_1 s_2$, $\sigma_4 = (s_1 + s_2) \gamma_c$.

We therefore assume a quasi steady-state for the viral population and thus from equation (10) we have

$$V^* = \frac{(1 - \zeta_p) N \delta_2 T_4^{i*}}{\mu_v}.$$

Substituting V^* into equation (9) we obtain

$$T_4^{i*} \left(\frac{(1 - \zeta_p)(1 - \zeta_r) \mu_2 N \delta_2 T_4^*}{\mu_v} - \mu_5 \right) = 0.$$

This gives

$$T_4^{i*} = 0 \quad \text{or} \quad T_4^* = \frac{\mu_v \mu_5}{(1 - \zeta_p)(1 - \zeta_r) \mu_2 N \delta_2}.$$

From the above, it implies that T_4 has one solution given by

$$T_4^* = \frac{\mu_v \mu_5}{(1 - \zeta_p)(1 - \zeta_r) \mu_2 N \delta_2}.$$

For $T_4^{i*} = 0$, our system at the steady state relates to HIV-free tumor equilibrium. Since our objective is to investigate the role of HIV in the NHLs, we therefore analyse hereinafter the steady state in which there is HIV in the system, that is, co-infection of HIV and the tumor in the presence of HIV treatment.

We now solve for the steady states, $E = (M_1^*, M_2^*, T_4^*, T_4^{i*}, V^*, T_8^*, C^*)$ where the state of the tumor is also influenced by the presence of the HIV in the tumor environment. Firstly, we

substitute T_4 with the solutions T_4^* into equations (8) and (11). We notice that in the solution T_4^* , the number of virions, N , has an effect on the concentration of the CD4⁺ T cells in the tumor environment, therefore the virus and the infected T cells play a crucial role in our model.

From (8) we solve for the solution of V at HIV-related NHL steady state denoted by V^* so that

$$V^* = \frac{\left(\left(s_3 + \frac{T_4^{*2}\beta_2\gamma_3}{K_2+T_4^*\gamma_3} + \frac{\gamma_1\sigma_1^2}{K_{10}(\Lambda+C^*\sigma_2)^2+(\sigma_3+C^*\sigma_4)(\Lambda+C^*\sigma_2)} \right) - \mu_1 T_4^* \right)}{(1-\zeta_r)\mu_2 T_4^*}.$$

From $V = \frac{(1-\zeta_p)N\delta_2 T_4^{i*}}{\mu_v}$ we have

$$T_4^{i*} = \mu_v \left(\frac{\left(\left(s_3 + \frac{T_4^{*2}\beta_2\gamma_3}{K_2+T_4^*\gamma_3} + \frac{\gamma_1\sigma_1^2}{K_{10}(\Lambda+C^*\sigma_2)^2+(\sigma_3+C^*\sigma_4)(\Lambda+C^*\sigma_2)} \right) - \mu_1 T_4^* \right)}{(1-\zeta_p)(1-\zeta_r)\mu_2 N\delta_2 T_4^*} \right).$$

We then obtain the steady state T_8^* as a function of C from equation (11). We have

$$T_8^* = \frac{\epsilon\gamma_1\sigma_1 [(1-\zeta_p)(1-\zeta_r)\mu_2\delta_2NK_2 + \gamma_3\mu_5\mu_v]}{[(1-\zeta_p)(1-\zeta_r)\mu_2\mu_4\delta_2NK_2 - \gamma_3\mu_5(\beta_2 - \mu_4)\mu_v] [K_{10}(\Lambda + C^*\sigma_2) + \gamma_2(\sigma_3 + C^*\sigma_4)]},$$

Since β_2 is the proliferation/activation rate of T_8 due to IL-2 and μ_4 , the decay rate of T_8 , it therefore suffice to assume that, for the existence of CD8⁺ T- cells, the proliferation rate must always be greater than the death rate that is, $\beta_2 > \mu_4$. Which implies that, the solution T_8^* is positive if and only if

$$N > \frac{\gamma_3\mu_5\mu_v(\beta_2 - \mu_4)}{(1-\zeta_p)(1-\zeta_r)\mu_2\mu_4\delta_2K_2} = N_{\text{crit}}^*$$

The existence of T_8^* at endemic steady state is subject to $N > N_{\text{crit}}^*$. Therefore, the viral particles must exceed a certain threshold, N_{crit}^* .

From equation (12) we have

$$g(C) = C \left[rC^{-1/4} \left(1 - (C/C_0)^{1/4} \right) - \beta_3 T_8^* \right] = 0. \quad (13)$$

The solutions of (13) are

$$C^* = 0 \quad \text{or} \quad rC^{-1/4} \left(1 - (C/C_0)^{1/4} \right) - \beta_3 T_8^* = 0.$$

$C^* = 0$ corresponds to a tumor free environment.

We define

$$g(C^*) = rC^{-1/4} \left(1 - (C/C_0)^{1/4} \right) - \beta_3 T_8^* = 0,$$

for the non-zero steady states.

Once the solutions of T_8 are in terms of C , their substitution into the non-zero equilibria i.e endemic equilibria result in an implicit function whose solutions can only be established numerically. We begin by considering the tumor free steady state. The non-zero solutions of C are subject to $N > N_{\text{crit}}^*$.

Tumor-free steady state

The tumor-free steady state, E_0 exists and represents the state of HIV infection in the presence of HIV treatment with no tumor cells in the host immune system. It reflects the possibility of tumor development prevention by the immune system (i.e the tumors are not able to evade the immune system. The state, E_0 is therefore given given by

$$\begin{aligned}
 & \text{Tumor-free equilibrium, } E_0 = (M_1^*, M_2^*, T_4^*, T_4^{0*}, V^*, T_8^*, C^*), \quad \text{where} \\
 & M_1^* = \frac{\sigma_1}{\Lambda}, \quad M_2^* = \frac{\sigma_3}{\Lambda}, \quad T_4^* = \frac{\mu_v \mu_5}{(1 - \zeta_p)(1 - \zeta_r)\mu_2 N \delta_2}, \quad C^* = 0, \\
 & T_4^{i*} = \frac{s_3}{\mu_5} + \frac{\beta_2 \gamma_3 \mu_v^2 \mu_5}{((1 - \zeta_r)(1 - \zeta_p)N K_2 \mu_2^2 \delta_2 + \gamma_3 \mu_5 \mu_v \mu_2)((1 - \zeta_r)(1 - \zeta_p)N \delta_2)} + \frac{\gamma_1 \sigma_1^2}{\Lambda^2 K_{10} \mu_5 + \Lambda \gamma_2 \mu_5 \sigma_3} \\
 & \quad - \frac{\mu_1 \mu_v}{(1 - \zeta_r)(1 - \zeta_p)N \delta_2 \mu_2}, \\
 & T_8^* = \frac{(\epsilon \gamma_1 ((1 - \zeta_p)(1 - \zeta_r)\mu_2 \delta_2 N K_2 + \gamma_3 \mu_5 \mu_v) \sigma_1)}{((1 - \zeta_p)(1 - \zeta_r)\mu_2 \mu_4 \delta_2 N K_2 + \gamma_3 \mu_5 (\mu_4 - \beta_2) \mu_v)(K_{10} \Lambda + \gamma_2 \sigma_3)}, \\
 & V^* = \frac{(1 - \zeta_r)N \delta_2 s_3}{\mu_v \mu_5} + \frac{\beta_2 \gamma_3 \mu_v \mu_5}{(1 - \zeta_r)(1 - \zeta_p)^2 N K_2 \mu_2^2 \delta_2 + \gamma_3 \mu_5 \mu_v \mu_2} + \frac{N \delta_2 \gamma_1 \sigma_1^2}{\Lambda^2 K_{10} \mu_v \mu_5 + \Lambda \gamma_2 \mu_v \mu_5 \sigma_3} \\
 & \quad - \frac{\mu_1}{(1 - \zeta_p)\mu_2},
 \end{aligned}$$

The existence of tumor-free equilibrium, E_0 is subject to $\bar{N}_{\text{crit}} < N$, where $\bar{N}_{\text{crit}} = \max \{N_{\text{crit}}, N_{\text{crit}}^*\}$, and

$$\begin{aligned}
 N_{\text{crit}} &= \frac{\mu_5 \mu_v \mu_1}{(1 - \zeta_p)(1 - \zeta_r)\mu_2 \delta_2 s_3} \\
 N_{\text{crit}}^* &= \frac{\gamma_3 \mu_5 \mu_v (\beta_2 - \mu_4)}{(1 - \zeta_p)(1 - \zeta_r)\mu_2 \mu_4 \delta_2 K_2} = N_{\text{crit}} \frac{\gamma_3 s_3 (\beta_2 - \mu_4)}{\mu_1 \mu_4 K_2}
 \end{aligned}$$

The stability of this state is discussed in Section 3.

Tumor-persistence steady states

The steady-state analysis for the model discussed in this section (without the chemotherapy) above clearly shows the existence of some feasible (non-negative) and non-zero tumor equilibria (tumor-persistence steady states). However, due to mathematical intractability we are unable to explicitly express the endemic states interms of the model parameters. We resort to numerical simulations. To understand the effect of chemotherapy in the evolution of the cancer, we will also perform numerical simulations in the following section.

3 Numerical Simulations

3.1 Parameter Estimation.

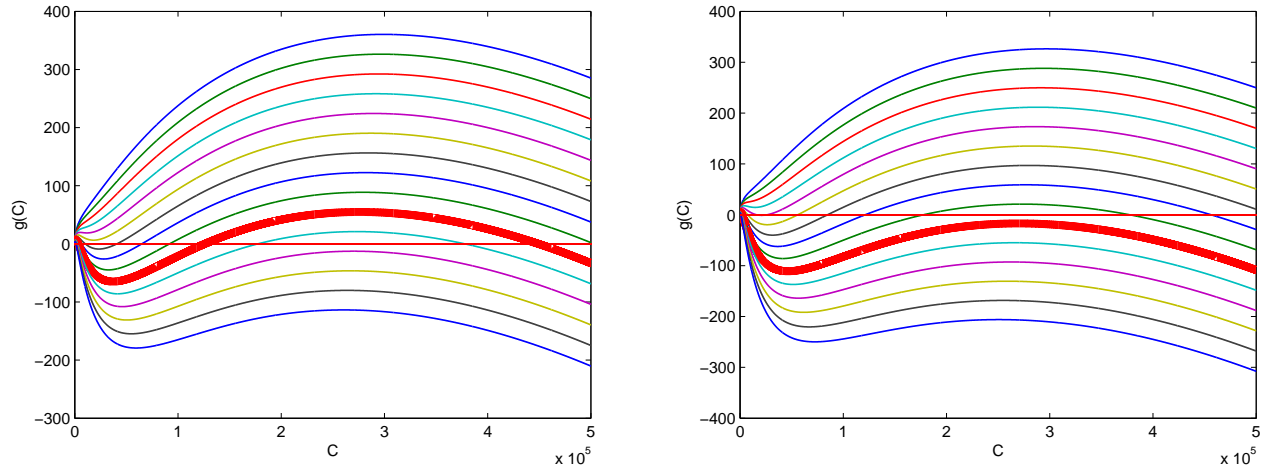
Parameter values used in the numerical simulation are presented in Table 2 below where most of the parameter values were obtained from different sources as indicated. Some of the parameters that do not have known values in the literature, were estimated to be close to the others for instance, α_6 was estimated to be close to α_1 . The initial conditions used in the numerical simulations were set as follows; the initial value for the tumor density was set at 100 cells/ml while the rest of the state variables used in our model the initial values were set at their quasi steady-states. For instance, the patients are assumed to be in homeostasis, constant cell population/concentration. We note that the parameter N used in our simulation is 1000 virion particles, though it varies as indicated in most of the studies, see for instance [29].

Table 2: Estimated Parameter values.

Parameter	Description	Values	Units	Source
α_1	production rate of TGF- β due to cancers cells	7×10^{-4}	pg/cell day	[34]
α_2	production rate of IL-2 due to CD4 $^+$ T cells	5	pg/cell day	[32, 42]
α_6	production rate of IL-6 due to cancers cells	7×10^{-7}	pg/cell day	Estimated
α_{10}	production rate of IL-10 due to M_2	5×10^{-4}	pg/cell day	[34, 36]
α_{12}	production rate of IL-12 due to M_1	3×10^{-2}	pg/cell day	[36]
d_1	degradation rate of TGF- β	10	day $^{-1}$	[42]
d_2	degradation rate of IL-2	10	day $^{-1}$	[32]
d_6	degradation rate of IL-6	0.173	day $^{-1}$	[?]
d_{10}	degradation rate of IL-10	5	day $^{-1}$	[36]
d_{12}	degradation rate of IL-12	1.188	day $^{-1}$	[36, 44]
s_1	influx rate of M_1	40	day $^{-1}$	[16, 36]
s_2	influx rate of M_2	20	day $^{-1}$	[16, 36]
s_3	production of CD4 $^+$ T cells by the sources	10^4	cells/ml day	[29]
k_1	per capita death rate of M_1	0.02	day $^{-1}$	[36, 44]
k_2	per capita death rate of M_2	8×10^{-3}	day $^{-1}$	[36]
λ_1	transformation rate of M_1 by TGF- β	0.075	ml/pg day	[34]
λ_2	transformation rate of M_2 by IL-6	0.075	day $^{-1}$	[34]
ν	transition rate from M_2 to M_1	5×10^{-2}	day $^{-1}$	[34]
β_1	activation rate of T cells by IL-12	10^6	cells/ ml day	[44]
β_2	proliferation rate of T cells by IL-2	0.1245	pg/cell day	[32, 42]
β_3	loss of cancer cells	10^{-7}	day $^{-1}$	[35] (10^{-5}) [16] (10^{-7})
K_2	saturation constant of proliferation by IL-2	2×10^7	pg/ml	[32]
K_{10}	saturation constant for anti-proliferation by IL-10	2.5×10^7	pg/ml	[44]
ϵ	modification parameter	0.5		Estimated
μ_1	per capita death rate of uninfected CD4 $^+$ T cells	0.02	day $^{-1}$	[29]
μ_2	infection rate of CD4 $^+$ T cells due to infiltration by free viruses	2.4×10^{-8}	ml/ day	[29]
μ_3	infection rate of CD4 $^+$ T cells due to direct contact with infected T cells	2×10^{-6}	day $^{-1}$	[46]
μ_4	per capita death rate of CD8 $^+$ T cells	0.03	day $^{-1}$	[32]
μ_v	clearance rate (loss) of free viruses	2.4	day $^{-1}$	[29]
μ_5	per capita death rate of infected CD4 $^+$ T cells	0.26	day $^{-1}$	[29]
δ_2	lytic death rate of infected CD4 $^+$ T cells	0.24	day $^{-1}$	[29]
δ_3	elimination rate of infected CD4 $^+$ T cells by CD8 $^+$ effector cells	0.78	day $^{-1}$	[33]
N	Virions produced during a lifetime by an infected CD4 $^+$ T cells	Varies		[29]
r	cancer growth rate	0.19	day $^{-1}$	[32, 35]
C_0	maximum cancer density	10^6	cells/ml	[16]
ζ_r	the measure of efficacy of reverse transcriptase inhibitors(RTI)	[0, 1]		
ζ_p	the measure of efficacy of protease inhibitors(PI)	[0, 1]		
$P_{M_1}, P_{M_2}, P_{T_4}, P_{T_4^i}, P_{T_b}$	chemo-induced immune cell death rates	0.6	day $^{-1}$	[47, 48]
P_C	chemo-induced tumor cell death rate	0.9	day $^{-1}$	[47, 48]
d_D	chemo drug elimination rate	0.9	day $^{-1}$	[47, 48]

3.2 Results with no chemotherapeutic drug

The results presented below of the numerical simulations for system (3) were obtained using Matlab ODE45 Solver which employ simultaneously the fourth and fifth order Runge Kutta schemes.



(a) With no HIV treatment; $\zeta_p = \zeta_r = 0$ and $\beta_3 = 2.0 \times 10^{-5} - 5.5 \times 10^{-5}$ steps of 2.5×10^{-6}
(b) With HIV treatment; $\zeta_p = \zeta_r = 0.8$ and $\beta_3 = 2.0 \times 10^{-5} - 5.5 \times 10^{-5}$ steps of 2.5×10^{-6}

Figure 2: The $g(C)$ as a function of C with different values of β_3 (rate of cancer loss in the population) with other parameters as in Table 2 and the other variables at their steady states. No chemotherapy treatment initiated.

Figure (2) shows the results of our simulation for $g(C)$ as a function of C , with different values of tumor killing rate, β_3 . Every one of the trajectories represents different parameter value of β_3 and the values increase from top to the bottom line. The values considered were in the range 2×10^{-5} to 5.5×10^{-5} for both cases; with and without HIV treatment with a step size of 2.5×10^{-6} (arithmetic distribution). A closer look at the trajectories, interestingly show that HIV treatment is important in cancer growth control. A typical example is to consider $\beta_3 = 4.25 \times 10^{-5}$ represented by the thicker trajectories. Without treatment we can have three possible cancer steady states while one steady state is observed for the case with treatment.

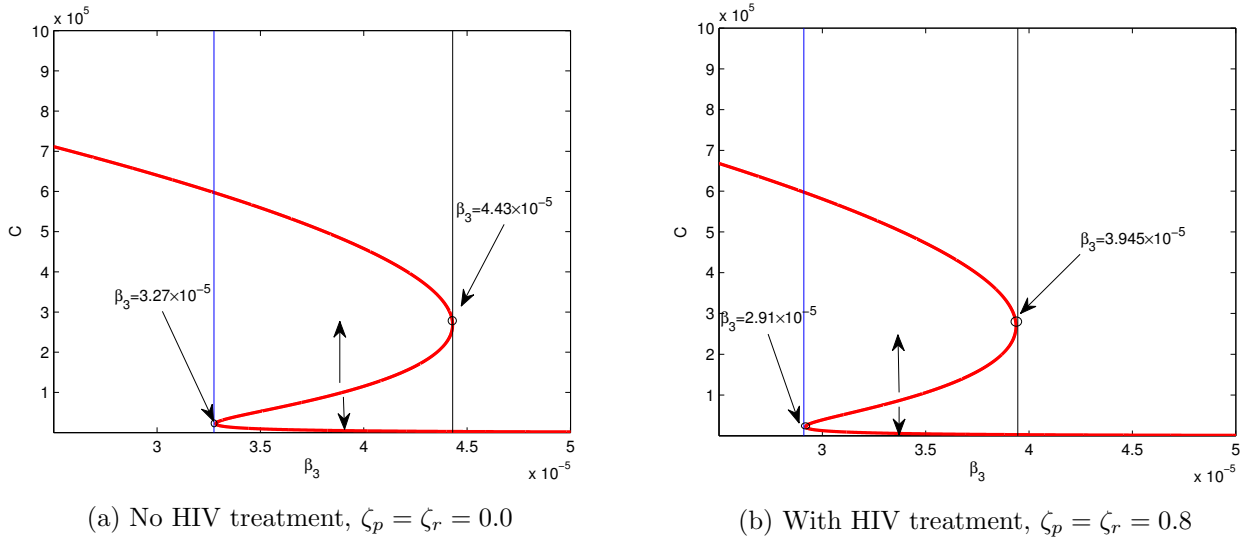


Figure 3: Bifurcation diagram: Non-trivial solutions of $g(C^*) = 0$ as a function of β_3 with the rest of parameters as in Table (2) with the other variables at their steady states.

From the analysis in Figure (2), we observe that the parameter β_3 is important in our model since it plays an effective role in defining the tumor behaviour. We thus investigate numerically, the bifurcation of the model for parameter β_3 , responsible for the immune response. The graphs in Figure (3), display the bifurcation diagrams for the treatment and no treatment cases. Figures (3a) and (3b) are plots of the non-zero steady state solutions of $g(C^*) = 0$ as a function of the parameter, β_3 . This analysis helps in understanding the behaviours of the model, i.e the critical values of the bifurcation parameter where the behaviour of the model system (3) changes. Figure 3 shows two saddle node bifurcation points. We observe the existence of multiple equilibria with respect to the different range of values for β_3 . Considering Figure 3a, one steady state exists for both $\beta_3 < 3.27 \times 10^{-5}$ and $\beta_3 > 4.43 \times 10^{-5}$ (these exact values where the bifurcation occurs are obtained from the plots in Figure 2a). However, for $3.27 \times 10^{-5} < \beta_3 < 4.43 \times 10^{-5}$ we have three equilibria. It is also clear from the figure that the upper branch where $\beta_3 < 4.43 \times 10^{-5}$ and the lower branch of the graph where $\beta_3 > 3.27 \times 10^{-5}$, we have stable equilibrium of the tumor whereas for the middle is unstable equilibrium. The same is evident for Figure 3b where one solution exists for both $\beta_3 < 2.91 \times 10^{-5}$ and $\beta_3 > 3.945 \times 10^{-5}$ and three for $2.91 \times 10^{-5} < \beta_3 < 3.945 \times 10^{-5}$. This implies that for the regions $\beta_3 > 4.43 \times 10^{-5}$ in Figure 3a and $\beta_3 > 3.945 \times 10^{-5}$ in Figure 3b, all the trajectories are attracted to the trivial tumor solution or the non-aggressive steady state disregarding the initial conditions. For $\beta_3 < 3.27 \times 10^{-5}$ in Figure 3a and $\beta_3 < 2.91 \times 10^{-5}$ in Figure 3b, the aggressive tumor equilibrium is an attractor for all the initial conditions.

A consideration of the same initial conditions, say $(C, \beta_3) = (1 \times 10^5, 3.5^{-5})$, in Figures (3a) and (3b) yields different long term dynamic results. In the absence of treatment, the system will eventually settle to the aggressive steady state. On the hand, in the presence of treatment, the system settles to a non-aggressive steady state. This underscores the importance of HIV treatment and early identification of the cancer.

The population dynamics of the tumor cell of our system is depicted in the time series plot, Figure (4), where the solution is observed to stabilize after around $5\frac{1}{2}$ years for a value of $\beta_3 = 1^{-7}$.

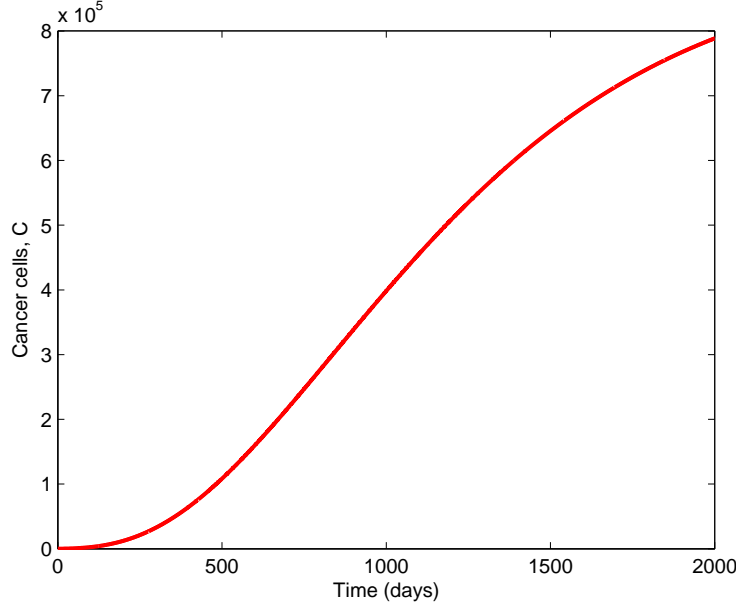


Figure 4: Population dynamics of the tumor cells in model system (3) with the parameters as in Table (2). Initial conditions: $M_1(0) = 2000$ cells/ml, $M_2(0) = 2500$ cells/ml, $T_4(0) = 5 \times 10^5$ cells/ml, $T_4^i(0) = 0$ cells/ml, $V(0) = 1000$ copies/mL, $T_8(0) = 100$ cells/ml and $C(0) = 100$ cells/ml.

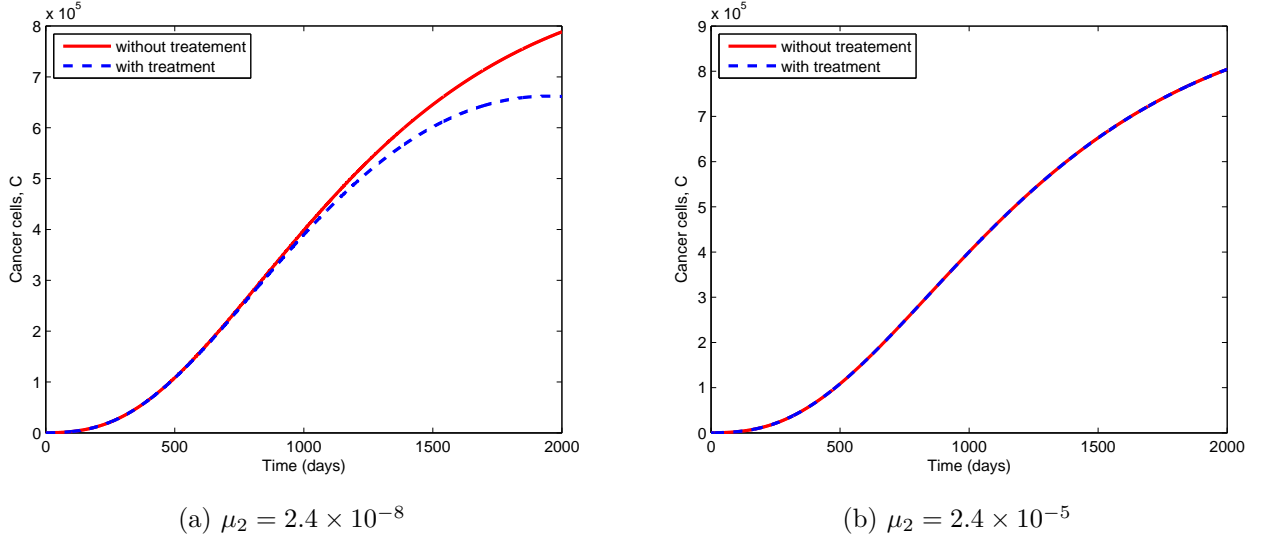


Figure 5: Population dynamics of the tumor cells in model system (3) with only HAART therapy, with $\zeta_r = \zeta_p = 0.5$ and the rest of the parameters as in Table (2). Initial conditions: $M_1(0) = 2000$ cells/ml, $M_2(0) = 2500$ cells/ml, $T_4(0) = 5 \times 10^5$ cells/ml, $T_4^i(0) = 0$ cells/ml, $V(0) = 1000$ copies/mL, $T_8(0) = 100$ cells/ml and $C(0) = 100$ cells/ml.

The time series plot in Figure (4) is considered for different infection rates, $\mu_2 = 2.4 \times 10^{-8}$ and

$\mu_2 = 2.4 \times 10^{-5}$ in the presence of HIV treatment. The results are presented in Figure 5. As seen in Figures 5a and 5b, for a smaller infection rate, treatment reduces tumor growth while treatment has no effect on the tumor growth for high infection rate values. So, treatment alone in the absence of reduced infection rates does not have a significant impact on cancer growth dynamics.

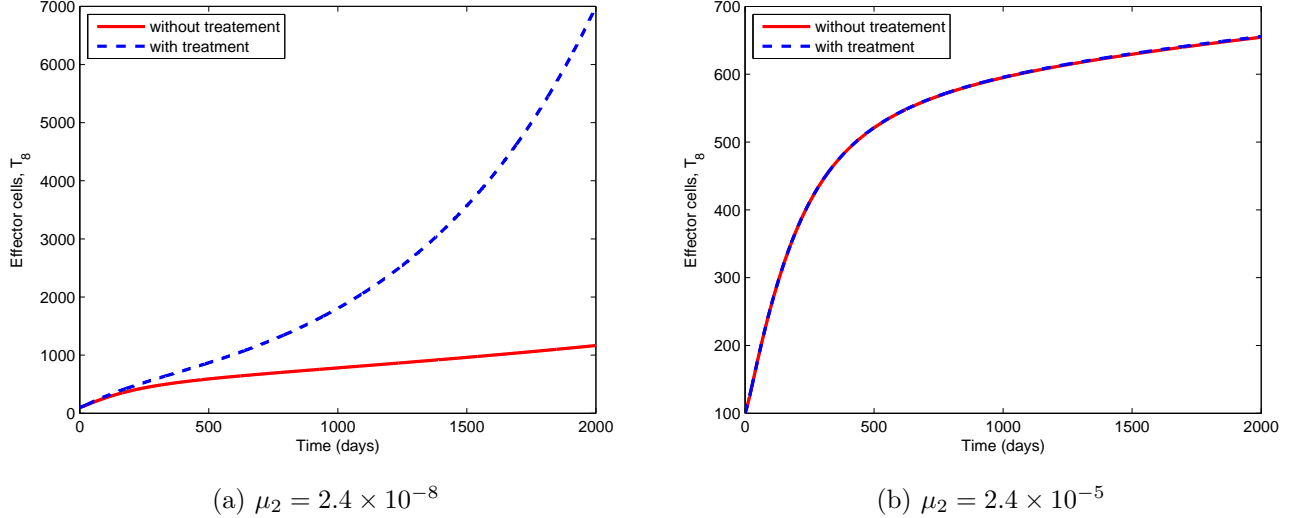


Figure 6: Numerical simulation of model system (3) for the evolution of the CD8⁺ T cells (effector cells) with RTIs and PIs treatment of efficacies, $\zeta_r = \zeta_p = 0.5$ and the rest of the parameters as in Table (2). Initial conditions: $M_1(0) = 2000$ cells/ml, $M_2(0) = 2500$ cells/ml, $T_4(0) = 5 \times 10^5$ cells/ml, $T_4^i(0) = 0$ cells/ml, $V(0) = 1000$ copies/mL, $T_8(0) = 100$ cells/ml and $C(0) = 100$ cells/ml.

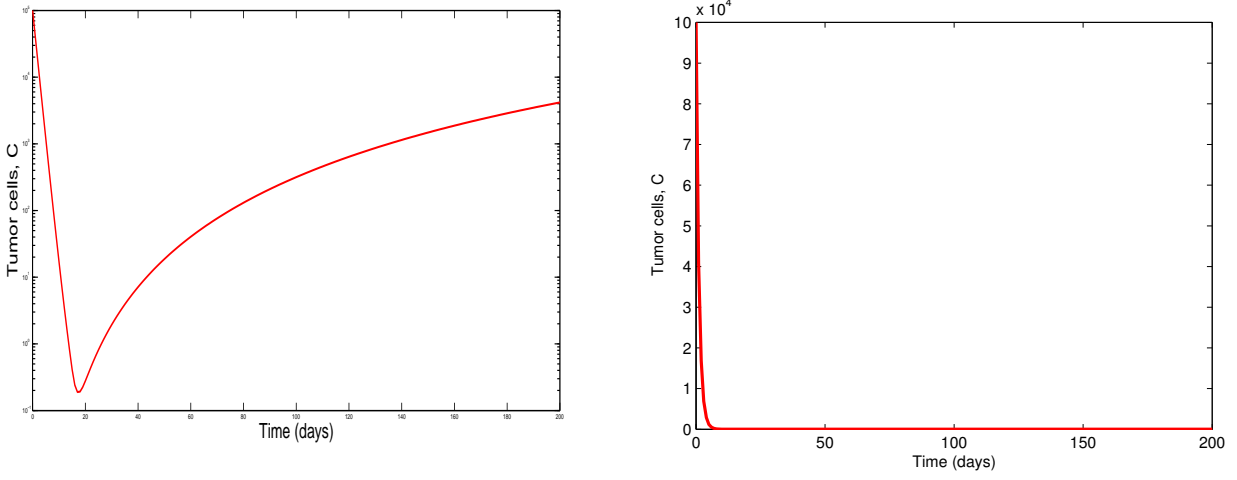
Figure (6) shows the dynamics of the CD8 T cell population. For Figure 6(a), where the infection rate of the CD4⁺ T cells is low, we observe significant growth of the CD8 T cells in the presence of treatment. Similarly, as in Figure 5b, no changes are obtained for higher infection rates.

3.3 Results with chemotherapeutic drug

Considering the parameter associated with chemotherapy intervention, $u_{in}(t)$, we assume administration of 2.3869 mg/L $\simeq 2386900$ pg/mL per every 21 days for tumors, as suggested in [48]. Therefore, if T (every 21 days) is the drug infusion time, then the mass inflow is given by

$$u_{in} = \begin{cases} 2.3869, & t = T = 21n, \quad n = 1, 2, \dots \\ 0, & \text{otherwise} \end{cases}$$

With the inclusion of chemotherapy in the model, no difference is seen for the cases with and without HAART therapy. Chemotherapy administration occurs when the tumor is large and detectable, thus considering the initial state of tumor as 1×10^5 cells/ml, we observe that the drug is very effective in eliminating the tumors when the decay rate in the system is smaller. Administering same therapy but with a higher decay rate in the system, the tumor will not be eliminated and instead the tumors will regrow as seen in Figure 7a. This implies that the length



(a) Drug elimination rate, $d_D = 0.9$ with a log scale on the vertical axis.

(b) Drug elimination rate, $d_D = 0.1$

Figure 7: Population dynamics for a period of 200 days of the tumor cells in model system (3) with both therapies (HAART and chemotherapy) with parameters as in Table (2). Initial conditions: $M_1(0) = 2000$

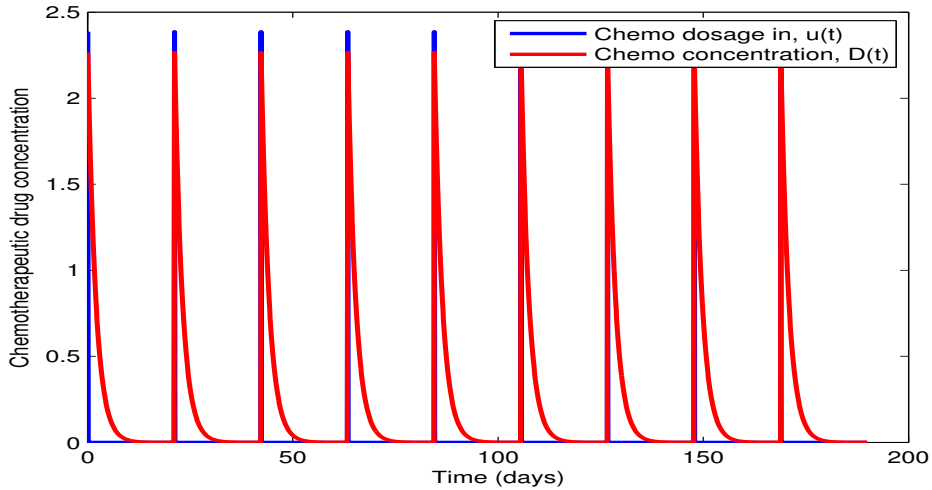


Figure 8: Chemotherapeutic drug dose concentration in the system administered 1 day every 21 days for 200 days i.e 9 doses every 21 days.

of time a chemotherapeutic drug has to act against the tumor is very critical since smaller decay rate/ elimination rate implies a longer time required to act against the tumor. Figure 7b thus shows the effect of smaller decay rate on tumor elimination.

4 Discussion and Conclusions

In this paper we investigated the role of HIV in the model of AIDS-related non-Hodgkin Lymphoma by considering cytokines, macrophages, CD4⁺ T helper cells, CD8⁺ T effector cells and the virus in the tumor environment.

From the analysis, it suffices to deduce that when HIV is present in the tumor environment and no treatment of the HIV initiated in the patient, for a non-aggressive tumor state to be achieved the tumor killing rate has to be higher , i.e. higher immune response as compared to the case where treatment of HIV with HAART is initiated. This implies that the timing of initiating HIV treatment in patients with the tumor is an important factor since the tumor can remain in a non-aggressive state despite lower immune response (the comparison is done with respect to no treatment case). The bifurcation analysis shows that treatment plays an important role in shifting the steady states. We notice that given the same value of parameter β_3 , the steady states values decrease when HIV treatment is included in the model system and for most of the parameter value β_3 , the existence of only low endemic tumor state is observed. This implies that, as opposed to the no HIV treatment scenario, the tumor can be controlled to a non-aggressive state despite low immune response.

We also observe that when the HIV infection rate is low, initiating treatment in patients with HIV-related NHLs reduces tumor growth. Also, no effective control of the tumor will be observed despite HIV treament as long as the tumor killing rate is small, i.e. weak immune response. Our model represents a possible long-lasting coexistence of HIV-related NHLs and HIV, because of the existence of the non-zero equilibria. Despite a patient's strong immune response and treatment of the HIV with the reverse transcriptase inhibitors (RTIs) and protease inhibitors (PIs) drugs of efficacy for instance, 50% in our case, complete elimination of the tumor by the immune system is actually not possible. The tumors will still remain in the host system unless the tumor elimination rate is very high, though at a lower state that is not so destructive and thus the patient survives with the tumors for a longer period of time. This could also explain why some people live with cancer for many years. Moreover, it can also explain why late initiation of HIV treatment is not very helpful to NHL patients. In the case of chemotherapy, the time taken by the drug to act on the tumor is an important factor and thus to reduce cancer related deaths, the chemotherapeutic drugs used should have low elimination rates. This implies that the absorption, distribution and clearance of the drugs take much longer time and this might explain why a few of these drugs are more effective when given at a slow continuous rate for a few days at a time.

The model presented in this paper is a very simplified caricature of a complex biological interaction of immune cells, cytokines and HIV in a tumor environment and therefore it has some lucid limitations. The model does not take into account the spatial growth of the tumors and the associated metabolic elements and pathways. We also restrict the NHL to some environment, like the lymph nodes despite the fact that they can be found in many parts of the body. There is also paucity of experimental data for model verification. Despite these limitations, the model results have significant bearings on NHL dynamics and its coexistence with HIV.

Acknowledgments

The authors are grateful to the University of Stellenbosch and African Institute for Mathematical Sciences (AIMS) for their support during the production of the manuscript. They are also

grateful for the support and help of Avner Friedman in setting up the model.

References

- [1] Cancer facts and figures 2014. A publication of the American Cancer Society Incorporated. Available at: <http://www.cancer.org/acs/groups/content/@research/documents/webcontent/acspc-042151.pdf>
- [2] Barros M.H.M., Hauck F., Dreyer J.H., Kempkes B., Niedobitek G., Macrophage polarisation: an immunohistochemical approach for identifying M_1 and M_2 macrophages, PLoS ONE 8(11) (2013) e80908. doi:10.1371/journal.pone.0080908.
- [3] Buske C., Hannig H., Schneider E.M., Blaschke S., Hunsmann G., Bodemer W., Hiddemann W., Transforming growth factor beta is a growth-inhibitory cytokine of B cell lymphoma in SIV-infected macaques, AIDS Res Hum Retroviruses, 15(16) (1999) 1477-1485.
- [4] National Cancer Institute. What is Non-Hodgkin Lymphoma? <http://www.cancer.gov/cancertopics/wyntk/non-hodgkin-lymphoma/page2>, Accessed 7 May, 2014.
- [5] Duff D.K., Thompson S., Braye S., Price D., Loewenthal M., Boyle M.J., The cytokine milieu of HIV-associated non-Hodgkin's lymphoma favours aggressive tumors, AIDS, 14(1) (2000) 92-94.
- [6] Dong M., Blobel G.C., Role of transforming growth factor- β in hematologic malignancies, Blood, 107 (2006) 4589-4596.
- [7] Fassone L., Gaidano G., Ariatti C., Vivenza D., Capello D., Gloghini A., Cilia A.M., Buonaiuto D., Rossi D., Pastore C., Carbone A., Saglio G., The role of cytokines in the pathogenesis and management of AIDS-related lymphomas, Leuk Lymphoma, 38(5-6) (2000) 481-488
- [8] Goedert J.J., The epidemiology of acquired immunodeficiency syndrome malignancies. Semin. Oncol., 27(4) (2000) 390-401.
- [9] Gordon S., Martinez F.O. Alternative activation of macrophages: mechanism and functions. Immunity. 32(5) (2010) 593-604.
- [10] Grulich A.E., Vajdic C.M., The epidemiology of non-Hodgkin lymphoma, Path. 25 (2005) 409-419.
- [11] Gu Y., Circulating cytokines and risk of B-cell non-Hodgkin lymphoma, UMI, 2008.
- [12] Heusinkveld M., van der Burg S.H., Identification and manipulation of tumor associated macrophages in human cancers, J. Translat. Med. 9 (2011) 216.
- [13] Hsu S., Waldron Jnr J.W., Hsu P., Hough Jnr A.J., Cytokines in malignant lymphomas, Hum. Pathol., 24 (1993) 1040-1056.
- [14] Levine A.M., Seneviratne L., Espina B.M., Wohl A.R. et al., Tulpule A., Nathwani B. N. , Gill P.S., Evolving characteristics of AIDS-related lymphoma, Blood, 96(13) (2000) 4084-4090.
- [15] Liao K., Bai X., Friedman A., The role of CD200-CD200R in tumor immune evasion, J Theor. Biol., 328 (2013) 65-76.

- [16] Louzoun Y., Xue C., Lesinski G.B., Friedman A., A Mathematical model for pancreatic cancer growth and treatment, *J Theor. Biol.*, 351 (2014) 74-82.
- [17] Nogai H., Dörken B., Lenz G., Pathogenesis of non-hodgkins lymphoma, *J. Clin. Oncol.*, 29(14) (2011) 1803-1811.
- [18] Pastore C., Gaidano G., Ghia P., Fassone L., Cilia A.M., Gloghini A., Capello D., Buonaiuto D., Gonella S., Roncella S., Carbone A., Saglio G., Patterns of cytokine expression in AIDS related non-Hodgkin's lymphoma, *Brit. J. Haematol.*, 103 (1998) 143-149.
- [19] Pluda J.M., Venzon D.J., Tosato G., Lietzau J., Wyvill K., Nelson D.L., Jaffe E.S., Karp J.E., Broder S., Yarchoan R., Parameters affecting the development of non-Hodgkin's lymphoma in patients with severe human immunodeficiency virus infection receiving antiretroviral therapy, *J. Clin. Oncol.*, 11 (1993) 1099-1107.
- [20] Ruff K.R., Puettner A., Levy L.S., Growth regulation of simian and human AIDS-related non-Hodgkin's lymphoma cell lines by TGF- β_1 and IL-6, *BMC Cancer*, 7 (2007) 35.
- [21] Shek F.W., Benyon R.C., Walker F.M., McCrudden P.R., Pender S.L., Williams E.J., Johnson P.A., Johnson C.D., Bateman A.C., Fine D.R., Iredale J.P., Expression of transforming growth factor-beta 1 by pancreatic stellate cells and its implications for matrix secretion and turnover in chronic pancreatitis, *Am. J. Pathol.*, 160 (2002), 1787-1798.
- [22] Sica A., Mantovani A., Macrophage plasticity and polarization: in vivo veritas, *J Clin Invest.* 122(3) (2012) 787-795.
- [23] Takeuchia E., Yanagawa H., Suzukia Y., Shinkawaa K., Ohmotoa Y., Bandob H., Sonea S., IL-12 induced production of IL-10 and interferon- γ by nonnuclear cells in lung cancer-associated malignant pleural effusions, *Elsevier*, 35 (2002) 171-177.
- [24] Trinchieri G., Cytokines acting on or secreted by macrophages during intracellular infection (IL-10, IL-12, IFN- γ), *Curr. Opin. Immunol.* 9(1) (1997) 17-23.
- [25] Villinger F., Ansari A.A., Role of IL-12 in HIV infection and vaccine, *Eur. Cytokines Netw.*, 21(3) (2010) 215-218.
- [26] Zhang L., Yang J., Qian J., Li H., Romaguera J.E., Kwak L.W., Wang M., Yi Q., Role of the microenvironment in mantle cell lymphoma: IL-6 is an important survival factor for the tumor cells, *Blood*, 120 (2012) 3783-3792.
- [27] Asadullah K., Sterry W., Volk H.D., Interleukin-10 therapy-review of a new approach, *Pharmacological Reviews*, 55(2) (2003), 241-269.
- [28] Judie Alimonti B., Blake Ball T., Keith Fowke R., Mechanisms of CD4 $^{+}$ T lymphocyte cell death in human immunodeficiency virus infection and AIDS, *J Gen Virol*, 84(7) (2003), 1649-1661.
- [29] Rebecca V.C, Sigui R., A delay-differential equation model of HIV infection of CD4 $^{+}$ T-cells, *Mathematical Biosciences* 165 (2000) 27-39.
- [30] Nathalie V., Robert T., Eric G., Henry-Jacques D., Franoise R., Irene J., Marie C., and Jean-Yves Blay, Interleukin (IL)-10 and IL-6 Are Produced in Vivo by Non-Hodgkin's Lymphoma Cells and Act as Cooperative Growth Factors, *Cancer Research*, 56 (1996) (5499-5505).

- [31] Kogan Y., Agur Z., Elishmereni M., A mathematical model for the immunotherapeutic control of the Th1/Th2 imbalance in melanoma, Discrete and Continuous Dynamical Systems Series B, 18(4) (2013) 1017-1030.
- [32] Kirschner D., Panetta J.C., Modeling immunotherapy of the tumor-immune interaction, J Math Biol, 37(1998) 235-252
- [33] Mugwagwa. T., Mathematical models of coreceptor usage and a dendritic cell-based vaccine during HIV-1 infection., 2005, Available at:
<http://theory.bio.uu.nl/tendai/theses.pdf>
- [34] Yunji W., Tianyi Y., Yonggang M., Ganesh V. H., Jianqiu Z., Merry L. L., Yu-Fang J., Mathematical modeling and stability analysis of macrophage activation in left ventricular remodeling post-myocardial infarction, BMC Genomics ,13(6) (2012) doi:10.1186/1471-2164-13-S6-S21, <http://www.biomedcentral.com/1471-2164/13/S6/S21>
- [35] Wilson S., Levy D., A Mathematical Model of the Enhancement of tumor Vaccine Efficacy by Immunotherapy,Bull Math Biol 74(2012) 1485-1500 doi: 10.1007/s11538-012-9722-4
- [36] Day J., Friedman A., Schlesinger L.S., Modelling the immune rheostat of macrophages in the lung in response to infection, Proc Natl Acad Sci U.S.A 106(27) 11246-11251
- [37] Titanji B. K., Aasa-Chapman M., Pillay D., Jolly C.,Protease inhibitors effectively block cell-to-cell spread of HIV-1 between T cells, Retrovirology , 10(161) (2013)
- [38] Fathalla A. Rihan, Duaa H. Abdel Rahman (): Delay differential model for tumor-immune dynamics with HIV infection of CD4 T-cells, International Journal of Computer Mathematics, DOI:10.1080/00207160.2012.726354 <http://dx.doi.org/10.1080/00207160.2012.726354>
- [39] Lai Y., Jeng C., Chen S., The roles of CD4⁺ T Cells in tumor immunity, ISRN Immunology, 2011. doi:5402/2011/497397
- [40] Kekow J., Wachsman W., McCutchan J. A., Gross W. L., Zachariah M., Carson D. A., Lotz M., Transforming growth factor-beta and suppression of humoral immune responses in HIV infection, J Clin Invest, 87(3) (1991) 1010-1016 doi: 10.1172/JCI115059
- [41] Wilson S., Levy D., A Mathematical Model of the Enhancement of Tumor Vaccine Efficacy by Immunotherapy, Bull Math Biol 74(2012) 1485-1500 doi: 10.1007/s11538-012-9722-4
- [42] Arciero J.C., Jackson T.L., Kirschner D.E, A mathematical model of tumor-immune evasion and siRNA treatment, Discrete and Continuous Dynamical Systems-series B, 4(1) 2004 39-58. <http://AIMsciences.org>
- [43] M. Y. Li, H. Shu, Global dynamics of a mathematical model for HTLV-I infection of CD4+ T cells with delayed CTL response, Non linear Analysis: Real World Applications (2011), doi:10.1016/j.nonrwa.2011.02.026
- [44] Hao W, Friedman A, The LDL-HDL profile determines the risk of atherosclerosis: A mathematical model. PLoS ONE 9(3) (2014): e90497. doi:10.1371/journal.pone.0090497
- [45] Guiota C., Delsanto P P., Carpinteri A., Pugno N., Mansurye Y., Deisboeck T.S., The dynamic evolution of the power exponent in a universal growth model of tumors, Journal of Theoretical Biology, 240(3) (2006), Pages 459-463 doi:10.1016/j.jtbi.2005.10.006

- [46] Rebecca V. C., Shigui R., Glenn W., A mathematical model of cell-to-cell spread of HIV-1 that includes a time delay, *J. Math. Biol.* 46 (2003) 425-444, doi: 10.1007/s00285-002-0191-5
- [47] Kwang S.K, Giphil C., Il H.J, Optimal treatment strategy for a tumor model under immune suppression, *Computational and Mathematical Methods in Medicine*, 2014, <http://dx.doi.org/10.1155/2014/206287>
- [48] L.G. de Pillis, W. Gu., A.E. Radunskaya, Mixed immunotherapy and chemotherapy of tumors: modelling, applications and biological interpretations, *J Theor. Biol.*, 238(2006), 841-862.

Noname manuscript No.
(will be inserted by the editor)

The effect of anti HIV drugs on HIV associated cancer *.

Rosemary Aogo · Farai Nyabadza · Avner Friedman

Received: date / Accepted: date

Abstract Highly active antiretroviral therapy (HAART) used for HIV treatment is a combination therapy, that includes reverse transcriptase inhibitor (RTI) and protease inhibitor (PI) in different proportions; it is more effective in treating HIV than a single drug therapy. HIV/AIDS associated cancers are cancers whose incidence is much higher in HIV/AIDS patients than in the general population. In many communities in sub-Saharan Africa, HAART is available but not anti cancer drugs. In this paper we develop a mathematical model to explore how effective is the combination therapy in HIV associated cancer in reducing cancer growth. Our model simulations show how to choose the proportions of RTI and PI in order to maintain an acceptable level of $CD4^+$ T cells and, at the same time, reduce the growth of cancer cells as much as possible. Although our model is generic, it could be used as a first step in developing a more detailed model for a specific HIV-associated cancer.

Keywords HAART · HIV · HIV/AIDS · associated cancer · simulation

1 Introduction

The hallmark of Human immunodeficiency virus (HIV) is deficiency in $CD4^+$ T cells, caused by the virus which infects them and causes their destruction. The disease is characterised as acquired immunodeficiency syndrome (AIDS) when the number of T cells falls from 700000 in ml of blood to 200000. The most effective anti HIV drug is HAART, a combination drug of reverse transcriptase inhibitor (RTI) and protease inhibitor (PI). Since $CD4^+$ T cells are an important component of the immune defense against diseases and in particular against cancer, people with advanced stage of HIV are at risk of developing cancer.

The majority of cancers affecting HIV-positive people are Kaposi sarcoma (KS), non-Hodgkin's Lymphoma (NHL) and invasive cervical cancer ([Newcomb-Fernandez, 2003](#)). Other types of cancer which occur somewhat more frequently in HIV/AIDS patients include, anal cancer ([Newcomb-Fernandez, 2003](#)), lung cancer ([Mani et al., 2012](#); [Newcomb-Fernandez, 2003](#)), and colorectal cancer ([Ford et al., 2008](#)). KS is an indolent cancer, involving multiple tumor of the lymph nodes or skin, and occurring mainly in people with depressed immune system. Cervical cancer is caused by several types of virus, the most common one is human papillomavirus (HPV). NHL is a blood disease which is characterised by abnormal growth of

* This work was funded by CANSA, South Africa

R. Aogo *
Department of Mathematics, University of Stellenbosch P. Bag X 1, Matieland, 7602, South Africa
Tel.: +277-40-653383
E-mail: rosemary@aims.ac.za

F. Nyabadza
Department of Mathematics, University of Stellenbosch P. Bag X 1, Matieland, 7602, South Africa
E-mail: nyabadzaf@sun.ac.za

A. Friedman
Mathematical Biosciences Institute, The Ohio State University 1735 Jennings Hall, Neil Avenue, Columbus OH, 43210
E-mail: afriedman@math.osu.edu

mutated lymphocytes (Hoffmann et al., 2015; Moosa, 2012; Stebbing et al., 2004). A positive correlation between immunosuppression and increased incidence of Hodgkin disease (HD) has been demonstrated in several studies, and those infected with HIV are 7.6 to 11.5 times more likely to have HD compared to the general population (Newcomb-Fernandez, 2003).

Cancer is treated by surgery, radiation, immunotherapy and chemotherapy. An individual with HIV who develops cancer, should be treated for both cancer and HIV. However, in poor communities around the world where anti HIV drugs are nevertheless available, anti cancer treatment is almost non-existent. For example, the estimates regarding access to or coverage of the cytotoxic chemotherapy in sub-Saharan Africa are largely unknown (Mwamba et al., 2012). The study by (Gopal et al., 2012) also indicates that, out of the 54 sub-Saharan Africa countries, only 21 have operational radiotherapy service units. The delay and misdiagnosis of lymphoma, more specifically the diffuse large B-cell NHL in HIV patients, remains a major problem in South Africa (Puvaneswaran and Shoba, 2013): Cancer, especially NHL, is often misdiagnosed as tuberculosis, and this implies that patients living with HIV and HIV-related NHL are only introduced to HAART, instead of receiving the anti-cancer drugs.

We quantify the efficacy of RTI by a parameter ζ_r where $0 \leq \zeta_r \leq 1$ and say that the efficacy of RTI is $n\%$ if $\zeta_r = n/100$. Similarly we quantify the efficacy of PI by a parameter ζ_p , where $0 \leq \zeta_p \leq 1$. In view of the inadequate supply of chemotherapeutic drugs and radiotherapy equipments as well as increased incidences of NHL misdiagnosis and the lack of trained personnel in Sub-Saharan Africa (Gopal et al., 2012; Mwamba et al., 2012; Puvaneswaran and Shoba, 2013), the question arises; Can RTI and PI be combined in a way that will reduce the cancer load as much as possible, while maintaining acceptable level of $CD4^+$ T cells?

To answer this question we develop a mathematical model that describes the interactions of macrophages (pro-inflammatory, M_1 and anti-inflammatory, M_2), T cells (healthy $CD4^+$ T cells, HIV-infected $CD4^+$ T cells and $CD8^+$ T cells), HIV, and cancer cells. The various cells interact with each other through several cytokines.

Human tumor microenvironment includes macrophages and these tumor associated macrophages (TAMs) are phenotypically classified as M_1 and M_2 (Gordon and Martinez, 2010; Heusinkveld and van der Burg, 2011). The M_1 macrophages are associated with acute inflammation and T-cell immunity, and are characterized by the expression of high levels of pro-inflammatory cytokines. The M_2 macrophages are anti-inflammatory and are associated with the promotion of cancer growth (Gordon and Martinez, 2010; Heusinkveld and van der Burg, 2011; Roda et al., 2012). TAMs can switch type between pro-inflammatory M_1 and anti-inflammatory M_2 in the tumor environment (Heusinkveld and van der Burg, 2011). IL-6 has been identified as a key cytokine for the B-cell NHLs' growth and survival (Zhang et al., 2012). TGF- β has an inhibitory factor in the regulatory network of AIDS-related lymphomagenesis (Buske et al., 1999; Ruff et al., 2007), and an immunosuppressive role, mediated predominantly by its effects on T cells and antigen-presenting cells (APCs) (Dong and Blobel, 2000). IL-6 and TGF- β induce polarization of M_2 into M_1 macrophages and promote an immunosuppressive environment (Zhang et al., 2012). One of the most important features of M_1 macrophages is the production of a T-cell stimulating cytokine IL-12 which enhances natural killer cell activities by activation of CD8 effector T cells (Villinger and Ansari, 2010). M_2 macrophages produce IL-10 which down regulates the activities of IL-12, and thus inhibits the activation of T cells by IL-12 (Asadullah et al., 2003; Groux et al., 1998; Trinchieri, 1997). $CD4^+$ T cells produce cytokine IL-2 which induces growth, proliferation and activation of both $CD4^+$ T cells and $CD8^+$ T cells. $CD8^+$ T cells, also called cytotoxic T cells (CTL), are directly involved in killing cancer cells (Lai et al., 2011).

The model we develop is not specific to any cancer, and as clinical data becomes available, for instance in the case of NHL, some of the parameters could be made more precise. The present model aims to establish the concept that combination drugs available only against HIV can be judiciously adjusted to be useful against cancer. The model focuses on the role of T cells in killing the cancer cells, since in HIV infected individuals, the reduced number of T cells exacerbates cancer growth.

2 Mathematical model

The mathematical model therefore includes the variables listed in Table 1. The mathematical model is based on the network described in Figure 1.

Variable	Description	Units
M_1	density of pro-inflammatory tumor associated macrophages	cells/ml
M_2	density of anti-inflammatory tumor associated macrophages	cells/ml
T_4	density of healthy CD4 ⁺ T cells	cells/ml
T_4^i	density of virus-infected CD4 ⁺ T cells	cells/ml
V	density of extracellular HIV	virus/ml
T_8	density of CD8 ⁺ T cells	cells/ml
C	density of cancer cells	cells/ml
T_β	concentration of transforming growth factor (TGF- β)	pg/ml
I_6	concentration of interleukin 6 (IL-6)	pg/ml
I_{10}	concentration of interleukin 10 (IL-10)	pg/ml
I_{12}	concentration of interleukin 12 (IL-12)	pg/ml
I_2	concentration of interleukin 2 (IL-2)	pg/ml

Table 1: Variables and their units

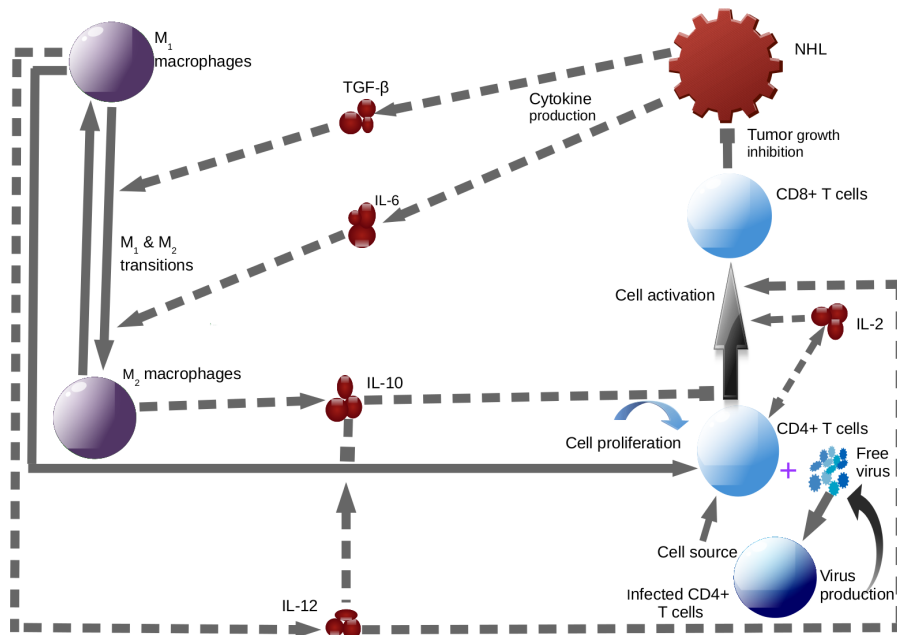


Fig. 1: Schematic representation of interactions of cells and cytokines in HIV-NH Lymphoma. We have macrophages M_1, M_2 , T-cells (immune cells) T_4, T_4^i, T_8 , cytokines ($T_\beta, I_6, I_{10}, I_{12}, I_2$), the cancer cells, C and HIV, V . The pool of viruses V , through infection, affects the movement of the CD4⁺ T cells into the infected compartment T_4^i . We have used dotted lines with arrow heads to represent cytokine production, and cell activation and with square head to represent inhibition. The bold lines with arrow head represent induction, transition or activation, and with square head represents killing.

2.1 Model equations

2.1.1 Equations of the cytokines.

$$\left. \begin{array}{l} \frac{dT_\beta}{dt} = \alpha_1 C - d_1 T_\beta, \\ \frac{dI_6}{dt} = \alpha_6 C - d_6 I_6, \\ \frac{dI_{10}}{dt} = \alpha_{10} M_2 - d_{10} I_{10}, \\ \frac{dI_{12}}{dt} = \alpha_{12} M_1 - d_{12} I_{12}, \\ \frac{dI_2}{dt} = \alpha_2 T_4 - d_2 I_2. \end{array} \right\} \quad (1)$$

T_β and I_6 are produced by cancer cells (Fassone et al., 2000; Louzoun et al., 2014; Ruff et al., 2007), I_{12} and I_{10} are produced primarily by M_1 and M_2 macrophages respectively (Louzoun et al., 2014; Takeuchia et al., 2002; Trinchieri, 1997), and I_2 is produced by T_4 cells (Lai et al., 2011). The parameters α_i represent the production of the cytokines by the respective cells the parameters d_i represent cytokines decay.

2.1.2 Immune cell equations

The dynamics of macrophages are given by the following equations

$$\frac{dM_1}{dt} = s_1 - k_1 M_1 + \nu M_2 - (\lambda_1 T_\beta + \lambda_2 I_6) M_1, \quad (2)$$

$$\frac{dM_2}{dt} = s_2 + (\lambda_1 T_\beta + \lambda_2 I_6) M_1 - k_2 M_2 - \nu M_2, \quad (3)$$

Here s_1 and s_2 are source terms for M_1 and M_2 macrophages, ν represents the unbiased interchange between these two macrophage phenotypes, and $(\lambda_1 T_\beta + \lambda_2 I_6)$ is the rate by which additional transformation occurs from M_1 to M_2 (Louzoun et al., 2014).

The density of CD4⁺ T cells, T_4 satisfies the equation

$$\frac{dT_4}{dt} = s_3 + \beta_1 \frac{I_{12} M_1}{K_{10} + I_{10}} + \beta_2 \frac{I_2 T_4}{K_2 + I_2} - \mu_1 T_4 - (1 - \zeta_r) \mu_2 V T_4, \quad (4)$$

with source term s_3 and apoptosis rate μ_1 . T_4 is further activated (from naive T cells) by I_{12} while in contact with M_1 , a process resisted by I_{10} (Asadullah et al., 2003; Groux et al., 1998; Louzoun et al., 2014). The third term on the right-hand side of equation (4) is the proliferation enhanced by I_2 (Lai et al., 2011), and the fourth term is the natural death of T_4 cells. The last term is depletion of T_4 as a result of invasion by external virus, a process which is reduced by RTI drug as represented by the factor $1 - \zeta_r$, where $0 \leq \zeta_r \leq 1$. The RTI works by blocking the reverse transcription of viral DNA and can therefore effectively prevent the target cell from becoming productively infected by the free virus. It is worth noting that the inhibition process by RTI occurs after the virus has been attached to the cell and therefore the drug does not directly affect the infection rate, μ_2 of the target cells.

The density of infected T_4 cells, T_4^i satisfies the equation

$$\frac{dT_4^i}{dt} = (1 - \zeta_r) \mu_2 V T_4 - \mu_5 T_4^i, \quad (5)$$

where in μ_5 we included both the natural death rate and the burst rate δ_2 of infected T_4 cells, hence $\mu_5 > \delta_2$. We assume that without HIV drugs, upon burst of one infected T_4 cell, N virions are released. However, this number will be decreased by a factor $1 - \zeta_p$, ($0 \leq \zeta_p \leq 1$) under treatment with PI drug.

PI blocks the action of HIV protease by preventing it from cleaving the viral polyprotein into functional sub units which ultimately prevents the production of mature viruses. Hence

$$\frac{dV}{dt} = (1 - \zeta_p)N\delta_2 T_4^i - \mu_v V, \quad (6)$$

where μ_v is the death, or degradation rate of extracellular virus.

T_8 cells are activated by I_{12} , a process inhibited by I_{10} (Asadullah et al., 2003; Groux et al., 1998; Louzoun et al., 2014), and by I_2 (Lai et al., 2011). Since HIV does not invade into T_8 cells, we have the following equation;

$$\frac{dT_8}{dt} = \beta_3 \frac{I_{12}}{K_{10} + I_{10}} + \beta_4 \frac{I_2 T_8}{K_2 + I_2} - \mu_4 T_8. \quad (7)$$

As in (Louzoun et al., 2014), we assume that the density of cancer cells (for instance, NHL cells which are mutated B cells) follows universal growth law and that the killing of cancer cells by T_8 cells follows mass-action law:

$$\frac{dC}{dt} = rC^{\frac{3}{4}} \left(1 - \left(\frac{C}{C_0} \right)^{\frac{1}{4}} \right) - \mu_c C T_8. \quad (8)$$

The parameters in the model system described in equations (1) - (8) are all non-negative.

2.2 The simplified model

The dynamics of cytokines is on a much faster scale than the dynamics of cells. Hence, following (Louzoun et al., 2014), we simplify the model (1) - (8) by taking the cytokines dynamics in the equation (1) to be in steady state, so that

$$T_\beta = \frac{\alpha_1}{d_1} C, \quad I_6 = \frac{\alpha_6}{d_6} C, \quad I_{10} = \frac{\alpha_{10}}{d_{10}} M_2, \quad I_{12} = \frac{\alpha_{12}}{d_{12}} M_1, \quad I_2 = \frac{\alpha_2}{d_2} T_4.$$

Substituting these cytokines into Eqs.(2) - (8) we obtain

$$\left. \begin{aligned} \frac{dM_1}{dt} &= s_1 - k_1 M_1 + \nu M_2 - \gamma_c C M_1, \\ \frac{dM_2}{dt} &= s_2 + \gamma_c C M_1 - k_2 M_2 - \nu M_2, \\ \frac{dT_4}{dt} &= s_3 + \frac{\gamma_1 M_1 M_1}{K_{10} + \gamma_2 M_2} + \beta_2 \frac{\gamma_3 T_4 T_4}{K_2 + \gamma_3 T_4} - \mu_1 T_4 - (1 - \zeta_r) \mu_2 V T_4, \\ \frac{dT_4^i}{dt} &= (1 - \zeta_r) \mu_2 V T_4 - \mu_5 T_4^i, \\ \frac{dV}{dt} &= (1 - \zeta_p) N \delta_2 T_4^i - \mu_v V, \\ \frac{dT_8}{dt} &= \frac{\gamma_4 M_1}{K_{10} + \gamma_2 M_2} + \beta_4 \frac{\gamma_3 T_4 T_8}{K_2 + \gamma_3 T_4} - \mu_4 T_8, \\ \frac{dC}{dt} &= r C^{\frac{3}{4}} \left(1 - \left(\frac{C}{C_0} \right)^{\frac{1}{4}} \right) - \mu_c C T_8, \end{aligned} \right\} \quad (9)$$

where $\gamma_c = \lambda_1 \frac{\alpha_1}{d_1} + \lambda_2 \frac{\alpha_6}{d_6}$, $\gamma_1 = \beta_1 \frac{\alpha_{12}}{d_{12}}$, $\gamma_2 = \frac{\alpha_{10}}{d_{10}}$, $\gamma_3 = \frac{\alpha_2}{d_2}$ and $\gamma_4 = \beta_3 \frac{\alpha_{12}}{d_{12}}$.

3 Parameter estimation

Table 2 provides the description and values of all the parameters that appear in Eqs.(1)-(8). Most of the parameters are taken from the literature, although not always from cancer experimental data. The parameters s_3 and α_1 are estimated as follows;

We assume that at steady state of HIV infected person, when he/she still appears to be normal, $T_4 = 500000$ cells/ml. Since $\mu_1 = 0.02/\text{day}$ (V.C.Rebecca and Sigui, 2000), from the cancer-free steady state equation $s_3 - \mu_1 T_4 = 0$ and $\mu_1 = 0.02/\text{day}$ we then get $s_3 = 10000$ cells/ml day. In normal healthy individual, the average monocyte content is 400000cells/ml (mon). We assume that monocytes differentiate mostly into M_1 macrophages as they move from the blood into the tissue, and thus take $M_1 = 400000$ cells/ml. From the cancer-free steady state equation $s_1 - k_1 M_1 = 0$ and $k_1 = 0.02/\text{day}$, we get $s_1 = 8000$ cells/ml/day. It is known that tumor attracts myeloid derived suppressor cells (MDSC), cells that have similar behaviour to M_2 cells(Sevko and Umansky, 2013). We identify MDSC with M_2 , and for simplicity consider this source of macrophages as a source term s_2 . We assume that this source is small in comparison to the source of M_1 macrophages, and take $s_2 = s_1/10 = 800$ cells/ml/day. Since $k_2 = 0.008/\text{day}$, the steady state equation $s_2 - k_2 M_2 = 0$ yields the steady state density $M_2 = 100000$ cells/ml. We take the values of parameters λ_1 and λ_2 to be 0.075 day^{-1} as in (Yunji et al., 2012). We also assume that $\beta_4 = \beta_2$ and $\beta_3 = 0.5\beta_1$. We finally take $N = 1000$, although this number varies in different studies (V.C.Rebecca and Sigui, 2000).

Table 2: Estimated Parameter values.

Parameter	Description	Values	Units	Source
α_2	production rate of IL-2 due to CD4 ⁺ T cells	5	pg/cell day	(Arciero et al., 2004; Kirschner and Panetta, 1998)
α_1	production rate of TGF- β due to cancers cells	7×10^{-4}	pg/cell day	(Arciero et al., 2004; Tzai et al., 1999)
α_6	production rate of IL-6 due to cancers cells	7×10^{-5}	pg/cell day	Estimated
α_{10}	production rate of IL-10 due to M_2	5×10^{-4}	pg/cell day	(J.Day et al., 2008; J.P.Edwards et al., 2006; Yunji et al., 2012)
α_{12}	production rate of IL-12 due to M_1	3×10^{-2}	pg/cell day	Estimated in(J.Day et al., 2008)
d_1	degradation rate of TGF- β	10	day ⁻¹	Estimated in (Arciero et al., 2004)
d_2	degradation rate of IL-2	10	day ⁻¹	(Kirschner and Panetta, 1998; Rosenberg and M.T.Lotze, 1986)
d_6	degradation rate of IL-6	0.173	day ⁻¹	(Lu et al., 1995)
d_{10}	degradation rate of IL-10	5	day ⁻¹	(J.Day et al., 2008)
d_{12}	degradation rate of IL-12	1.188	day ⁻¹	(J.Day et al., 2008; Ohno et al., 2000)
s_1	influx rate of M_1	8000	cells/ml day	Estimated
s_2	influx rate of M_2	800	cells/ml day	Estimated
s_3	production of CD4 ⁺ T cells by the sources	10000	cells/ml day	Estimated
k_1	per capita death rate of M_1	0.02	day ⁻¹	(J.Day et al., 2008)
k_2	per capita death rate of M_2	8×10^{-3}	day ⁻¹	(J.Day et al., 2008; Keane et al., 1997)
λ_1	transformation rate of M_1 to TGF- β	0.075	day ⁻¹	Estimated in (Yunji et al., 2012)
λ_2	transformation rate of M_2 by IL-6	0.075	day ⁻¹	Estimated in (Yunji et al., 2012)
ν	transition rate from M_2 to M_1	5×10^{-2}	day ⁻¹	(Steinmiller et al., 2000; Yunji et al., 2012)
β_1	proliferation rate of T_4 cells due to IL-12	10 ⁶	cells/ml day	(Hao and Friedman, 2014)
β_2	proliferation rate of T_4 cells by IL-2	0.1245	pg/cell day	(Arciero et al., 2004; Kirschner and Panetta, 1998; Kuznetsov et al., 1994)
β_3	proliferation rate of T_3 cells due to IL-12	0.5×10^6	cells/ml day	assumed
β_4	proliferation rate of T_3 cells by IL-2	0.1245	pg/cell day	assumed
μ_c	loss of cancer cells	$10^{-10} \sim 10^{-9}$	day ⁻¹	(Louzon et al., 2014; Seki et al.; Wilson and Levy, 2012) and estimated (10^{-9})*
K_2	saturation constant of proliferation by IL-2	2×10^7	pg/ml	(Kirschner and Panetta, 1998; Kuznetsov et al., 1994)
K_{10}	saturation constant for anti-proliferation by IL-10	2.5×10^7	pg/ml	(Hao and Friedman, 2014)
μ_1	per capita death rate of uninfected CD4 ⁺ T cells	0.02	day ⁻¹	Estimated in (V.C.Rebecca and Sigui, 2000)
μ_2	infection rate of CD4 ⁺ T cells due to infiltration by free viruses	2.4×10^{-8}	ml/day	Estimated in (V.C.Rebecca and Sigui, 2000)
μ_4	per capita death rate of CD8 ⁺ T cells	0.03 ~ 0.0412	day ⁻¹	(Kirschner and Panetta, 1998; Kuznetsov et al., 1994)0.03*
μ_5	clearance rate (loss) of free viruses	2.4	day ⁻¹	Estimated in (V.C.Rebecca and Sigui, 2000)
μ_6	per capita death rate of infected CD4 ⁺ T cells	0.26	day ⁻¹	Estimated in (V.C.Rebecca and Sigui, 2000)
δ_2	lytic death rate of infected CD4 ⁺ T cells	0.24	day ⁻¹	Estimated in (V.C.Rebecca and Sigui, 2000)
N	Virions produced during a lifetime by an infected CD4 ⁺ T cells	Varies	day ⁻¹	Estimated in (V.C.Rebecca and Sigui, 2000)
r	cancer growth rate	$0.18 \sim 0.19$	cells/ml	(Arciero et al., 2004; Kirschner and Panetta, 1998; Kuznetsov et al., 1994; Wilson and Levy, 2012) 0.19*
C_0	maximum cancer density	10^6	cells/ml	Estimated in (Louzon et al., 2014)
N	number of virions released upon burst by an infected T4 cell	1000	cells/ml	(V.C.Rebecca and Sigui, 2000) and assumed
ζ_r	the measure of efficacy of reverse transcriptase inhibitors(RTIs)	[0, 1]		
ζ_p	the measure of efficacy of protease inhibitors(PIs)	[0, 1]		

* value chosen in the simulation.

4 Simulation results

The results presented below of the numerical simulations for system (9) were obtained using Matlab ODE45 Solver which employs simultaneously the fourth and fifth order Runge Kutta schemes. Unless otherwise stated, parameters are as stated in Table 2.

We take the following initial conditions: $M_1(0) = 400000$ cells/ml, $M_2(0) = 100000$ cells/ml, $T_4(0) = 500000$ cells/ml, $T_4^i(0) = 0$ cells/ml, $V(0) = 1000$ copies/ml, $T_8(0) = 100$ and $C(0) = 100$ cells/ml.

We explore the effect of combined HIV therapy on the cancer. Recall that one type of drugs (RTIs) reduces the infection of T_4 cells by virus by a factor $1 - \zeta_r$, while another type of drugs (PIs) reduces the proliferation rate of virus within infected T_4 cells by a factor $1 - \zeta_p$. As mentioned in the introduction, we shall say that RTI has efficacy of $n\%$ if $\zeta_r = n/100$, and similarly PI has efficacy of $n\%$ if $\zeta_p = n/100$.

Figure 2 is a combination therapy map for cancer cells. Starting with $C(0) = 100$ cells/ml, it shows the density of cancer cells at days 350, 1000 and 20000 for any combination of ζ_r and ζ_p . In particular,

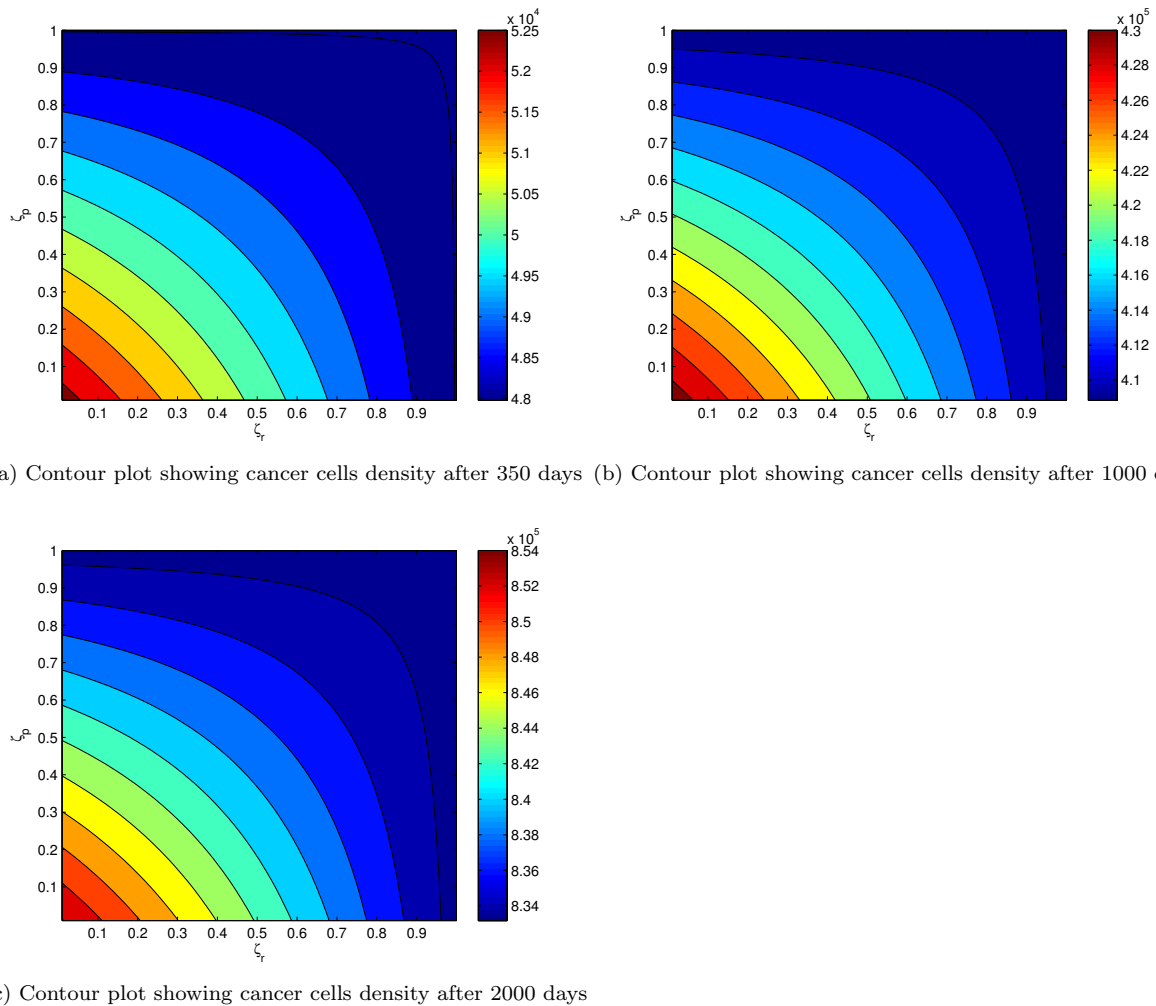
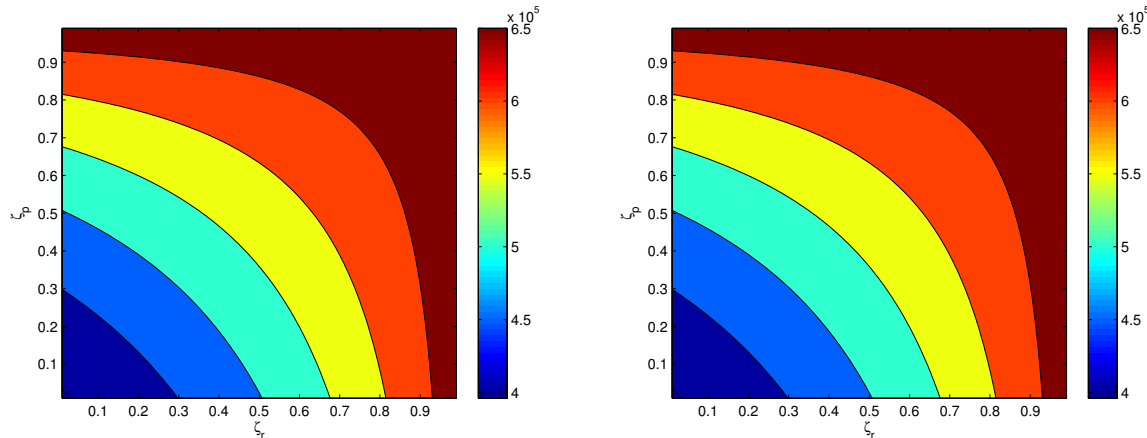
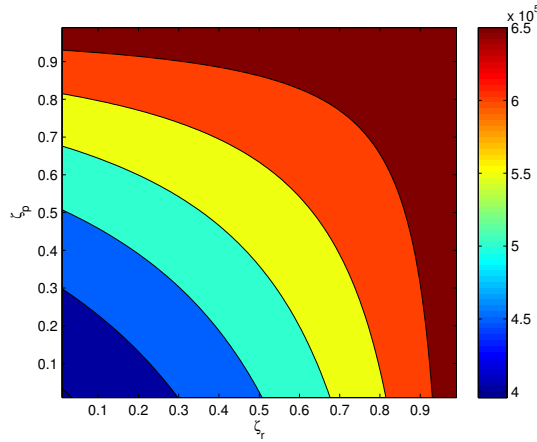


Fig. 2: Combination therapy map: $C(t)$, for $t=350, 1000$ and 2000 days as a function of RTI (ζ_r) and PI (ζ_p) combination, the parameters are as in Table 2. The color bar shows the $C(t)$ values for various drug combination.

with no drugs, $C(350) = 5.25 \times 10^4$ cells/ml, $C(1000) = 4.3 \times 10^5$ and $C(2000) = 8.54 \times 10^5$. From the convex shape of the equi-cancer-cell-number curves we see that if two drugs, ζ_r with efficacy $n\%$ and ζ_p with efficacy $m\%$, ($n + m < 100$) can be replaced by just one drug, say ζ_r , with efficacy $\zeta_r = (n + m)\%$ then the result will lead to a decrease in the growth of the cancer.



(a) Contour plot showing CD4 T cells density after 350 days (b) Contour plot showing CD4 T cells density after 1000 days



(c) Contour plot showing CD4 T cells density after 2000 days

Fig. 3: Combination therapy map: $T_4(t)$, for $t=350, 1000$ and 2000 days as a function of RTI (ζ_r) and PI (ζ_p) combination, the parameters are as in Table 2. The color bar shows the $T_4(t)$ values for various drug combination.

Figure 3 is a color map of T cells at $t=350, 100$ and 2000 days as a function of ζ_r and ζ_p . Similar to Figure 2, we see that if the two drugs with efficacies $m\%$ and $n\%$ can be replaced by one drug with efficacy $(n + m < 100)$ then the resulting number of CD4+ T cells will increase.

5 Discussion and conclusions

In this paper we investigated the effect of HIV treatment on AIDS-related cancers (including for example NHL). We developed a mathematical model which includes; macrophages, CD4⁺ T helper cells and CD8⁺ T effector cells, various cytokines produced by these cells and by cancer cells, and the virus. We investigated the effect of combined RTI and PI drugs on reduction of cancer load. We created a combination therapy map for cancer-cells number, $C(t)$, for $t=350, 1000$ and 2000 days as a function of ζ_r and ζ_p combination. The results show how to best choose a combination of the two drugs that reduces the cancer load in the host environment while maintaining the CD4+ T cells at an 'acceptable' level.

Indeed, suppose we wish to maintain the CD4+ T cells population at level $\bar{T}_4 = 500000$ cells/ml after 1000 days. We use Figure 4 to determine the pairs ζ_r, ζ_p for which the corresponding equi-color curve indicates the level \bar{T}_4 ; we can write these pair of points as $\zeta_p = h(\zeta_r)$ where h is a monotone decreasing function. Next, for each pair $\zeta_r, h(\zeta_r)$ we depict from Figure 3 the corresponding value of $C(1000)$, and denote it by $C(\zeta_r)$. As we vary ζ_r over the range of all possible efficacy levels, say $a < \zeta_r < b$, for which $\zeta_r = h(\zeta_r)$ is also a realizable efficacy level, we obtain a range of values $C(\zeta_r)$. Figure 4 shows a typical curve $C = C(\zeta_r)$; we see that the smallest number of cancer cells occurs at one of the extreme points, i.e at $\zeta_r = a$ or $\zeta_r = b$. Thus, the best strategy is to choose the minimum or maximum level of efficacy for ζ_r and the corresponding ζ_p by $\zeta_p = h(\zeta_r)$.

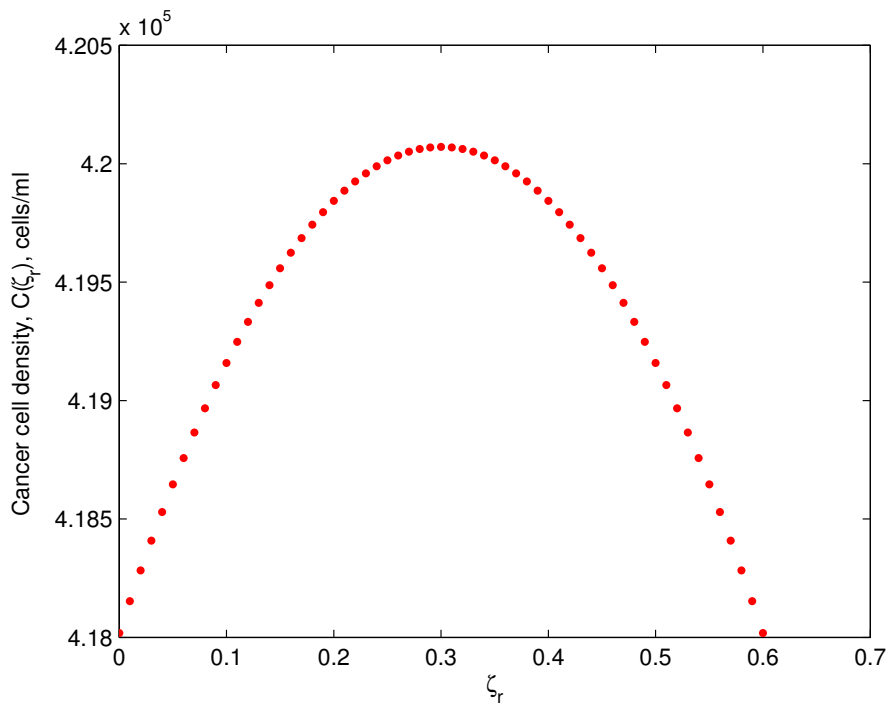


Fig. 4: Cancer cell density curve, $C(\zeta_r)$ at $t = 1000$ days, for each pair $(\zeta_r, h(\zeta_r))$, the parameters are as in Table 2.

We developed a mathematical model of HIV-associated cancer, and determined how to optimally choose the proportions of RTI and PI in the anti HIV combination drug HAART in order to maintain an acceptable level of CD4+ T cells and, at the same time, to reduce cancer growth as much as possible. The model however is generic; it is not cancer specific. Building on this model, future work should consider specific cancers, for example NHL, and by expanding the model to include additional relevant cells and cytokines, and more precise clinically or experimentally derived parameters, provide an improved prediction of the optimal combination of RTI and PI.

Acknowledgements The authors are grateful to the University of Stellenbosch, African Institute for Mathematical Sciences (AIMS) and the Mathematical Biosciences Institute at the Ohio State University for their support during the preparation of the manuscript.

References

- Monocyte. Available at <http://en.wikipedia.org/wiki/Monocyte>.
- J.C. Arciero, T.L. Jackson, and D.E. Kirschner. A mathematical model of tumor-immune evasion and siRNA treatment. *Discrete and Continuous Dynamical Systems-series B*, 4(1):39–58, 2004. <http://AIMsciences.org>.
- K. Asadullah, W. Sterry, and H.D. Volk. Interleukin-10 therapy-review of a new approach. *Pharmacological Reviews*, 55(2):241–269, 2003.
- C. Buske, H. Hannig, E.M. Schneider, S. Blaschke, G. Hunsmann, W. Bodemer, and W. Hiddeemann. Transforming growth factor beta is a growth-inhibitory cytokine of B cell lymphoma in SIV-infected macaques. *AIDS Res Hum Retroviruses*, 15(16):1477–1485, 1999.
- M. Dong and G.C. Blobe. Role of transforming growth factor- β in hematologic malignancies. *Blood*, 107: 44589–4596, 2000.
- L. Fassone, G. Gaidano, C. Ariatti, D. Vivenza, D. Capello, A. Gloghini, A.M. Cilia, D. Buonaiuto, D. Rossi, C. Pastore, A. Carbone, and G. Saglio. The role of cytokines in the pathogenesis and management of AIDS-related lymphomas. *Leuk Lymphoma*, 38(5):81–488, 2000.
- R.M. Ford, M.M. McMahon, and M.A. Wehbi. HIV/AIDS and colorectal cancer . *Gastroenterol Hepatol*, 4(4):274–278, 2008.
- S. Gopal, W. A. Wood, S. J.Lee, T.C. Shea, K.N. Naresh, P.N. Kazembe, C. Casper, P.B. Hesseling, and R.T. Mitsuyasu. Meeting the challenge of hematologic malignancies in sub-Saharan Africa. *Blood*, 2012. doi: 10.1182/blood-2012-02-387092.
- S. Gordon and F.O. Martinez. Alternative activation of macrophages: mechanism and functions. *Immunity*, 32(5):593–604, 2010.
- H. Groux, M. Bigler, J..E de Vries, and M.G. Roncarolo. Inhibitory and stimulatory effects of il-10 on human cd8+ t cells. *The Journal of Immunology*, 160(7):3188–3193, 1998.
- W. Hao and A. Friedman. The LDL-HDL profile determines the risk of atherosclerosis: A mathematical model. *PLoS ONE*, 9(3), 2014. doi:10.1371/journal.pone.0090497.
- M. Heusinkveld and S.H. van der Burg. Identification and manipulation of tumor associated macrophages in human cancers. *J. Translat. Med.*, 9(16), 2011.
- C. Hoffmann, M. Henrich, D. Gillor, G. Behrens, B. Jensen, A. Stoehr, S. Esser, J. van Lunzen, I. Krznaric, M. Mller, M. Oette, M. Hensel, J. Thoden, G. Ftkenheuer, and C. Wyen. Hodgkin lymphoma is as common as non-Hodgkin lymphoma in HIV-positive patients with sustained viral suppression and limited immune deficiency: a prospective cohort study. *HIV Medicine*, 16(4):261–264, 2015. doi: 10.1111/hiv.12200.
- J.Day, A. Friedman, and L.S.Schlesinger. Modelling the immune rheostat of macrophages in the lung in response to infection. *Proc Natl Acad Sci U.S.A*, 106(27), 2008.
- J.P.Edwards, X.Zhang, K.A. Frauwirth, and D.M. Mosser. Biochemical and functional characterization of three activated macrophage populations. *J Leukoc Biol.*, 80(6):1298–1307, 2006.
- J. Keane, M.K. Balcewicz-Sablinska, H.G. Remold, G.L. Chupp, B.B. Meek, M.J. Fenton, and H. Kornfeld. Infection by Mycobacterium tuberculosis promotes human alveolar macrophage apoptosis. *Infect Immun.*, 65(1):298–304, 1997.
- D. Kirschner and J.C. Panetta. Modeling immunotherapy of the tumor-immune interaction. *J Math Biol*, 37:235–252, 1998.
- V.A. Kuznetsov, I.A. Makalkin, M. A. Taylor, and A. S. Perelson. Nonlinear dynamics of immunogenic tumors: Parameter estimation and global bifurcation analysis. *Bull. Math. Biol.*, 56(2):295–321, 1994.
- Y. Lai, C.J. Jeng, and S.C. Chen. The roles of CD4 $^{+}$ T cells in tumor immunity. *ISRN Immunology*, 2011, 2011. doi:5402/2011/497397.
- Y. Louzoun, C. Xue, G.B. Lesinski, and A. Friedman. A mathematical model for pancreatic cancer growth and treatment. *J Theor. Biol.*, 351:74–82, 2014.

- Z.Y Lu, H. Brailly, J. Wijdenes, R. Bataille, J.F. Rossi, and Klein B. Measurement of whole body interleukin-6 (il-6) production: prediction of the efficacy of anti-il-6 treatments. *Blood*, 86(8):3123–31, 1995.
- D. Mani, M. Haigentz, and D.M. Aboulafia. Lung cancer in HIV infection. *Clin Lung Cancer*, 13(1): 5–13, 2012. doi:10.1016/j.cllc.2011.05.005.
- P. Moosa. Hodgkins Lymphoma and Human Immunodeficiency Virus Infection. *Immunodeficiency*, 2012. doi:10.5772/51671.
- P.M. Mwamba, W. O. Mwanda, N. W. Busakhala, R. M Strother, P. J. Loehrer, and S.C. Remick. AIDS-Related Non-Hodgkins Lymphoma in Sub-Saharan Africa: Current Status and Realities of Therapeutic Approach. *Hindawi Publishing Corporation*, 2012. doi:10.1155/2012/904367.
- J. Newcomb-Fernandez. Cancer in the HIV-infected population. *The Center for AIDS*, 2003.
- R. Ohno, Y. Yamaguchi, T. Toge, T. Kinouchi, T. Kotake, M. Shibata, Y. Kiyohara, S. Ikeda, I. Fukui, A. Gohchi, Y. Sugiyama, S. Saji, S. Hazama, M. Oka, K. Ohnishi, Y. Ohhashi, S. Tsukagoshi, and T. Taguchi. A dose-escalation and pharmacokinetic study of subcutaneously administered recombinant human interleukin 12 and its biological effects in Japanese patients with advanced malignancies. *Clin Cancer Res.*, 6(7):2661–9, 2000.
- B. Puvaneswaran and B. Shoba. Misdiagnosis of tuberculosis in patients with lymphoma. *South African Medical Journal*, 103(1), 2013.
- J.M Roda, Y. Wang, L.A Sumner, G.S Phillips, C.B. Marsh, and T.D. Eubank. Stabilization of HIF-2 α induces sVEGFR-1 production from tumor-associated macrophages and decreases tumor growth in amurine melanoma model. *J. Immunol.*, 189:3168–3177, 2012. doi:10.4049/jimmunol.1103817.
- S.A. Rosenberg and M.T. Lotze. Cancer immunotherapy using interleukin-2 and interleukin-2-activated lymphocytes. *Annu Rev Immunol.*, 4:681–709, 1986.
- K.R. Ruff, A. Puetter, and L.S. Levy. Growth regulation of simian and human AIDS-related non-hodgkin's lymphoma cell lines by TGF- β_1 and IL-6. *BMC Cancer*, 7(35), 2007.
- N. Seki, A.D. Brooks, C.R. Carter, T.C. Back, E.M. Parsoneault, M.J. Smyth, R.H. Wiltrot, and T.J. Sayers. Tumor-specific CTL kill murine renal cancer cells using both perforin and Fas ligand-mediated lysis in vitro, but cause tumor regression in vivo in the absence of perforin.
- A. Sevko and V. Umansky. Myeloid-derived suppressor cells interact with tumors in terms of myelopoiesis, tumorigenesis and immunosuppression; thick as thieves. *J Cancer*, 4(1):3–11, 2013. doi:10.7150/jca.5047.
- J. Stebbing, B. Gazzard, S. Mandalia, A. Teague, A. Waterston, V. Marvin, M. Nelson, and M. Bower. Antiretroviral treatment regimens and immune parameters in the prevention of systemic AIDS-related non-Hodgkin's lymphoma. *J. Clin.oncol.*, 22(11):2177–2183, 2004.
- C. Steinmller, G. Franke-Ullmann, M.L. Lohmann-Matthes, and A. Emmendrffer. Local activation of nonspecific defense against a respiratory model infection by application of interferon-gamma: comparison between rat alveolar and interstitial lung macrophages. *Am J Respir Cell Mol Biol.*, 22(4):481–490, 2000.
- E. Takeuchia, H. Yanagawa, Y. Suzukia, K. Shinkawaa, Y. Ohmotoa, H. Bandob, and S. Sone. IL-12 induced production of IL-10 and interferon- γ by nonneclear cells in lung cancer-associated malignant pleural effusions. *Lung Cancer*, 35(2):171–177, 2002.
- G. Trinchieri. Cytokines acting on or secreted by macrophages during intracellular infection (IL-10, IL-12, IFN- γ). *Curr. Opin. Immunol.*, 9(1):17–23, 1997.
- T.S. Tzai, A.L. Shiao, L.L. Liu, and C.L. Wu. Immunization with TGF-beta antisense oligonucleotide-modified autologous tumor vaccine enhances the antitumor immunity of MBT-2 tumor-bearing mice through upregulation of MHC class I and Fas expressions. *Anticancer Research*, 20(3A):1557–1562, 1999.
- V.C. Rebecca and R. Sigui. A delay-differential equation model of HIV infection of CD4 $^+$ T-cells. *Mathematical Biosciences*, 165:27–39., 2000.
- F. Villinger and A.A. Ansari. Role of IL-12 in HIV infection and vaccine. *Eur. Cytokines Netw.*, 21(3): 215–218, 2010.
- S. Wilson and D. Levy. A mathematical model of the enhancement of tumor vaccine efficacy by immunotherapy. *Bull Math Biol*, 74, 2012. doi: 10.1007/s11538-012-9722-4.
- W. Yunji, Y. Tianyi, M. Yonggang, V. H. Ganesh, Z. Jianqiu, L. L. Merry, and J. Yu-Fang. Mathematical modeling and stability analysis of macrophage activation in left ventricular remodeling post-myocardial

- infarction. *BMC Genomics*, 13(6), 2012. Available at <http://www.biomedcentral.com/1471-2164/13/S6/S21>.
- L. Zhang, J. Yang, J. Qian, H. Li, J.E. Romaguera, L.W. Kwak, M. Wang, and Q. Yi. Role of the microenvironment in mantle cell lymphoma: IL-6 is an important survival factor for the tumor cells. *Blood*, 120:3783–3792, 2012.